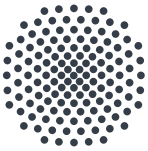

Universität Stuttgart

Dissertation

# Thermodynamic Uncertainty Relations for Time-Dependent Driving

---

*Von der Fakultät Mathematik und Physik der Universität Stuttgart zur Erlangung der Würde eines Doktors der Naturwissenschaften (Dr. rer. nat.) genehmigte Abhandlung*

---


Vorgelegt von

Timur Koyuk

aus Waiblingen


| | |
|---|---|
| Hauptbericht: | Prof. Dr. Udo Seifert |
| Mitbericht: | Prof. Dr. Christian Holm |


| | |
|---|---|
| Tag der Einreichung: | 14. Juni 2022 |
| Tag der mündlichen Prüfung: | 21. Juli 2022 |



II. Institut für Theoretische Physik



2022

CONTENTS

# ACRONYMS

| | |
|---|---|
| TUR | thermodynamic uncertainty relation |
| GTUR | generalized thermodynamic uncertainty relation |
| SCGF | scaled cumulant generating function |
| LDF | large deviation function |
| MTUR | multidimensional thermodynamic uncertainty relation |
| NESS | non-equilibrium steady state |
| PSS | periodic steady state |
| REL | relaxation process |
| TDD | time-dependent driving |
| FRI | fluctuation-response inequality |
| EQ | equilibrium state |
| FDT | fluctuation-dissipation theorem |

# PUBLICATIONS

Parts of this thesis are based on the following publications:

- T. Koyuk and U. Seifert, *Operationally accessible bounds on fluctuations and entropy production in periodically driven systems*, Phys. Rev. Lett. **122**, 230601 (2019)
  © 2019 American Physical Society. Chapter 5 and Appendix A are based on this publication.

- T. Koyuk and U. Seifert, *Thermodynamic uncertainty relation for time-dependent driving*, Phys. Rev. Lett. **125**, 260604 (2020)
  © 2020 American Physical Society. Chapter 6 and Appendix B are based on this publication.

- T. Koyuk and U. Seifert, *Quality of the thermodynamic uncertainty relation for fast and slow driving*, J. Phys. A: Math. Theor. **54**, 414005 (2021)
  © 2021 The Author(s). Published by IOP Publishing Ltd. Chapter 7, Appendix C and parts of Chapter 4 are based on this publication.

Further publications:

- T. Koyuk, U. Seifert, and P. Pietzonka, *A generalization of the thermodynamic uncertainty relation to periodically driven systems*, J. Phys. A Math. Theor. **52**, 02LT02 (2019)

- J. Degünther, T. Koyuk, and U. Seifert, *Phase shift in periodically driven non-equilibriumsystems: its identification and a bound*, J. Stat. Mech.: Theor. Exp., 033207 (2022)

- T. Koyuk and U. Seifert, *Thermodynamic uncertainty relation in interacting many-body systems*, arXiv:2202.12220 (2022)

# SUMMARY

As one of the most dynamic developments in the recent years, the thermodynamic uncertainty relation (TUR) has led to a diverse research field with many applications within stochastic thermodynamics. Crucially, it relates the key properties of small mesosopic non-equilibrium systems by bundling them into one single inequality: the inverse relative fluctuations of *any* current bounds the total entropy production from below. This implies a trade-off between precision and thermodynamic cost since a higher precision, i.e., a lower uncertainty inevitably requires a larger amount of entropy production. Moreover, the TUR has refined macroscopic principles and their implications adapted to mesoscopic systems. For example, as a stronger statement than the second law, the TUR adds the new ingredient of fluctuations to the well-known trade-off between power and efficiency of heat engines. From the perspective of thermodynamic inference, the TUR yields a model-free estimate for entropy production by measuring solely experimentally or operationally accessible quantities. Although the TUR can be applied universally without knowledge about the underlying details of the system, it is restricted to systems driven into a non-equilibrium steady state (NESS), which obey an overdamped Langevin equation or a Markovian dynamics on a discrete set of states.

In this thesis, we substantially extend the range of applicability of the TUR by deriving its generalizations to periodically driven and arbitrary time-dependently driven systems. With these relations, we unify several other TURs known so far including the original one for steady-state systems. For periodically driven systems, we derive an upper bound on the efficiency of cyclic heat engines, which implies a trade-off between power, efficiency and constancy at maximum output power. Moreover, we show that these relations cannot only be applied to current observables but also to state variables. This is especially useful from the perspective of thermodynamic inference since a further model-free estimate for entropy production can be obtained by measuring a new large class of observables. We illustrate our results not only for simple toy models but also for the folding and unfolding of a protein using real experimental data. Furthermore, we analyze the TUR in the limit of fast and slow driving and discuss which observables yield the best estimate for entropy production. Here, we show that the TUR can even be saturated in the limit of fast driving.

This thesis is structured into five different parts. In Part i, we give a general introduction to small mesoscopic systems described by the framework of stochastic thermodynamics, whereas Part ii gives a specific introduction to the field of stochastic thermodynamics and

is based on Refs. [3, 7–11]. In Part iii, which is based on Refs. [1, 2], we generalize the TUR to periodically and arbitrary time-dependently driven systems. Part iv is based on Ref. [3] and focuses on a systematic analysis of the quality of TUR in the limit of fast and slow driving. In the last Part v, we give a concluding perspective.

In the following, we briefly summarize the content of individual chapters that are part of this thesis.

CHAPTER 1: In the first chapter, we give an introduction to the basic concepts of stochastic thermodynamics and stress its important role as a theoretical framework to describe various types of non-equilibrium systems. To build up this framework, we separate the phase space of the total system into slow and fast degrees of freedom from which we identify slow observable mesostates consisting of fast possibly unobservable microstates. We assume that the microstates within a mesostate equilibrate much faster than transitions between mesostates occur. This timescale separation leads to a Markovian dynamics on the mesostates and enables us to define observables along single fluctuating trajectories in non-equilibrium systems.

CHAPTER 2: In this chapter, we first introduce the concepts of stochastic thermodynamics for continuous overdamped Langevin systems and, then, for a Markovian dynamics on a discrete set of states. We define the dynamics for both types of systems, which are driven out of equilibrium, and discuss three distinct choices of forces and rates, which lead to three different stationary states: an equilibrium state, a NESS and a periodic steady state (PSS). Moreover, we formulate the requirements for the dynamics to model a discrete system in a thermodynamic consistent way and introduce the local detailed balance condition. Last but not least, we define fluctuating thermodynamic notions like work, heat and internal energy by formulating the first law along discrete as well as continuous trajectories and introduce two equivalent definitions of entropy production, which are consistent with the second law.

CHAPTER 3: We define general current observables and state variables for continuous overdamped Langevin systems and for a Markovian dynamics on a discrete set of states. To quantify their fluctuations, we define the diffusion coefficient and the precision of an observable. Moreover, we introduce the scaled cumulant generating function (SCGF), which quantifies fluctuations completely on an ensemble of trajectories. We further relate this function to the mean and diffusion coefficient of an observable.

CHAPTER 4: In this chapter, we give a brief introduction to the TUR and highlight its significance in the field of stochastic thermo-

dynamics by summarizing recent research directions and give a broad overview about its impact on related fields of research. Furthermore, we provide a simple proof of the TUR for continuous and discrete steady-state systems, which is solely based on the Cauchy-Schwarz inequality and discuss the advantages and disadvantages of recent methods for deriving the TUR. Finally, we focus on one important application of the TUR: a bound on the efficiency of heat engines, which yields a trade-off relation between power, efficiency and fluctuations.

CHAPTER 5: We derive a substantial generalization of the thermodynamic uncertainty relation to periodically driven systems for various types of observables. This relation is operationally accessible and requires the experimentalist to measure only the mean, its dependence on the driving frequency and the variance of an observable. In contrast to the ordinary TUR, our generalization additionally includes the response of an observable with respect to the driving frequency. Remarkably, we show that entropy production can be bounded by just observing the time spent in a certain state. As an important application of our generalization, the thermodynamic efficiency of isothermal cyclic engines like molecular motors under a periodic load or of cyclic heat engines can be bounded using experimental data without requiring knowledge of the specific interactions within the system. Most prominently, these bounds imply a trade-off between power, efficiency and constancy for machines operating at maximum power. We illustrate these results for a driven three-level system and for a colloidal Stirling engine.

CHAPTER 6: In this chapter, we derive the most general form of the thermodynamic uncertainty relation for arbitrary time-dependent driving and from arbitrary initial states. We show that this relation is not restricted to current-type observables but holds also for the huge class of state variables. With these relations, we unify several TURs valid for steady-states, relaxation processes and periodic driving. The crucial step to derive our main results is the identification of a speed parameter of a protocol controlled by the experimentalist. Our bounds do not require specific knowledge about the system or its coupling to the time-dependent control. Hence, they are widely applicable tools for thermodynamic inference in time-dependently driven systems. The quality of the bounds is discussed for an interacting pair of colloidal particles in a moving laser trap and for the dynamical unfolding of a small protein using real experimental data.

CHAPTER 7: We analyze the quality of the thermodynamic uncertainty relation for time-dependent driving by defining a quality factor in the limiting cases of fast and slow driving for state vari-

ables and for current observables. We show that in both limiting cases observables can be found that yield an estimate of order 1 for the total entropy production and derive a generic scaling of the quality factor for different observables. We further prove that the uncertainty relation can even be saturated in the limit of fast driving when choosing as a current the total entropy production rate. We illustrate the scaling of the quality factors for different setups of a three-state system. In the limit of slow driving, the scaling depends on whether or not a non-conservative force is applied to the system.

# ZUSAMMENFASSUNG

Als eine der dynamischsten Entwicklungen in den letzten Jahren führte die TUR zu einem diversen Forschungsfeld mit vielen Anwendungen in der stochastischen Thermodynamik. Mithilfe der TUR werden die Schlüsseleigenschaften kleiner mesoskopischer Nichtgleichgewichtssysteme in Relation gesetzt und in eine einzige Ungleichung gebündelt: Die totale Entropieproduktion wird von unten durch die inversen relativen Fluktuationen eines *beliebigen* Stromes begrenzt. Dies führt zu einer Kosten-Nutzen Relation zwischen Präzision und thermodynamischen Kosten, denn für eine höhere Präzision, d.h. kleinere Unsicherheit, wird unausweichlich eine größere Menge an Entropieproduktion benötigt. Darüber hinaus wurden etablierte makroskopische Prinzipien sowie deren Schlussfolgerungen, welche auf mesoskopische Systeme übertragen werden können, durch die TUR weiterentwickelt. Beispielsweise trifft die TUR eine stärkere Aussage über Entropieproduktion als der zweite Hauptsatz. Dadurch wird die etablierte Kosten-Nutzen Relation zwischen Ausgangsleistung und Effizienz für Wärmekraftmaschinen um Fluktuationen ergänzt. Aus der Perspektive der thermodynamischen Inferenz liefert die TUR unabhängig vom betrachteten Modell eine Abschätzung an die Entropieproduktion, indem ausschließlich experimentell oder operational zugängliche Größen gemessen werden. Obwohl die TUR universell ohne Kenntnisse über Details des betrachteten Systems angewandt werden kann, ist sie auf stationäre Nichtgleichgewichtssysteme beschränkt, welche durch eine überdämpfte Langevin Gleichung oder durch ein diskretes Markovnetzwerk beschrieben werden können.

In der vorliegenden Arbeit wird der Gültigkeitsbereich der TUR erheblich erweitert, indem ihre Verallgemeinerungen für periodisches Treiben sowie beliebig zeitabhängiges Treiben hergeleitet werden. Mit diesen Relationen werden bisher bekannte TURs einschließlich derjenigen für stationäre Nichtgleichgewichtssysteme vereinheitlicht. Für periodisch getriebene Systeme erfolgt die Herleitung einer Schranke an die Effizienz von Wärmekraftmaschinen, welche eine Kosten-Nutzen Relation zwischen Leistung, Effizienz und Zuverlässigkeit bei maximaler Ausgangsleistung impliziert. Darüber hinaus wird gezeigt, dass diese Relationen nicht nur für Ströme, sondern auch für Zustandsgrößen angewandt werden können. Dies ist vor allem aus der Perspektive der thermodynamischen Inferenz nützlich, da eine zusätzliche Abschätzung der Entropieproduktion, unabhängig vom physikalischen Modell, durch eine neue Klasse von Observablen möglich ist. Die obigen Resultate werden nicht nur durch simple „Toy"-Modelle, sondern auch durch einen Proteinfaltungsprozess basierend auf echten

experimentellen Daten illustriert. Des Weiteren wird die TUR in den Grenzfällen des schnellen und langsamen Treibens analysiert sowie die optimale Wahl der Observablen untersucht, welche die beste Abschätzung der Entropieproduktion liefert. Hierbei wird aufgezeigt, dass die TUR im Grenzfall des schnellen Treibens sogar gesättigt werden kann.

Die vorliegende Arbeit ist in fünf verschiedene Teile gegliedert. In Teil i wird eine allgemeine Einführung in kleine mesoskopische Systeme gegeben, welche innerhalb des Gebiets der stochastischen Thermodynamik beschrieben werden können. Im Gegensatz dazu findet sich in Teil ii eine spezifische Einführung in die stochastische Thermodynamik, die auf Refs. [3, 7–11] basiert. In Teil iii, welcher auf Refs. [1, 2] beruht, wird die TUR für periodisch getriebene und für beliebig zeitabhängig getriebene Systeme verallgemeinert. Teil iv gründet sich auf Ref. [3] und behandelt eine systematische Analyse der Qualität der TUR im Grenzfall des schnellen und langsamen Treibens. Im letzten Teil v folgt ein zusammenfassender Ausblick.

Im Folgenden wird der Inhalt einzelner Kapitel der vorliegenden Arbeit zusammengefasst.

KAPITEL 1: Im ersten Kapitel wird eine Einführung in die grundlegenden Konzepte der stochastischen Thermodynamik gegeben. Dieser theoretische Forschungsbereich ist in der Lage zahlreiche Arten von Nichtgleichgewichtssystemen zu beschreiben. Um die Theorie zu formulieren, wird der Phasenraum des gesamten Systems in langsame und schnelle Freiheitsgrade aufgeteilt, wodurch eine Identifizierung von langsamen und sichtbaren Mesozuständen möglich ist, welche sich aus schnellen unzugänglichen Mikrozuständen zusammensetzen. Hierbei wird angenommen, dass Mikrozustände innerhalb eines Mesozustandes schneller ins Gleichgewicht relaxieren als Übergänge zwischen zwei Mesozuständen stattfinden. Diese Zeitskalenseparation führt effektiv zu einer Markovdynamik, welche auf den Mesozuständen stattfindet und es ermöglicht Observablen entlang einzelner fluktuierender Trajektorien in Nichtgleichgewichtsystemen zu definieren.

KAPITEL 2: In diesem Kapitel werden die grundlegenden Konzepte der stochastischen Thermodynamik zunächst für kontinuierliche Langevin Systeme und anschließend für diskrete Makrovnetzwerke eingeführt. Hierbei wird die Dynamik für beide Arten von Nichtgleichgewichtssystemen definiert und anschließend drei spezielle Wahlen für Kräfte und Raten diskutiert, welche zu jeweils drei verschiedenen stationären Zuständen führen: Einem Gleichgewichtszustand, einem stationären Nichtgleichgewichtszustand sowie einem periodischen stationären Zustand. Darüber hinaus werden die Anforderungen formuliert, die nötig sind, um ein diskretes System thermodynamisch konsistent zu mo-

dellieren. Hierzu wird die sogenannte „local detailed balance"-Bedingung eingeführt. Des Weiteren werden fluktuierende thermodynamische Größen wie z.B. Arbeit, Wärme oder innere Energie definiert, indem der erste Hauptsatz entlang diskreter und kontinuierlicher Trajektorien formuliert wird. Schließlich werden zwei äquivalente Definitionen für Entropieproduktion eingeführt, welche konsistent mit dem zweiten Hauptsatz sind.

KAPITEL 3: Es werden allgemeine Strom- und Zustandsobservablen für kontinuierliche überdämpfte Langevin Systeme und diskrete Markovnetzwerke definiert. Zur Quantifizierung von Fluktuationen werden der Diffusionskoeffizient sowie die Präzision einer Observablen eingeführt. Darüber hinaus wird die SCGF definiert, welche Fluktuationen auf einem gesamten Ensemble von Trajektorien quantifiziert. Hierbei wird auf den Zusammenhang zwischen der SCGF und dem Mittelwert sowie dem Diffusionskoeffizienten eingegangen.

KAPITEL 4: In diesem Kapitel wird eine kurze Einführung in das Themengebiet der TUR gegeben und deren Relevanz im Feld der stochastischen Thermodynamik erörtert. Hierzu werden verschiedene Richtungen aktueller Forschung betrachtet und ein breiter Überblick über den Einfluss auf verwandte Themengebiete gegeben. Des Weiteren wird ein simpler Beweis der TUR für kontinuierliche und diskrete stationäre Nichtgleichgewichtssysteme vorgestellt, der ausschließlich auf der Cauchy-Schwarz Ungleichung beruht. Anschließend werden die Vor- und Nachteile aktueller Beweismethoden der TUR diskutiert. Zuletzt wird eine wichtige Anwendung der TUR vorgestellt: Eine Schranke an die Effizienz von Wärmekraftmaschinen, die eine Kosten-Nutzen Relation zwischen Leistung, Effizienz und Fluktuationen impliziert.

KAPITEL 5: Es wird eine bedeutende Verallgemeinerung der thermodynamischen Unschärferelation für periodisch getriebene Systeme und für verschiedene Arten von Observablen hergeleitet. Diese Relation ist operational zugänglich und erfordert für eine experimentelle Durchführung lediglich den Mittelwert, dessen Abhängigkeit von der Frequenz und die Varianz einer Observablen zu messen. Im Gegensatz zur konventionellen TUR beinhaltet die Verallgemeinerung für periodisch getriebene Systeme den Antwortterm bezüglich der Frequenz einer beliebigen Observablen. Bemerkenswerterweise wird gezeigt, dass die Entropieproduktion durch eine Größe beschränkt wird, für die lediglich die verbrachte Zeit in einem ausgewählten Zustand gemessen werden muss. Eine wichtige Anwendung dieser Relationen ist eine Schranke an die Effizienz von zyklisch arbeitenden isothermen Maschinen wie z.B. molekulare Motoren unter periodisch

wechselnder Last oder zyklisch arbeitende Wärmekraftmaschinen. Zur Aufstellung dieser Schranke werden ausschließlich, ohne zusätzliches Wissen über spezifische Wechselwirkungen innerhalb des Systems, experimentell zugängliche Daten benötigt. Die Schranke an die Effizienz impliziert eine Kosten-Nutzen Relation zwischen Ausgangsleistung, Effizienz und Zuverlässigkeit für zyklisch arbeitende Maschinen, welche mit maximaler Ausgangsleistung operieren. Die oben genannten Relationen für periodisch getriebene Systeme werden anhand eines getriebenen Drei-Niveau Systems und einer kolloidalen Stirling Maschine illustriert.

KAPITEL 6: In diesem Kapitel wird die allgemeinste Form der thermodynamischen Unschärferelation aufgestellt, welche für beliebiges Treiben und für beliebige Anfangszustände gültig ist. Es wird gezeigt, dass diese Relation nicht nur für Ströme, sondern auch für die große Klasse von Zustandsobservablen angewandt werden kann. Mit diesen Resultaten werden zahlreiche Unschärferelationen vereinheitlicht, welche für stationäre Nichtgleichgewichtszustände, Relaxationsprozesse sowie periodisches Treiben gelten. Der entscheidende Schritt für den Beweis dieser Relation liegt in der Identifikation eines Geschwindigkeitsparameters des Protokolls, welcher durch den Experimentator kontrolliert werden kann. Diese Schranken benötigen keine näheren Informationen über das System oder dessen Kopplung zum zeitabhängigen Protokoll. Daher sind sie universell zur thermodynamischen Inferenz einsetzbare Werkzeuge in zeitlich getriebenen Systemen. Die Qualität der Schranken wird für ein wechselwirkendes Paar von kolloidalen Teilchen und für einen dynamischen Proteinfaltungsprozess, basierend auf echten experimentellen Daten, diskutiert.

KAPITEL 7: Die Qualität der thermodynamischen Unschärferelation wird für zeitabhängiges Treiben durch Einführung eines Qualitätsfaktors in den Grenzfällen des schnellen und langsamen Treibens für Zustandsobservablen und für Ströme untersucht. Hierbei wird gezeigt, dass in beiden Grenzfällen Observablen existieren, die zu einer Abschätzung von Entropieproduktion auf Ordnung 1 führen. Ebenso wird eine generische Skalierung von Qualitätsfaktoren für verschiedenen Observablen in den jeweiligen Grenzfällen hergeleitet. Des Weiteren wird bewiesen, dass die Unschärferelation im Grenzfall des schnellen Treibens sogar gesättigt werden kann, wenn der gewählte Strom proportional zur totalen Entropieproduktion ist. Die Skalierungen der Qualitätsfaktoren werden für verschiedene Konfigurationen eines Drei-Niveau Systems illustriert. Im Grenzfall des lang-

samen Treibens hängen diese Skalierungen davon ab, ob eine nicht-konservative Kraft angelegt wird oder nicht.

# Part I

# INTRODUCTION

# INTRODUCTION

The arguably most important feature that characterizes non-equilibrium processes is the total rate of entropy production. As a universal measure of irreversibility, it quantifies how far from equilibrium the system indeed is. In the early days of thermodynamics, Rudolf Clausius first has introduced the notion of entropy as a macroscopic quantity [12], whereas later Boltzmann and Gibbs have given a statistical definition on a microscopic basis [13, 14]. Moreover, Clausius has stated that in an isolated system, entropy can only increase or remains constant. With this consideration, he has contributed to the formulation of the second law of thermodynamics [15, 16], which equivalently states that the total rate of entropy production is always positive or zero. While the second law makes predictions about the direction of spontaneous processes, the first law of thermodynamics introduced by Robert Mayer in 1842 states a conservation of energy in the sense that the change in internal energy of a system must be transformed into heat and work [17].

The first and the second law of thermodynamics provide the basics to describe heat engines, which are cyclic processes that convert heat into useful work. Since it laid the foundation of thermodynamics, the probably most prominent of such processes is the Carnot cycle [18]. For such a process, the first law deals with energetic considerations, i.e., it allows one to determine the efficiency. The second law implies that the efficiency of any cyclic process is bounded from above by the Carnot efficiency, which is reached only if the engine operates reversibly. This condition is typically satisfied for quasi-static slow processes with infinite cycle duration. However, for these slow processes, the output power vanishes, which inevitably leads to a trade-off between power and efficiency.

The above discussed concepts have been originally formulated for macroscopic systems in the 19th century. In contrast, recent research focuses on small mesoscopic systems coupled to a heat bath like colloidal particles embedded in an aqueous solution. Such a system has been studied in 1827 by Robert Brown, who observed the random motion of pollen immersed in water under the microscope [19]. This phenomenon has been fully understood not until the beginning of the 20th century, where the works of Einstein, Smoluchowski, Langevin and Perrin have led to a theory, in which the random motion is modeled by a stochastic Gaussian noise, which effectively resembles the collisions of the pollen or colloids with the surrounding solvent molecules [20–24]. In such systems, the relevant energy scales are on the same order of magnitude as the thermal energy. Hence, in contrast

to macroscopic thermodynamic systems, fluctuations in these small systems play a fundamental role.

Nowadays, for small mesoscopic non-equilibrium systems, a theoretical framework called stochastic thermodynamics [8, 25] has been established and provides proper definitions of entropy or entropy production that are consistent with the second law. Moreover, it allows one to formulate the first law along single fluctuating trajectories and, hence, thermodynamic notions like heat and work can be properly defined. One of the main objectives in the field of stochastic thermodynamics deals with the quantification of the total rate of entropy production. While its proper measurement requires the experimentalist to observe all degrees of freedom, systems of interest contain hidden degrees of freedom like unobservable folded or unfolded states of a protein (see, e.g., Ref. [26]). Obviously, this makes an exact inference of entropy production impossible.

Recently, a prominent and universally applicable inequality called the TUR has been discovered [27, 28]. As a trade-off between precision and thermodynamic cost, the TUR yields a lower bound on the total entropy production in terms of *any* current and its fluctuations. An important application of this inequality is the inference of entropy production since the measurement of an arbitrary current and its fluctuations within a limited number of degrees of freedom yields an estimator for entropy production. Moreover, the TUR can be interpreted as a stronger statement about entropy production in comparison to the second law. Thus, it yields a stronger bound on the efficiency of heat engines than the bound imposed by the Carnot efficiency [29]. Despite its universal applicability without knowledge about interactions or forces, the TUR is restricted to systems driven into a NESS and violations have been observed for different types of dynamics such as discrete-time Markovian processes [30], periodically driven systems [31], and underdamped Langevin systems with and without a magnetic field [32–34]. Therefore, recent research, including this thesis, deals with generalizations of the TUR to further types of dynamics.

# Part II

# STOCHASTIC THERMODYNAMICS

# 1 BASIC CONCEPTS

In the continuously growing research area about non-equilibrium phenomena, the framework of stochastic thermodynamics is one of the most successful theories since it is able to describe various types of mesoscopic non-equilibrium systems. For example, it allows one to model suspensions of colloidal particles, the folding and unfolding of proteins, enzymatic reactions and molecular motors in a thermodynamic consistent way [8–10, 25]. All these systems are coupled to a heat bath with a well-defined temperature.

A fundamental assumption of stochastic thermodynamics that enables us to describe systems far away from equilibrium is the separation of the total phase space into slow observable degrees of freedom and fast unobservable ones. Typically, these slow degrees of freedom correspond to the system of interest, whereas the fast ones are associated with the heat bath or internal degrees of freedom. We separate the total phase space into sets of microstates, which are called mesostates (see Figure 1.1). For example, we consider the motion of a colloidal particle or the folding and unfolding of a protein, which are both embedded in an aqueous solution functioning as a heat bath. Then, a mesostate corresponds to the position of the colloidal particle or the folded or unfolded state of a protein and all configurations of the solvent particles compatible with these. From an operational or experimental point of view, it suffices to observe solely the colloidal particle or the protein to determine the mesostate of the system. In contrast, a microstate contains all positions and momenta of the solvent particles and the system of interest. For each of these microstates, there is a unique mapping to a corresponding mesostate.

The crucial assumption for building a thermodynamic consistent framework is the equilibration of microstates within a mesostate, which is much faster than transitions between mesostates occur. This timescale separation allows us to define thermodynamic quantities for mesostates like internal energy or free energy. These definitions are important for identifying thermodynamic notions along a trajectory of mesostates, which is the key concept of stochastic thermodynamics.

Finally, the timescale separation implies that the dynamics on the mesostates becomes Markovian since the future mesostate of the system depends neither on the state occupied before nor on the time spent in this state due to the fast equilibration of microstates within a mesostate. For systems with continuous degrees of freedom, the dynamics of the mesostates is described by a Langevin equation or,

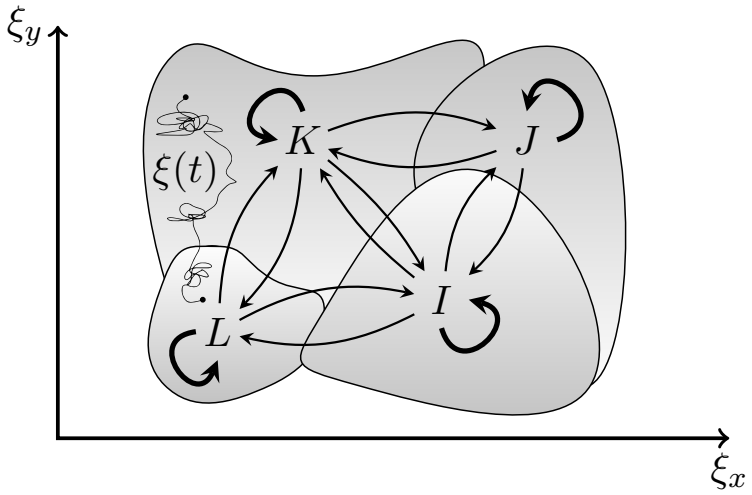


Figure 1.1: Phase space consisting of microstates $\xi = (\xi_x, \xi_y)$ and separated into several mesostates $I, J, K$ and $L$, e.g., different folded or unfolded states of a protein. A trajectory $\xi(t)$ visits different mesostates. Here, transitions within mesostates occur often (thick arrows), whereas transitions between them happen rarely (thin arrows). This effectively leads to a timescale separation implying microstates that equilibrate much faster within a mesostate than transitions between mesostates occur.

equivalently, by the Fokker-Planck equation, whereas the dynamics on a discrete set of mesostates is described by a master equation. We will discuss these different types of the dynamics in the next Chapter 2.

# 2

# THERMODYNAMICS ALONG SINGLE TRAJECTORIES

## 2.1 CONTINUOUS DEGREES OF FREEDOM

In this section, we introduce the concepts of stochastic thermodynamics for a single colloidal particle embedded in an aqueous solution [8, 11]. Here, we are interested in the position of the particle, which corresponds to the mesostate and assume that the microstates associated with the solvent particles and compatible with the particle position equilibrate much faster than the position of the particle changes. We further assume that the particle is driven out of equilibrium by a time-dependent force that evolves slowly enough in time to ensure that the microstates of the solvent particles still equilibrate.

We first introduce the theory to describe the dynamics of an overdamped colloidal particle. Then, we discuss three distinct choices for the type of dynamics and follow the steps of Sekimoto to formulate the first law along a trajectory [35, 36]. Moreover, we define the total entropy production and show that this definition is consistent with the second law. While we focus on a system with a single continuous degree of freedom in this section, generalizations of the concepts for systems with multiple interacting degrees of freedom or systems with state-dependent friction are straightforward (see, e.g., Refs. [8, 37]).

### 2.1.1 *Dynamics*

We consider the one-dimensional motion of a time-dependently driven colloidal particle embedded in an aqueous solution, which acts as a heat bath with inverse temperature $\beta$. The position $x_t$ of the particle at time $t$ obeys the overdamped Langevin equation

$$\partial_t x_t \equiv \dot{x}_t = \mu F(x_t, \lambda_t) + \sqrt{2D}\zeta_t. \tag{2.1}$$

Here, $\mu$ denotes the mobility and

$$F(x_t, \lambda_t) \equiv F_c(x_t, \lambda_t) + f(x_t, \lambda_t) \tag{2.2}$$

is the time-dependent total force acting on the particle, where the conservative force $F_c(x_t, \lambda_t) \equiv -\partial_x V(x, \lambda_t)|_{x=x_t}$ can be derived from the potential $V(x, \lambda_t)$ and $f(x_t, \lambda_t)$ is a non-conservative force, which both depend on the external protocol $\lambda_t$. The diffusion coefficient $D \equiv \mu/\beta$ obeys the Einstein relation [17, 20, 38] and $\zeta_t$ denotes the

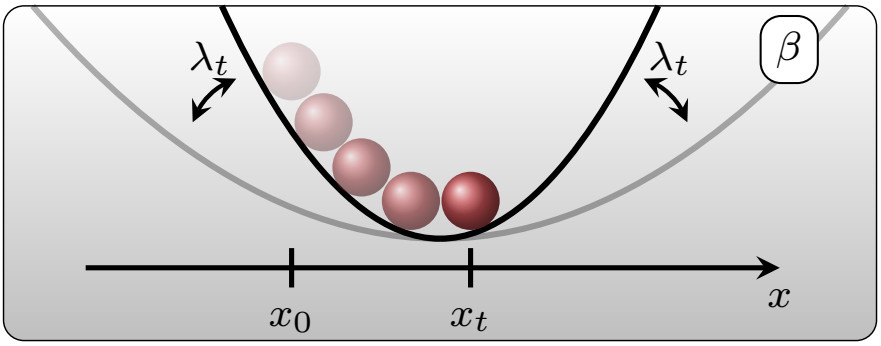


Figure 2.1: Schematic of a colloidal particle trapped in a harmonic potential and coupled to a heat bath with inverse temperature $\beta$. The particle moves from position $x_0$ to position $x_t$. The stiffness of the trap is controlled by the time-dependent protocol $\lambda_t$.

random force described by a Gaussian random variable with mean and correlations given by

$$\langle \zeta_t \rangle = 0 \tag{2.3}$$

and

$$\langle \zeta_t \zeta_{t'} \rangle = \delta(t - t'), \tag{2.4}$$

respectively, where $\langle \cdot \rangle$ denotes the mean value over all noise realizations. A paradigmatic example for such a system is a colloidal particle trapped in a harmonic potential as shown in Fig. 2.1. Here, the stiffness of the trap $k(\lambda_t)$ is controlled by a time-dependent protocol $\lambda_t$. In this system, there is only a time-dependent conservative force $F_c(x, \lambda_t) = -k(\lambda_t)x$. The non-conservative force is zero, i.e., $f(x_t, \lambda_t) = 0$.

Equivalently, the dynamics of the colloidal particle can be described on an ensemble level by the overdamped Fokker-Planck equation

$$\partial_t p(x,t) = -\partial_x j(x,t), \tag{2.5}$$

where $p(x,t)$ is the probability to find the particle at position $x$ at time $t$ and

$$j(x,t) \equiv \left(\mu F(x,\lambda_t) - D\partial_x\right) p(x,t) \tag{2.6}$$

is the time-dependent probability current. The Fokker-Planck equation (2.5) can be written as

$$\partial_t p(x,t) = \mathcal{L}_{\mathrm{FP}}(x,\lambda_t) p(x,t) \tag{2.7}$$

with the Fokker-Planck operator

$$\mathcal{L}_{\mathrm{FP}}(x,\lambda_t) \equiv -\partial_x \left(\mu F(x,\lambda_t) - D\partial_x\right). \tag{2.8}$$

We now discuss three different choices of the forces leading to three different special states.

First, for a constant protocol $\lambda_t = \lambda$ and in the absence of a non-conservative force $f(x,\lambda) = 0$, every system prepared in an arbitrary initial distribution $p(x,0)$ will reach the equilibrium distribution

$$p^{\mathrm{eq}}(x,\lambda) \equiv \exp[-\beta V(x,\lambda)]/Z(\lambda) \tag{2.9}$$

in the long-time limit, where $Z(\lambda) \equiv \int \mathrm{d}x \exp[-\beta V(x,\lambda)]$ is the normalization. Obviously, in this case the probability current vanishes, i.e., $j(x,\lambda) = 0$.

Second, for a constant protocol but with a non-vanishing non-conservative force $f(x,\lambda) \neq 0$ and for a system with periodic boundary conditions $F(x,\lambda) = F(x+L,\lambda)$, where $L$ is the length of the ring, the system will reach a unique NESS. For a constant force $f(x,\lambda) = f(\lambda)$, the formal expression of the distribution is given by

$$p^{\mathrm{s}}(x,\lambda) \equiv e^{\beta \int_0^x \mathrm{d}x' F(x',\lambda)} \left[ c + \frac{j^{\mathrm{s}}(\lambda)}{D} \int_0^x \mathrm{d}x'\, e^{-\beta \int_0^{x'} \mathrm{d}x'' F(x'',\lambda)} \right], \tag{2.10}$$

where $c$ is an integration constant and the stationary probability current $j^{\mathrm{s}}(\lambda) \equiv (\mu F(x,\lambda) - D\partial_x)\, p^{\mathrm{s}}(x,\lambda) \neq 0$ is non-zero and position-independent. Both quantities can be determined by using the periodicity condition $p^{\mathrm{s}}(0,\lambda) = p^{\mathrm{s}}(L,\lambda)$ and normalization condition $\int_0^L \mathrm{d}x\, p^{\mathrm{s}}(x,\lambda)$. For an arbitrary force $f(x,\lambda)$, the steady-state distribution can be determined by using the Eigenvalue equation

$$\mathcal{L}_{\mathrm{FP}}(x,\lambda) p^{\mathrm{s}}(x,\lambda) = 0, \tag{2.11}$$

which follows from Eq. (2.7). A NESS is typically used to model Brownian ratchets [39] or molecular motors [40].

Third, for periodic time-dependent driving with a protocol $\lambda_t = \lambda(\Omega t) = \lambda(\Omega\,[t+\mathcal{T}])$ depending on frequency $\Omega$ and period $\mathcal{T}$, the system will reach a unique PSS

$$p^{\mathrm{ps}}(x,t) = p^{\mathrm{ps}}(x,t+\mathcal{T}), \tag{2.12}$$

which is the periodic solution of the Fokker-Planck equation and fulfills the Eigenvalue equation

$$\overrightarrow{\exp}\left( \int_0^{\mathcal{T}} \mathrm{d}t\, \mathcal{L}_{\mathrm{FP}}(x,\lambda_t) \right) p^{\mathrm{ps}}(x,0) = p^{\mathrm{ps}}(x,0), \tag{2.13}$$

where $\overrightarrow{\exp}\,(\cdot)$ denotes the time-ordered exponential. Furthermore, there is a time-dependent periodic probability current $j^{\mathrm{ps}}(x,t) = j^{\mathrm{ps}}(x,t+\mathcal{T})$. This class of dynamics is typically used to model microscopic heat engines [41, 42] or molecular pumps [43–45].

Beside the trajectory-based description of the Langevin equation (2.1) or the ensemble-based approach of the Fokker-Planck equation (2.5), the dynamics can be described equivalently by a path integral $\mathcal{P}[x_t]$

providing a measure of probability to observe the trajectory $x_t$. For a proper definition of the path weight $\mathcal{P}[x_t]$, the trajectory $x_t$ must be discretized in time since the position $x_t$ is not differentiable due to the noise. Thus, a trajectory of length $T$ becomes a set of $n$ positions $\{x_1, ..., x_i, ..., x_n\}$ with $x_i \equiv x_{t_i}$ and $t_i \equiv i\Delta t$, where $\Delta t$ is a small time step and $n\Delta t = T$ is kept fixed. When discretizing the Langevin equation (2.1) one has to chose between two discretization schemes: the Stratonovich scheme and the Itô scheme. In the Itô scheme, the Langevin equation reads

$$x_i - x_{i-1} = \mu F(x_{i-1}, \lambda_{i-1})\Delta t + \sqrt{2D\Delta t}\zeta_{i-1}, \tag{2.14}$$

whereas in the Stratonovich scheme (midpoint discretization) it reads

$$x_i - x_{i-1} = \mu F([x_i + x_{i-1}]/2, \lambda_{\Delta t(i-1/2)})\Delta t + \sqrt{2D\Delta t}\zeta_{i-1}, \tag{2.15}$$

where $\zeta_{i-1} \equiv \zeta_{t_{i-1}}$ and $\lambda_{i-1} \equiv \lambda_{t_{i-1}}$. Here, we have scaled the diffusion constant by $1/\Delta t$ due to the discretized delta-distribution $\delta(t_i - t_j) \to \delta_{ij}/\Delta t$. To derive an expression for a path weight, we will use the Stratonovich scheme in Eq. (2.15).

To build the path weight for a trajectory $x_t$, we define the probability $\mathcal{P}(\zeta_1, ..., \zeta_n)$ to observe a discrete noise history $\{\zeta_1, ..., \zeta_n\}$. Since the noise is Gaussian distributed according to $\langle \zeta_i \rangle = 0$ and $\langle \zeta_i \zeta_j \rangle = \delta_{ij}$, the probability to observe the history of noises is given by

$$\mathcal{P}[\zeta_t] \equiv \mathcal{P}(\zeta_1, ..., \zeta_n) = \left(\frac{\Delta t}{4\pi D}\right)^{n/2} \exp\left(-\frac{\Delta t}{4D}\sum_{i=1}^{n}\zeta_i^2\right). \tag{2.16}$$

With this path weight, mean values over noise realizations can be expressed as

$$\langle \cdot \rangle = \int \mathrm{d}[\zeta_t]\mathcal{P}[\zeta_t] \equiv \left(\prod_{i=1}^{n}\int \mathrm{d}\zeta_i\right)\mathcal{P}(\zeta_1, ..., \zeta_n). \tag{2.17}$$

Our goal is to define a path weight for a mean value over all trajectory realizations $x_t$ and, hence, we have to transform (2.17) according to

$$\left(\prod_{i=1}^{n}\int \mathrm{d}x_i\right)\mathcal{P}(x_1, ..., x_n|x_0) \equiv \left(\prod_{i=1}^{n}\int \mathrm{d}x_i\right)\det\left(\frac{\partial\zeta_i}{\partial x_j}\right) \times \mathcal{P}(\zeta_1, ..., \zeta_n)|_{\zeta_i=\zeta_i(x_i,x_{i+1})} \tag{2.18}$$

with the Jacobian given by

$$\begin{aligned}\det\left(\frac{\partial\zeta_i}{\partial x_j}\right) &= \frac{1}{\Delta t^n}\exp\left(\sum_{i=1}^{n}\ln\left(1 - \frac{\Delta t\mu}{2}F'([x_i + x_{i-1}]/2, \lambda_{(i-1/2)\Delta t})\right)\right) \\ &\approx \frac{1}{\Delta t^n}\exp\left(\sum_{i=1}^{n}\frac{-\Delta t\mu}{2}F'([x_i + x_{i-1}]/2, \lambda_{(i-1/2)\Delta t})\right),\end{aligned} \tag{2.19}$$

where we used Eq. (2.15) and $F'(x,\lambda_t) \equiv \partial_x F(x,\lambda_t)$. Thus, for the path weight of a trajectory in Eq. (2.18) we get

$$\mathcal{P}(x_1,...,x_n|x_0) = \left(\frac{1}{4\pi D\Delta t}\right)^{\frac{n}{2}} \exp\left[-\frac{\Delta t}{4D}\sum_{i=1}^{n}\left(\left[\frac{x_i - x_{i-1}}{\Delta t} - \mu F_i\right]^2 + 2D\mu F_i'\right)\right] \tag{2.20}$$

with the discretized force in the Stratonovich scheme

$$F_i \equiv F\left(\frac{x_i + x_{i-1}}{2}, \lambda_{(i-1/2)\Delta t}\right). \tag{2.21}$$

When taking the continuum limit $\Delta t \to 0$ and $n \to \infty$ with fixed $n\Delta t = T$, we define the path weight as

$$\mathcal{P}[x_t|x_0] \equiv \exp(-\mathcal{S}[x_t]) \tag{2.22}$$

with the action

$$\mathcal{S}[x_t] \equiv \frac{1}{4D}\int_0^T \mathrm{d}t\left([\dot{x}_t - \mu F(x_t,\lambda_t)]^2 + 2D\mu F'(x_t,\lambda_t)\right) \tag{2.23}$$

in the Stratonovich discretization, where the functional in Eq. (2.23) is called an Onsager-Machlup functional [46]. A mean value is then expressed as an integration over all paths as

$$\langle\cdot\rangle = \int \mathrm{d}[x_t]\mathcal{P}[x_t] \equiv \int \mathrm{d}[x_t]\mathcal{P}[x_t|x_0]p(x_0,0), \tag{2.24}$$

where $p(x_0,0)$ is the initial distribution and

$$\int \mathrm{d}[x_t] \equiv \int \mathrm{d}x_0 \prod_{i=1}^{n}\left(\frac{1}{\sqrt{4\pi D\Delta t}}\int \mathrm{d}x_i\right) \tag{2.25}$$

is the measure of integration. In the Itô scheme, the last term in Eq. (2.23), i.e., the derivative of the force does not occur since the force entering in the Jacobian in Eq. (2.18) does only depend on $x_{i-1}$ and not on $x_i$. We note that the path weight in Eq. (2.22) can be generalized to systems with state-dependent diffusion in a thermodynamic consistent way, see, e.g., Ref. [37].

Finally, a path weight in the continuum limit (2.22) has to be read always as a time-discretized path weight in Eq. (2.20) with a suitable small time step $\Delta t$. Thus, one has to choose between suitable discretization schemes such as the Stratonovich or Itô scheme. Throughout this thesis, we will use the Stratonovich scheme unless we explicitly indicate to use another scheme. The advantage of the Stratonovich scheme is that we are able to apply the chain rule as usual [47]. Furthermore, as we will show in the next section, physical observables along single trajectories are defined through the Stratonovich scheme.

### 2.1.2 *Stochastic energetics: first law*

The centerpiece of stochastic thermodynamics is the definition of well known thermodynamic notions like heat, work or entropy production along single fluctuating trajectories. Here, the first step is to formulate the first law along a trajectory $x_t$, which has been suggested by Sekimoto in 1997 and is termed as stochastic energetics [35, 36].

The first law along the trajectory $x_t$ reads

$$\mathrm{d}U[x_t] = \delta W[x_t] - \delta Q[x_t], \tag{2.26}$$

where $\mathrm{d}U[x_t]$ is the change in internal energy, $\delta W[x_t]$ is the work and $\delta Q[x_t]$ is the heat. Since in the overdamped dynamics the kinetic energy is assumed to relax fast to equilibrium due to large friction or small mass, we neglect this term in the position dependent internal energy of the system, which is, thus, given by

$$U(x_t, \lambda_t) \equiv V(x_t, \lambda_t), \tag{2.27}$$

i.e., the internal energy coincides with the potential energy. Consequently, the change in internal energy reads

$$\begin{aligned}\mathrm{d}U[x_t] &= \partial_x V(x, \lambda_t)|_{x=x_t} \circ \dot{x}_t \,\mathrm{d}t + \partial_\lambda V(x_t, \lambda)|_{\lambda=\lambda_t} \dot{\lambda}_t \,\mathrm{d}t \\ &= -F_\mathrm{c}(x_t, \lambda_t) \circ \dot{x}_t \,\mathrm{d}t + \partial_\lambda V(x_t, \lambda)|_{\lambda=\lambda_t} \dot{\lambda}_t \,\mathrm{d}t\,,\end{aligned} \tag{2.28}$$

where $\dot{\lambda}_t \equiv \partial_t \lambda_t$. Here, we used that in the Stratonovich scheme the chain rule can be applied and $\circ$ denotes the Stratonovich product, which has to be interpreted as

$$F_\mathrm{c}(x_{t_i}, \lambda_{t_i}) \circ \dot{x}_{t_i} \,\mathrm{d}t \equiv F_\mathrm{c}([x_i + x_{i-1}]/2, \lambda_{(i-1/2)\Delta t})[x_i - x_{i-1}]. \tag{2.29}$$

We define the work as

$$\delta W[x_t] \equiv f(x_t, \lambda_t) \circ \dot{x}_t \,\mathrm{d}t + \partial_\lambda V(x_t, \lambda)|_{\lambda=\lambda_t} \dot{\lambda}_t \,\mathrm{d}t\,, \tag{2.30}$$

where the first term is the well-known definition of "external force times displacement" and the second term is the definition of work used by Jarzynski [48], which corresponds to change of the external time-dependently evolving potential at fixed particle position. Using Eqs. (2.28) and (2.30) together with the first law in Eq. (2.26) yields the heat

$$\delta Q[x_t] = \delta W[x_t] - \mathrm{d}U[x_t] = F(x_t, \lambda_t) \circ \dot{x}_t \,\mathrm{d}t\,. \tag{2.31}$$

To summarize, along a trajectory $x_t$ of length $T$ work, heat and the change in internal energy are given by

$$W[x_t] = \int_0^T \mathrm{d}t \left[ f(x_t, \lambda_t) \circ \dot{x}_t + \partial_\lambda V(x_t, \lambda)|_{\lambda=\lambda_t} \dot{\lambda}_t \right], \tag{2.32}$$

$$Q[x_t] = \int_0^T \mathrm{d}t\, F(x_t, \lambda_t) \circ \dot{x}_t, \tag{2.33}$$

and

$$\Delta U[x_t] \equiv U(x_T, \lambda_T) - U(x_0, \lambda_0), \tag{2.34}$$

respectively. These three quantities obey the first law $\Delta U[x_t] = W[x_t] - Q[x_t]$. The mean values of Eqs. (2.31)–(2.34) are given by

$$\langle W[x_t] \rangle = \int_0^T \mathrm{d}t \int \mathrm{d}x \left[ f(x, \lambda_t) j(x,t) + \partial_\lambda V(x,\lambda)|_{\lambda=\lambda_t} \dot{\lambda}_t p(x,t) \right], \tag{2.35}$$

$$\langle Q[x_t] \rangle = \int_0^T \mathrm{d}t \int \mathrm{d}x \, F(x, \lambda_t) j(x,t), \tag{2.36}$$

and

$$\langle \Delta U[x_t] \rangle = \int \mathrm{d}x \left[ U(x, \lambda_T) p(x,T) - U(x, \lambda_0) p(x,0) \right], \tag{2.37}$$

respectively.

We note that in a NESS or in a PSS with averages over full periods $\mathcal{T}$, the mean internal energy vanishes and, thus, the mean work coincides with the mean heat. In systems driven into a NESS with periodic boundary conditions, e.g., a driven particle on a ring, the internal energy is typically bounded from below and above. For long observation times $T \to \infty$, this implies that the work coincides with the heat even on a fluctuating trajectory level since the change in internal energy is not time-extensive in contrast to work and heat. Therefore, for such systems observed in the long-time limit, even the fluctuations coincide for these two quantities.

### 2.1.3 *Stochastic entropy and total entropy production*

The second step for a complete description of thermodynamic notions along trajectories is to find proper definitions of entropy production and entropy, which has been first consistently identified in Ref. [7]. Here, the entropy of the system, i.e., of the colloidal particle is defined as the stochastic entropy [1]

$$S_{\mathrm{sys}}[x_t] \equiv -\ln(p(x_t, t)), \tag{2.38}$$

where we assume that there is no intrinsic [2] entropy associated with the particle.

In equilibrium, Eq. (2.38) is given by

$$S_{\mathrm{sys}}[x_t] = \beta \left( V(x_t, \lambda_t) - \mathcal{F}(\lambda_t) \right), \tag{2.39}$$

1 This quantity has to be read as $-\ln(p(x,t)\Delta x)$ with an arbitrary bin size $\Delta x$ to get a dimensionless quantity in the logarithm.

2 For a proper introduction to the definitions of stochastic and intrinsic entropy, see Section 2.2

where we used Eq. (2.9). Here, the second term is the free energy $\mathcal{F}(\lambda_t) \equiv -\ln(Z(\lambda_t))/\beta$. Furthermore, the mean value of Eq. (2.38) coincides with the definition of the non-equilibrium Gibbs entropy

$$\left\langle S_{\text{sys}}[x_t] \right\rangle = -\int \mathrm{d}x\, p(x,t) \ln(p(x,t)). \tag{2.40}$$

To derive an expression for the entropy production, we calculate the change in system entropy given by

$$\mathrm{d}S_{\text{sys}}[x_t] = -\frac{\dot{p}(x_t,t)}{p(x_t,t)}\,\mathrm{d}t + \left[\frac{j(x_t,t)}{Dp(x_t,t)} - \beta F(x_t,\lambda_t)\right] \circ \dot{x}_t\,\mathrm{d}t \tag{2.41}$$

with $\dot{p}(x,t) \equiv \partial_t p(x,t)$. Here, we used the chain rule in the Stratonovich scheme as well as the definition of the current in Eq. (2.6). The third term in Eq. (2.41) is the heat dissipation in the medium $\dot{S}_{\text{med}}[x_t]\,\mathrm{d}t \equiv \beta\delta Q[x_t]$, where the exchanged heat is associated with the increase of entropy in the medium at inverse temperature $\beta$. The total rate of entropy production consists of the change in system entropy (2.41) and the latter mentioned change in medium entropy and, thus, is given by

$$\begin{aligned}\dot{S}_{\text{tot}}[x_t] &\equiv \frac{\mathrm{d}}{\mathrm{d}t} S_{\text{sys}}[x_t] + \dot{S}_{\text{med}}[x_t] \\ &= -\frac{\dot{p}(x_t,t)}{p(x_t,t)} + \frac{j(x_t,t)}{Dp(x_t,t)} \circ \dot{x}_t.\end{aligned} \tag{2.42}$$

We note that the first term vanishes in a NESS and describes the change in the probability distribution due to relaxation from a non-stationary distribution or due to time-dependent driving.

To summarize, the total entropy production along a trajectory $x_t$ of length $T$ is given by

$$\Delta S_{\text{tot}}[x_t] \equiv \int_0^T \mathrm{d}t \left[-\frac{\dot{p}(x_t,t)}{p(x_t,t)} + \frac{j(x_t,t)}{Dp(x_t,t)} \circ \dot{x}_t\right] \tag{2.43}$$

and its mean value divided by $T$ reads

$$\sigma \equiv \frac{1}{T}\left\langle \Delta S_{\text{tot}}[x_t] \right\rangle = \frac{1}{T}\int_0^T \mathrm{d}t \int \mathrm{d}x\, \frac{j^2(x,t)}{Dp(x,t)} \geq 0, \tag{2.44}$$

which is the mean total rate of entropy production. While, in principle, negative total entropy production is possible on a fluctuating trajectory level, the mean total entropy production is always positive and obeys the second law of thermodynamics. We further note that for a system in a NESS or in a PSS averaged over a period $\mathcal{T}$, the mean total rate of entropy production (2.44) coincides with the medium entropy production, i.e., with the heat flux and with the total power since the changes in system entropy and internal energy vanish. Furthermore, in the long-time limit $T \to \infty$, the total entropy production coincides with the dissipated heat and, hence, with the total amount of work

even on a fluctuating trajectory level if the system is in a NESS, in which the internal energy is bounded from below and above.

A second approach of defining entropy production along a trajectory is obtained by measuring the broken time-reversal symmetry of a process [49]. Comparing the path weight for a given trajectory $x_t$ of length $T$ and protocol $\lambda_t$ with the path weight of their time-reversed counter parts $\tilde{x}_t \equiv x_{T-t}$ and $\tilde{\lambda}_t \equiv \lambda_{T-t}$ yields the definition of entropy production

$$\begin{aligned}\Delta S_{\text{tot}}[x_t] &\equiv \ln\left(\frac{\mathcal{P}[x_t;\lambda_t]}{\mathcal{P}[\tilde{x}_t;\tilde{\lambda}_t]}\right)\\ &= \ln\left(\frac{\mathcal{P}[x_t;\lambda_t|x_0]}{\mathcal{P}[\tilde{x}_t;\tilde{\lambda}_t|x_T]}\right) - \ln\left(\frac{p(x_T,T)}{p(x_0,0)}\right)\\ &= \int_0^T \mathrm{d}t\,[\beta F(x_t,\lambda_t)\circ\dot{x}_t] - \ln\left(\frac{p(x_T,T)}{p(x_0,0)}\right),\end{aligned} \tag{2.45}$$

where we explicitly introduced the dependence on the protocol as the second argument. Here, the first term comes from the conditional path weights and is identical to the dissipated heat. The second term is the change in the system entropy. The definition in Eq. (2.45) is equivalent to the expression in Eq. (2.43).

## 2.2 DISCRETE DEGREES OF FREEDOM

In this section, we introduce the framework of stochastic thermodynamics for discrete Markovian systems coupled to a heat bath with inverse temperature $\beta$ [9, 10]. We first consider a closed equilibrated system to build up the concepts that are necessary to obtain a theory for systems out of equilibrium. Then, we split up the closed system into a core system and reservoirs that drive the system out of equilibrium. We show that the dynamics of the core system can be described by a master equation and discuss three distinct choices for the type of dynamics. Analogously to continuous systems, we formulate the first law along a trajectory, define the total entropy production and show that this definition is consistent with the second law.

### 2.2.1 *Closed system and detailed balance*

We consider a closed system in equilibrium coupled to a heat bath with inverse temperature $\beta$. The system in microstate $\xi$ has an energy $H(\xi)$. The free energy, internal energy and entropy are given by

$$\mathcal{F} \equiv -\frac{1}{\beta}\ln\left(\sum_{\xi} e^{-\beta H(\xi)}\right), \tag{2.46}$$

$$U \equiv \partial_\beta\left(\beta\mathcal{F}\right), \tag{2.47}$$

and

$$S \equiv \beta^2 \partial_\beta \mathcal{F} = \beta \left( U - \mathcal{F} \right), \tag{2.48}$$

respectively. We now partition the total phase space into observable mesostates $\{I\}$ such that each microstate corresponds uniquely to a mesostate $\xi \in I$. Since the total system is in equilibrium the probability to find the system in mesostate $I$ is given by

$$p_I^{\text{eq}} = \sum_{\xi \in I} \exp(-\beta \left[ H(\xi) - \mathcal{F} \right]) = \exp(-\beta \left[ \mathcal{F}_I - \mathcal{F} \right]), \tag{2.49}$$

where we defined the free energy of mesostate $I$ as

$$\mathcal{F}_I \equiv -\frac{1}{\beta} \ln \left( \sum_{\xi \in I} e^{-\beta H(\xi)} \right). \tag{2.50}$$

Moreover, we define the internal energy of mesostate $I$ as

$$U_I \equiv \sum_{\xi \in I} H(\xi) p(\xi | I), \tag{2.51}$$

where the conditional probability for microstate $\xi$ given the mesostate $I$ is defined as

$$p(\xi | I) \equiv \exp(-\beta \left[ H(\xi) - \mathcal{F}_I \right]). \tag{2.52}$$

The definition in Eq. (2.51) fulfills $U_I = \partial_\beta (\beta \mathcal{F}_I)$ and, hence, is consistent with definition (2.47). We further define the *intrinsic* entropy [9, 10] of mesostate $I$ as the Shannon entropy of the conditional probability (2.52) given by

$$S_I \equiv S[p(\xi | I)] \equiv -\sum_{\xi \in I} p(\xi | I) \ln(p(\xi | I)), \tag{2.53}$$

which fulfills $S_I = \beta \left( U_I - \mathcal{F}_I \right) = \beta^2 \partial_\beta \mathcal{F}_I$. Beside the intrinsic entropy, there is a contribution of the Shannon entropy of the mesostates given by $S[p_I^{\text{eq}}] \equiv -p_I^{\text{eq}} \ln(p_I^{\text{eq}})$. Thus, the total entropy of the system reads

$$S = \sum_I S_I p_I^{\text{eq}} + S[p_I^{\text{eq}}]. \tag{2.54}$$

Analogously, the total internal energy and total free energy are given by

$$U = \sum_I p_I^{\text{eq}} U_I \tag{2.55}$$

and

$$\mathcal{F} = \sum_I \left( p_I^{\text{eq}} \mathcal{F}_I \right) - \frac{1}{\beta} S[p_I^{\text{eq}}], \tag{2.56}$$

respectively.

So far, we focused on a closed equilibrated system. The definitions of the thermodynamic quantities for a mesostate $I$ in Eqs. (2.50), (2.51) and (2.53) remain valid even if the system is out of equilibrium if we assume that microstates within a mesostate equilibrate much faster than transitions between mesostates occur. As outlined in the previous Chapter 1, this timescale separation implies a Markovian dynamics on a discrete set of mesostates $I$. Thus, the probability to find the system in mesostate $I$ obeys the master equation

$$\partial_t p_I(t) = \sum_J \left( p_J(t) k_{JI} - p_I(t) k_{IJ} \right), \tag{2.57}$$

where $k_{IJ}$ denotes the transition rate from state $I$ to $J$. These transition rates must be chosen in a thermodynamic consistent way. In equilibrium, there is no arrow of time and, hence, the probability to observe a transition from $I$ to $J$ must be equal to the probability from $J$ to $I$. This implies vanishing net currents and leads to the so-called *detailed balance condition* [9, 10, 38]

$$\frac{k_{IJ}}{k_{JI}} = \frac{p_J^{\mathrm{eq}}}{p_I^{\mathrm{eq}}} = \exp(-\beta \Delta_{IJ} \mathcal{F}) \tag{2.58}$$

with the free energy difference $\Delta_{IJ}\mathcal{F} \equiv \mathcal{F}_J - \mathcal{F}_I$ between states $I$ and $J$. We note that the dynamics on the mesostates in Eq. (2.57) hold for relaxation processes towards equilibrium, where the system has been initially prepared in an arbitrary initial condition. Here, every initial distribution will converge to the equilibrium distribution due to the Perron-Frobenius theorem [50].

Lastly, the above considerations can be applied to systems driven by a time-dependent protocol $\lambda_t$ as well if the driving is slow enough to ensure that the microstates within a mesostate still equilibrate. Consequently, internal energy, free energy and entropy become time-dependent through the protocol, i.e., $U_I = U_I(\lambda_t)$, $\mathcal{F}_I = \mathcal{F}_I(\lambda_t)$ and $S_I = S_I(\lambda_t)$. Hence, the transition rates become time-dependent as well and obey [9]

$$\frac{k_{IJ}(\lambda_t)}{k_{JI}(\lambda_t)} = \exp(-\beta \Delta_{IJ} \mathcal{F}(\lambda_t)). \tag{2.59}$$

### 2.2.2 *Open system and local detailed balance*

In the previous section, we focused on a closed system coupled to a heat bath. Now, we split the closed system into several subsystems consisting of the core system of interest and further components like particle reservoirs or a reservoir providing a mechanical force. For example, the core system is a molecular motor stepping along a filament against an external force and powered by an induced enzymatic reaction between solvent particles [9, 40]. Each mesostate

$I$ of the closed system can be uniquely mapped to a state of the core system $i_I$. We assume that each transition between different states of the reservoirs is associated with a transition of the core system. For example, a change in the number of solvents involves always a change of the state of the molecular motor. Thus, we are able to replace the state of the closed system $I$ by the state of the core system $i$. Therefore, we change the notation $IJ \to ij$ and focus on the core system.

Since the core system must be modeled in a thermodynamic consistent way such that the total system eventually reaches equilibrium, the transition rates $k_{ij}(\lambda_t)$ between two states $i$ and $j$ of the core system must fulfill the so-called *local detailed balance condition* [9, 10, 51]

$$\frac{k_{ij}(\lambda_t)}{k_{ji}(\lambda_t)} = \exp\left(-\beta\left[\Delta_{ij}\mathcal{F}(\lambda_t) + \mathcal{A}_{ij}(\lambda_t)\right]\right), \tag{2.60}$$

where we have split the free energy difference of the total system into the free energy difference of the core system $\Delta_{ij}\mathcal{F}(\lambda_t) \equiv \mathcal{F}_j(\lambda_t) - \mathcal{F}_i(\lambda_t)$ and the one of the other reservoirs defined as the driving affinity

$$\mathcal{A}_{ij}(\lambda_t) \equiv f_{ij}(\lambda_t)d_{ij} + \sum_\alpha \mu^{(\alpha)}(\lambda_t)N_{ij}^{(\alpha)} = -\mathcal{A}_{ji}(\lambda_t). \tag{2.61}$$

Here, $f_{ij}(\lambda_t)$ is the force at link $ij$, $d_{ij} = -d_{ji}$ is a length scale, e.g., the distance stepped by the molecular motor, $\mu^{(\alpha)}(\lambda_t)$ is the chemical potential of species $\alpha$ and $N_{ij}^{(\alpha)} = -N_{ji}^{(\alpha)}$ is the change in the number of solvents of species $\alpha$ associated with the transition $i \to j$. The first term in Eq. (2.61) is associated with the free energy difference due to the mechanical force, whereas the second term corresponds to the free energy differences of the particle reservoirs. With the rates fulfilling Eq. (2.60), the dynamics of the probability $p_i(t)$ to find the core system in state $i$ at time $t$ obeys the master equation

$$\partial_t p_i(t) = -\sum_j j_{ij}(t) \tag{2.62}$$

with probability current

$$j_{ij}(t) \equiv p_i(t)k_{ij}(\lambda_t) - p_j(t)k_{ji}(\lambda_t) \tag{2.63}$$

between states $i$ and $j$. Equivalently, the master equation (2.62) can be written as

$$\partial_t \mathbf{p}(t) = \mathbf{L}(\lambda_t)\mathbf{p}(t), \tag{2.64}$$

where $\mathbf{p}(t)$ is a vector with entries $p_i(t)$ and $\mathbf{L}(\lambda_t)$ is a matrix with elements $L_{ij}(\lambda_t) \equiv k_{ji}(\lambda_t) - \sum_j k_{ij}(\lambda_t)\delta_{i,j}$. An example for such a discrete system is the three-state system shown in Fig. 2.2.

We now discuss three distinct choices of the rates leading to three special probability distributions. First, for a constant protocol $\lambda_t = \lambda$

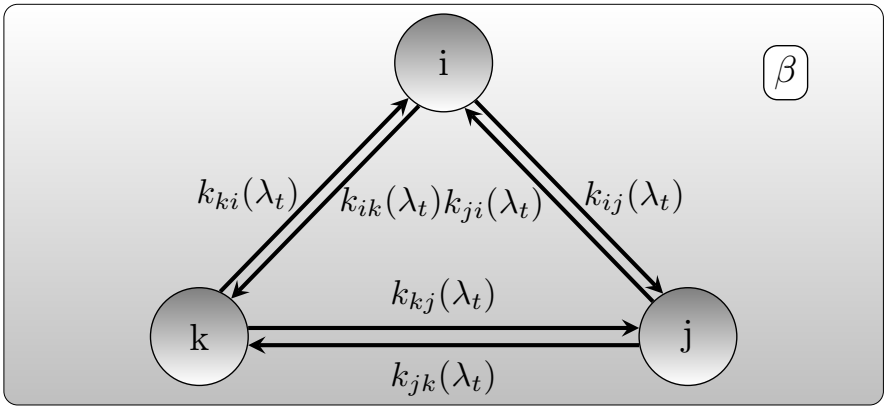


Figure 2.2: Schematic of a Markovian network consisting of three discrete states $i, j$ and $k$ coupled to a heat bath with temperature $\beta$. The transition rates are time-dependent through the protocol $\lambda_t$.

and a vanishing affinity $\mathcal{A}_{ij}(\lambda) = 0$, the system will reach equilibrium and, thus, the probability is given by

$$p_i^{\mathrm{eq}}(\lambda) \equiv \exp(-\beta\left[\mathcal{F}_i - \mathcal{F}(\lambda)\right]) \tag{2.65}$$

with total free energy of the system $\mathcal{F}(\lambda)$. Second, for a constant protocol $\lambda_t = \lambda$ but a non-vanishing affinity $\mathcal{A}_{ij}(\lambda) \neq 0$ and in the case of the existence of at least one cycle in the network topology, the system will reach a NESS in the long-time limit fulfilling the Eigenvalue equation

$$\mathbf{L}(\lambda)\mathbf{p}^{\mathrm{s}}(\lambda) = 0, \tag{2.66}$$

from which we can determine the steady-state probability $p_i^{\mathrm{s}}(\lambda)$. Here, the stationary net currents $j_{ij}^{\mathrm{s}}(\lambda) \neq 0$ do not vanish since the system is driven out of equilibrium by the driving affinity. For example, if a driving affinity is applied into the clockwise direction to the network shown in Fig. 2.2, the system is able to reach a NESS at constant $\lambda_t = \lambda$ with non-vanishing probability currents. Third, for periodic driving $\lambda_t = \lambda(\Omega t) = \lambda(\Omega\left[t + \mathcal{T}\right])$ with frequency $\Omega$ and period $\mathcal{T}$, the system will reach a periodic steady-state

$$p_i^{\mathrm{ps}}(t) = p_i^{\mathrm{ps}}(t + \mathcal{T}), \tag{2.67}$$

which is periodic in time and has the same period as the driving. The periodic steady-state distribution can be determined by using the Eigenvalue equation

$$\overrightarrow{\exp}\left(\int_0^{\mathcal{T}} \mathrm{d}t\, \mathbf{L}(\lambda_t)\right) \mathbf{p}^{\mathrm{ps}}(0) = \mathbf{p}^{\mathrm{ps}}(0), \tag{2.68}$$

where $\overrightarrow{\exp}\left(\cdot\right)$ denotes the time-ordered exponential. We note that the matrix on the l.h.s of Eq. (2.68) can be calculated by solving the master equation over a full period $\mathcal{T}$ for the initial conditions $p_i(0) = \delta_{i,\alpha}$.

Here, for each index $\alpha$ the solution of the master equation at time $\mathcal{T}$ yields one column of the matrix in Eq. (2.68). This scheme is especially useful to determine the PSS numerically.

### 2.2.3 *First law*

In stochastic thermodynamics, observables like work, heat and internal energy can be identified along a single fluctuating trajectory $n_t$ consisting of a discrete set of states visited at different times. The first law along such a discrete trajectory reads

$$\mathrm{d}U_{n_t}(\lambda_t) = \delta W[n_t] - \delta Q[n_t], \tag{2.69}$$

where $\mathrm{d}U_{n_t}(\lambda_t)$ is the change in internal energy, $\delta W[n_t]$ is the work and $\delta Q[n_t]$ denotes the heat. The internal energy along a trajectory $U_{n_t}(\lambda_t) \equiv \sum_j \delta_{n_t,j} U_j(\lambda_t)$ is a fluctuating quantity, where $\delta_{n_t,j}$ denotes the Kronecker-delta, which is 1, if state $j$ is occupied and 0, otherwise. The change in internal energy is given by

$$\mathrm{d}U_{n_t}(\lambda_t) = \sum_j \left[\dot{\delta}_{n_t,j} U_j(\lambda_t)\right] \mathrm{d}t + \dot{\lambda}_t \partial_\lambda U_{n_t}(\lambda)|_{\lambda=\lambda_t}\, \mathrm{d}t\,, \tag{2.70}$$

where $\dot{\delta}_{n_t,j}$ and $\dot{\lambda}_t$ denote the time derivatives of the Kronecker-delta and of the protocol, respectively. The work along a trajectory is defined as

$$\delta W[n_t] \equiv \sum_{i,j} \left[\mathcal{A}_{ij}(\lambda_t)\dot{m}_{ij}(t)\right] \mathrm{d}t + \dot{\lambda}_t \partial_\lambda \mathcal{F}_{n_t}(\lambda)|_{\lambda=\lambda_t}\, \mathrm{d}t\,, \tag{2.71}$$

where $m_{ij}(t)$ is the the total number of transitions from state $i$ to $j$ up to time $t$ and $\dot{m}_{ij}(t) \equiv \partial_t m_{ij}(t)$ is its time-derivative. The two variables $\delta_{n_t,i}$ and $m_{ij}(t)$ are connected through the relation $\dot{\delta}_{n_t,i} = -\sum_j [\dot{m}_{ij}(t) - \dot{m}_{ji}(t)]$. A schematic illustrating these variables is shown in Fig. 2.3. The first term in Eq. (2.71) arises due to the affinity $\mathcal{A}_{ij}(\lambda_t)$, which corresponds to, e.g., the product of a non-conservative force and the traveled distance along the transition $i \to j$. The second term is associated with the time-dependent change of the free energy through the protocol and corresponds to the definition of work of Jarzynski [48]. Inserting Eqs. (2.70) and (2.71) into the first law (2.69) yields the heat

$$\delta Q[n_t] = \sum_{i,j} \left[\mathcal{A}_{ij}(\lambda_t)\dot{m}_{ij}(t)\right] \mathrm{d}t - \sum_j \dot{\delta}_{n_t,j} \mathcal{F}_j(\lambda_t)\, \mathrm{d}t - \mathrm{d}S_{n_t}(\lambda_t)/\beta \tag{2.72}$$

with the change in intrinsic entropy

$$\mathrm{d}S_{n_t}(\lambda_t) \equiv \sum_j \left[\dot{\delta}_{n_t,j} S_j(\lambda_t)\right] \mathrm{d}t + \dot{\lambda}_t \partial_\lambda S_{n_t}(\lambda)|_{\lambda=\lambda_t}\, \mathrm{d}t\,, \tag{2.73}$$

where we used the relation $S_{n_t}(\lambda) = \beta\,[U_{n_t}(\lambda_t) - \mathcal{F}_{n_t}(\lambda_t)]$. Equation (2.72) shows that heat is not only exchanged when a transition

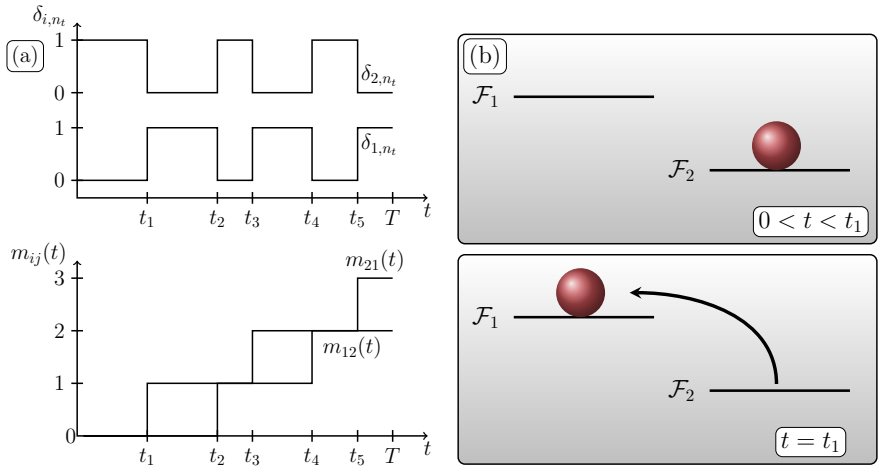


Figure 2.3: Schematic of the variables $\delta_{i,n_t}$ and $m_{ij}(t)$ (a) for a paradigmatic two-level system (b). For $0 < t < t_1$ the particle occupies state 2. Thus, the variables describing the occupation are given by $\delta_{2,n_t} = 1$ and $\delta_{1,n_t} = 0$ for $0 < t < t_1$. At time $t = t_1$ the particle jumps from state 2 to 1. Here, the variable describing the transitions $m_{21}(t_1)$ increases by 1, whereas the occupation quantities change their values accordingly.

between different states occurs but also when the system stays in a certain state since the intrinsic entropy is time-dependent through an external protocol.

To summarize, along a trajectory $n_t$ of length $T$ work and heat are given by

$$W[n_t] = \int_0^T \mathrm{d}t \left( \sum_{i,j} \left[ \mathcal{A}_{ij}(\lambda_t) \dot{m}_{ij}(t) \right] + \dot{\lambda}_t \partial_\lambda \mathcal{F}_{n_t}(\lambda)|_{\lambda=\lambda_t} \right), \quad (2.74)$$

and

$$Q[n_t] = \int_0^T \mathrm{d}t \left( \sum_{i,j} \left[ \mathcal{A}_{ij}(\lambda_t) + \Delta_{ij} \mathcal{F}(\lambda_t) \right] \dot{m}_{ij}(t) \right) - \Delta S[n_t]/\beta, \quad (2.75)$$

respectively, where $\Delta S[n_t] \equiv S_{n_T}(\lambda_T) - S_{n_0}(\lambda_0)$ is the change in intrinsic entropy. To derive Eq. (2.75), we used the relation $\dot{\delta}_{n_t,i} = -\sum_j [\dot{m}_{ij}(t) - \dot{m}_{ji}(t)]$. The change in internal energy reads

$$\Delta U[n_t] \equiv U_{n_T}(\lambda_T) - U_{n_0}(\lambda_0). \quad (2.76)$$

The definitions in Eqs. (2.74)–(2.76) obey the first law, i.e., $\Delta U[n_t] = W[n_t] - Q[n_t]$ and their mean values are given by

$$\langle W[n_t]\rangle = \int_0^T \mathrm{d}t \left( \sum_{i>j} \mathcal{A}_{ij}(\lambda_t) j_{ij}(t) + \sum_i \dot{\lambda}_t \partial_\lambda \mathcal{F}_i(\lambda)|_{\lambda=\lambda_t} p_i(t) \right), \tag{2.77}$$

$$\langle Q[n_t]\rangle = \int_0^T \mathrm{d}t \left( \sum_{i>j} \ln\left(\frac{k_{ij}(\lambda_t)}{k_{ji}(\lambda_t)}\right) j_{ij}(t) \right) - \sum_i \left[ S_i(\lambda_T) p_i(T) - S_i(\lambda_0) p_i(0) \right] / \beta, \tag{2.78}$$

and

$$\langle U[n_t]\rangle = \sum_i \left[ U_i(\lambda_T) p_i(T) - U_i(\lambda_0) p_i(0) \right], \tag{2.79}$$

respectively. Here, we used

$$\langle \delta_{n_t,i} \rangle = p_i(t), \tag{2.80}$$

$$\langle \dot{m}_{ij}(t) \rangle = p_i(t) k_{ij}(\lambda_t), \tag{2.81}$$

the local detailed balance relation (2.60) and $O_{n_t}(\lambda_t) = \sum_i \delta_{n_t,i} O_i(\lambda_t)$ for an arbitrary state variable $O_i(\lambda_t)$.

We note that in a NESS or PSS with averages over full periods, the internal energy difference vanishes after averaging over all trajectories. Moreover, the fluctuating internal energy difference can be neglected in the long-time limit $T \to \infty$ since it is not time-extensive. In these cases, the heat is identical to the work. Furthermore, in simple models one often assumes vanishing (or at least state- and time-independent) intrinsic entropy values since intrinsic entropy arises due to, e.g., coarse graining procedures of complex models with hidden degrees of freedom. Then, the free energy coincides with internal energy $\mathcal{F}_{n_t}(\lambda_t) = U_{n_t}(\lambda_t)$ and the last term in Eqs. (2.75) and (2.78) vanishes. For the models discussed in this thesis, we will assume such vanishing intrinsic entropy values.

### 2.2.4 *Entropy production*

We define the entropy of the system along a trajectory as

$$S_{\mathrm{sys}}[n_t] \equiv S_{n_t}(\lambda_t) - \ln(p_{n_t}(t)), \tag{2.82}$$

where the first contribution is the intrinsic entropy and the second one is the so-called *stochastic entropy* [7, 9]. While the intrinsic entropy arises from internal or hidden degrees of freedom within a mesostate, the stochastic entropy is the contribution of the observable mesostates.

The total entropy production is defined as

$$\dot{S}_{\mathrm{tot}}[n_t] \equiv \dot{S}_{\mathrm{med}}[n_t] + \frac{\mathrm{d}}{\mathrm{d}t} S_{\mathrm{sys}}[n_t] \tag{2.83}$$

with the medium entropy production rate $\dot{S}_{\mathrm{med}}[n_t]\,\mathrm{d}t \equiv \beta\delta Q[n_t]$. Using the time-derivative of the stochastic entropy

$$\frac{\mathrm{d}}{\mathrm{d}t}S_{\mathrm{sys}}[n_t] = -\sum_i \delta_{n_t,i}\frac{\dot{p}_i(t)}{p_i(t)} - \sum_{i,j}\dot{m}_{ij}(t)\ln\left(\frac{p_j(t)}{p_i(t)}\right) + \frac{\mathrm{d}}{\mathrm{d}t}S_{n_t}(\lambda_t) \quad (2.84)$$

together with Eq. (2.75), leads to the total entropy production

$$\Delta S_{\mathrm{tot}}[n_t] = \int_0^T \mathrm{d}t\left(\sum_{i,j}\ln\left(\frac{p_i(t)k_{ij}(\lambda_t)}{p_j(t)k_{ji}(\lambda_t)}\right)\dot{m}_{ij}(t) - \sum_i \delta_{n_t,i}\frac{\dot{p}_i(t)}{p_i(t)}\right). \quad (2.85)$$

Thus, the mean total entropy production rate is given by

$$\sigma \equiv \frac{1}{T}\left\langle \Delta S_{\mathrm{tot}}[n_t]\right\rangle = \frac{1}{T}\int_0^T \mathrm{d}t\sum_{i>j} j_{ij}(t)\ln\left(\frac{p_i(t)k_{ij}(\lambda_t)}{p_j(t)k_{ji}(\lambda_t)}\right) \geq 0, \quad (2.86)$$

where we used Eqs. (2.80) and (2.81). The expression of the mean total entropy production rate in Eq. (2.86) is always positive and, thus, is consistent with the second law of thermodynamics. We further note that in a NESS or a PSS with averages over full periods, the contribution of the change in system entropy in Eq. (2.85) vanishes in the long-time limit or after averaging over all trajectories. Thus, in these cases the total entropy production is identical to the medium entropy production.

Beside the definition in Eq. (2.83), entropy production can be defined as a measure of breaking the time-reversal symmetry [49]. This definition requires the introduction of a path weight $\mathcal{P}[n_t]$ for a discrete trajectory $n_t$ of length $T$. For a Markovian system obeying the master equation (2.62), the path weight is defined as

$$\mathcal{P}[n_t] \equiv p_{n_0}(0)\exp\left(-\int_0^T \mathrm{d}t\sum_i \delta_{n_t,i}r_i(\lambda_t)\right)\prod_{l=1}^{m(T)} k_{n_{t_l^-}n_{t_l^+}}(\lambda_{t_l}), \quad (2.87)$$

where $r_i(\lambda_t) \equiv \sum_j k_{ij}(\lambda_t)$ denotes the exit rate of state $i$, $m(T) \equiv \sum_{ij} m_{ij}(T)$ is the total number of transitions and $n_{t_l^-}$ and $n_{t_l^+}$ are the states before and after a transition at time $t_l$, respectively. The first term in Eq. (2.87) corresponds to the probability to stay in a certain state, which decays exponentially in the residence time. The second term is associated with the transition probabilities between different states. We can rewrite Eq. (2.87) in terms of the trajectory dependent variables $\delta_{n_t,i}$ and $m_{ij}(t)$ as

$$\mathcal{P}[n_t] \equiv p_{n_0}(0)k_0^{m(T)}\exp\left(\int_0^T \mathrm{d}t\sum_{i,j}\left[-\delta_{n_t,i}k_{ij}(\lambda_t) + \dot{m}_{ij}(t)\ln\left(\frac{k_{ij}(\lambda_t)}{k_0}\right)\right]\right) \quad (2.88)$$

by introducing an arbitrary irrelevant inverse timescale $k_0$. The definition of entropy production as a measure of breaking time-reversal

symmetry is given by the log-ratio between the path weight $\mathcal{P}[n_t;\lambda_t]$ and the path weight $\mathcal{P}[\tilde{n}_t;\tilde{\lambda}_t]$ for the time-reversed trajectory $\tilde{n}_t = n_{T-t}$ and protocol $\tilde{\lambda}_t = \lambda_{T-t}$. Here, we explicitly introduced the dependence on the protocol as the second argument. Using $\delta_{\tilde{n}_t,i} = \delta_{n_{T-t},i}$ and $\dot{\tilde{m}}_{ij}(t) = \dot{m}_{ji}(T-t)$ for the time-reversed trajectory-dependent quantities in Eq. (2.88) yields

$$\begin{aligned}\Delta S_{\mathrm{tot}}[n_t] &\equiv \ln\left(\frac{\mathcal{P}[n_t;\lambda_t]}{\mathcal{P}[\tilde{n}_t;\tilde{\lambda}_t]}\right)\\ &= \int_0^T \mathrm{d}t\left[\ln\left(\frac{k_{ij}(\lambda_t)}{k_{ji}(\lambda_t)}\right)\dot{m}_{ij}(t)\right] - \ln\left(\frac{p_{n_T}(T)}{p_{n_0}(0)}\right),\end{aligned} \tag{2.89}$$

which is equivalent to Eq. (2.85).

# 3

# OBSERVABLES AND THEIR FLUCTUATIONS

In the last chapter, we have introduced observables like work, heat and entropy production. Their time-averages, i.e., the power, heat flux and entropy production rate are current-type observables, which are odd under time-reversal. Moreover, we have defined quantities like internal energy or intrinsic entropy, which are state variables. Their time-averages depend on the time spent in a certain state and, thus, they can be even under time-reversal and should be clearly distinguished from current-type observables. In this chapter, we will define arbitrary current observables and state variables for continuous and discrete systems [2, 3]. To quantify their fluctuations, we will introduce the diffusion coefficient and the SCGF.

## 3.1 OBSERVABLES

A general current observable for continuous and discrete systems is given by

$$J[x_t] \equiv \frac{1}{T}\int_0^T \mathrm{d}t \left( d^{\mathrm{I}}(x_t,\lambda_t) \circ \dot{x}_t + \dot{\lambda}_t \partial_\lambda d^{\mathrm{II}}(x_t,\lambda)|_{\lambda=\lambda_t} \right) \tag{3.1}$$

and

$$J[n_t] \equiv \frac{1}{T}\int_0^T \mathrm{d}t \left( \sum_{ij} d^{\mathrm{I}}_{ij}(\lambda_t)\dot{m}_{ij}(t) + \sum_i \dot{\lambda}_t \partial_\lambda d^{\mathrm{II}}_i(\lambda)|_{\lambda=\lambda_t}\delta_{n_t,i} \right), \tag{3.2}$$

respectively, where $d^{\mathrm{I}}(x_t,\lambda_t)$, $d^{\mathrm{II}}(x_t,\lambda_t)$, $d^{\mathrm{I}}_{ij}(\lambda_t) = -d^{\mathrm{I}}_{ji}(\lambda_t)$ and $d^{\mathrm{II}}_i(\lambda_t)$ are arbitrary increments. A paradigm for such a current observable is the work defined in Eqs. (2.32) and (2.74) with increments $d^{\mathrm{I}}(x,\lambda_t) = f(x,\lambda_t)$, $d^{\mathrm{II}}(x,\lambda_t) = V(x,\lambda_t)$ and $d^{\mathrm{I}}_{ij}(\lambda_t) = \mathcal{A}_{ij}(\lambda_t)$, $d^{\mathrm{II}}_i(\lambda_t) = \mathcal{F}_i(\lambda_t)$, respectively. The mean values of the currents in Eqs. (3.1) and (3.2) are given by

$$\begin{aligned} J(T) &\equiv \langle J[x_t]\rangle \\ &= \frac{1}{T}\int_0^T \mathrm{d}t \int \mathrm{d}x \left( d^{\mathrm{I}}(x,\lambda_t) j(x,t) + \dot{\lambda}_t \partial_\lambda d^{\mathrm{II}}(x,\lambda)|_{\lambda=\lambda_t} p(x,t) \right) \end{aligned} \tag{3.3}$$

and

$$J(T) \equiv \langle J[n_t] \rangle = \frac{1}{T} \int_0^T \mathrm{d}t \left( \sum_{i>j} d_{ij}^{\mathrm{I}}(\lambda_t) j_{ij}(t) + \sum_i \dot{\lambda}_t \partial_\lambda d_i^{\mathrm{II}}(\lambda)|_{\lambda=\lambda_t} p_i(t) \right), \tag{3.4}$$

respectively.

A general state observable for continuous and discrete systems reads

$$A[x_t] \equiv \frac{1}{T} \int_0^T \mathrm{d}t \left( a^{\mathrm{I}}(x_t, \lambda_t) \right) + a^{\mathrm{II}}(x_T, \lambda_T) \tag{3.5}$$

and

$$A[n_t] \equiv \frac{1}{T} \int_0^T \mathrm{d}t \left( \sum_i a_i^{\mathrm{I}}(\lambda_t) \delta_{n_t,i} \right) + \sum_i a_i^{\mathrm{II}}(\lambda_T) \delta_{n_T,i}, \tag{3.6}$$

respectively, where $a^{\mathrm{I}}(x_t, \lambda_t)$, $a^{\mathrm{II}}(x_t, \lambda_t)$, $a_i^{\mathrm{I}}(\lambda_t)$ and $a_i^{\mathrm{II}}(\lambda_t)$ are arbitrary increments that cannot be written as a time-derivative. Examples for such quantities are the time spent in a set of certain states, the time-averaged or instantaneous internal energy and intrinsic entropy. The mean values of the state observables in Eqs. (3.5) and (3.6) are given by

$$A(T) \equiv \langle A[x_t] \rangle = \frac{1}{T} \int_0^T \mathrm{d}t \int \mathrm{d}x \left( a^{\mathrm{I}}(x, \lambda_t) p(x,t) \right) + \int \mathrm{d}x \, a^{\mathrm{II}}(x, \lambda_T) p(x,T) \tag{3.7}$$

and

$$A(T) \equiv \langle A[n_t] \rangle = \frac{1}{T} \int_0^T \mathrm{d}t \left( \sum_i a_i^{\mathrm{I}}(\lambda_t) p_i(t) \right) + \sum_i a_i^{\mathrm{II}}(\lambda_T) p_i(T), \tag{3.8}$$

respectively.

## 3.2 FLUCTUATIONS

We now quantify fluctuations for the observables defined in Eqs. (3.1), (3.2), (3.5) and (3.6). The first observable that quantifies fluctuations is the diffusion coefficient

$$D_X(T) \equiv \frac{T}{2} \mathrm{Var}(X[\Gamma_t]) \tag{3.9}$$

with the variance $\mathrm{Var}(X[\Gamma_t]) \equiv \langle X^2[\Gamma_t] \rangle - \langle X[\Gamma_t] \rangle^2$ of an arbitrary current observable or state variable $X \in \{A[\Gamma_t], J[\Gamma_t]\}$ along a continuous

or discrete trajectory $\Gamma_t \in \{x_t, n_t\}$ of length $T$. A large diffusion coefficient in Eq. (3.9) indicates large absolute fluctuations, whereas the precision $\mathfrak{p}(T) \equiv (T \langle X[\Gamma_t] \rangle^2)/D_X(T)$ of an observable $X[\Gamma_t]$ quantifies the inverse relative fluctuations. For example, choosing as an observable the output power $X[\Gamma_t] = P_{\text{out}}$ of a heat engine, the precision is a measure of how "reliable" the machine will work. Time-integrated current observables or state variables are time-extensive variables, where the variances of such quantities have typically a diffusive scaling. Thus, in the long-time limit, the diffusion coefficient of such quantities is of order 1 in time.

Beside the diffusion coefficient, the SCGF

$$\lambda_T(z) \equiv \frac{1}{T} \ln \left\langle e^{zTX[\Gamma_t]} \right\rangle , \tag{3.10}$$

quantifies fluctuations completely on an ensemble level of trajectories, where the derivatives at $z = 0$ yield the cumulants of the observable $X[\Gamma_t]$. For example, the first two derivatives at $z = 0$ are given by

$$\partial_z \lambda_T(z)|_{z=0} = \langle X[\Gamma_t] \rangle , \tag{3.11}$$

$$\partial_z^2 \lambda_T(z)|_{z=0} = 2D_X(T), \tag{3.12}$$

i.e., the first two cumulants are the mean value and the diffusion coefficient of the observable $X[\Gamma_t]$. We note that the SCGF in Eq. (3.10) is the Legendre-Fenchel transformation of the large deviation function (LDF) [52], which describes the exponential decay of the probability to observe a value of an observable in the long-time limit.

# 4 THE THERMODYNAMIC UNCERTAINTY RELATION

Recent progresses in the field of non-equilibrium statistical physics have reshaped our perspective on conventional thermodynamic notions such as work, heat or entropy production. Defining these thermodynamic observables along single fluctuating trajectories is the key step to build up the theoretical formalism of stochastic thermodynamics [8, 36, 53, 54]. As a key property of these small mesoscopic systems fluctuations and their relation to universal non-equilibrium properties are of special interest from a theoretical as well as from an operational or experimental point of view. A well-established paradigm for such a connection is the fluctuation-dissipation theorem (FDT) relating equilibrium fluctuations to the dissipation rate in driven systems near equilibrium [55]. Milestones in the field of stochastic thermodynamics *inter alia* deal with similar connections for systems *far away* from equilibrium: from fluctuation theorems [48, 56–64] and generalizations of the FDT [65–69] to the Harada-Sasa relation connecting the violation of the FDT to energy dissipation [70, 71].

## 4.1 STEADY-STATE UNCERTAINTY RELATION

A more recent development in this lineup is the so-called TUR, which connects the fluctuations or precision of *any* current in the system to the total entropy production rate. For an overdamped Langevin system or a Markovian system on a discrete set of states driven into a NESS the thermodynamic uncertainty relation for finite observation times $T$ reads

$$D_J(T)\sigma(T)/J(T)^2 \geq 1 \tag{4.1}$$

with current $J(T)$, its diffusion coefficient $D_J(T)$ quantifying fluctuations and the total entropy production rate $\sigma(T)$. In a steady state the current and the entropy production do not depend on the observation time, i.e., $J(T) = J$ and $\sigma(T) = \sigma$. However, the diffusion coefficients $D_J(T)$ are in general time-dependent for finite observation times. From the uncertainty relation in (4.1) follows that a higher precision, i.e., a lower uncertainty, inevitably requires a larger amount of entropy production. Thus, a high precision comes always along with a minimum thermodynamic cost.

The TUR has been originally conjectured in Ref. [27] and subsequently proven in Ref. [28] via the large deviation formalism in the long-time limit. It has been generalized to steady-state systems observed for finite times in Refs. [72, 73]. Moreover, recent research

re-derived the TUR using virtual perturbing forces [74, 75] or information theoretic bounds [76, 77]. These methods have the advantage that they hold for finite-observation times and are more accessible to a general physicist than the specialized mathematical formalism of large deviation theory. For example, in Ref. [75] the authors derive the so-called fluctuation-response inequality (FRI). The FRI has been derived using perturbing forces and, thus, shows similarities to the FDT. In contrast, the FRI is an *inequality* and not an *equality* like the FDT and provides a template for a proof of several TUR-like inequalities and of the TUR itself.

As a trade-off relation between precision and dissipation, the TUR has led to a variety of applications like bounds on the efficiency of biological processes or molecular machines [29, 78, 79], optimal design principles for self-assembly [80] or constraints on time windows in anomalously diffusing systems [81]. Moreover, beside more sophisticated methods [82–85], the TUR has been established as a useful tool for inferring entropy production [86–89]. To profit from these promising applications and tools in more complex systems, numerous attempts have been made to extend the range of applicability of the TUR including underdamped dynamics [32, 33, 76, 90–95], ballistic transport between different terminals [96], heat engines [29, 97–99], periodic driving [4, 30, 100, 101], stochastic field theories [102, 103], generalizations to observables that are even under time-reversal [104–106], first-passage time problems [107–109] and quantum systems [96, 110–119]. Moreover, several works have focused on comparing the quality of different uncertainty relations [120] and on the optimal choice of observables [121–123].

## 4.2 PROOF

In this section, we present a simple proof of the thermodynamic uncertainty relation that has been used similarly in Refs. [124, 125]. This proof is solely based on the Cauchy-Schwarz inequality and is equivalent to other methods using the linear response FRI in Ref. [75] and the Cramèr-Rao inequality [77, 124, 126]. Moreover, it provides a template for proving further thermodynamic inequalities like kinetic uncertainty relations [106, 108, 109].

We consider a system passing a trajectory $\Gamma_t$ of length $T$ and obeying, e.g., a Markovian dynamics on a discrete set of states or a continuous Langevin equation. We denote the path weight for a discrete or continuous trajectory $\Gamma_t \in \{n_t, x_t\}$ as $\mathcal{P}[\Gamma_t]$, where $n_t$ denotes a discrete and $x_t$ a continuous trajectory. Mean values in this dynamics are denoted by $\langle\cdot\rangle$. For deriving the TUR in a NESS, we introduce an auxiliary path weight $\mathcal{P}^\dagger[\Gamma_t;\epsilon]$, which describes a perturbed system. The parameter $\epsilon$ controls the perturbation and is chosen such that $\mathcal{P}^\dagger[\Gamma_t,\epsilon=0]=\mathcal{P}[\Gamma_t]$, i.e., for $\epsilon=0$ the perturbed dynamics coincides

with the original dynamics. Mean values in the perturbed dynamics are denoted by $\langle\cdot\rangle^\dagger$.

The deviation of the mean value of a fluctuating current $J[\Gamma_t]$ in the perturbed dynamics from the mean value in the original dynamics can be written as

$$\langle J[\Gamma_t]\rangle^\dagger - \langle J[\Gamma_t]\rangle = \langle J[\Gamma_t]C[\Gamma_t;\epsilon]\rangle \tag{4.2}$$

with

$$C[\Gamma_t;\epsilon] \equiv \left(\frac{\mathcal{P}^\dagger[\Gamma_t;\epsilon]}{\mathcal{P}[\Gamma_t]} - 1\right) \tag{4.3}$$

by using the Radon-Nikodým derivative and assuming that $\mathcal{P}^\dagger[\Gamma_t,\epsilon]$ is absolutely continuous with respect to $\mathcal{P}[\Gamma_t]$ [127]. Since $\langle C[\Gamma_t;\epsilon]\rangle = \langle \mathcal{P}^\dagger[\Gamma_t;\epsilon]/\mathcal{P}[\Gamma_t] - 1\rangle = 0$, we can rewrite Eq. (4.2) in terms of a covariance, i.e.,

$$\langle J[\Gamma_t]\rangle^\dagger - \langle J[\Gamma_t]\rangle = \mathrm{Cov}\left(J[\Gamma_t], C[\Gamma_t;\epsilon]\right). \tag{4.4}$$

For small $\epsilon \to 0$, the response of the current $J[\Gamma_t]$ is defined as

$$\Delta J(T) \equiv \lim_{\epsilon\to 0}\left(\langle J[\Gamma_t]\rangle^\dagger - \langle J[\Gamma_t]\rangle\right)/\epsilon = \mathrm{Cov}\left(J[\Gamma_t], \partial_\epsilon C[\Gamma_t;\epsilon]|_{\epsilon=0}\right) \tag{4.5}$$

with $\partial_\epsilon C[\Gamma_t;\epsilon]|_{\epsilon=0} = \partial_\epsilon \mathcal{P}^\dagger[\Gamma_t;\epsilon]|_{\epsilon=0}/\mathcal{P}[\Gamma_t]$. Using the Cauchy-Schwarz inequality, we finally get

$$\Delta J(T)^2 \leq D_J(T)\mathcal{C}(T) \tag{4.6}$$

with the diffusion coefficient of the current $D_J(T) = T\mathrm{Var}\left(J[\Gamma_t]\right)/2$ and the cost term

$$\mathcal{C}(T) \equiv \frac{2}{T}\left\langle \left(\partial_\epsilon C[\Gamma_t;\epsilon]|_{\epsilon=0}\right)^2\right\rangle. \tag{4.7}$$

We note that Eq. (4.6) is formally equivalent to the Cramèr-Rao inequality, where the cost term is associated with the Fisher-information [77, 124, 126]. Furthermore, the inequality (4.6) is widely applicable for numerous types of dynamics and several TURs or similar thermodynamic inequalities can be derived from this inequality [91, 92, 94, 95, 106, 109, 126, 128]. To derive the TUR in a NESS, we have to specify the auxiliary dynamics. While, in principle, it is sufficient to prove the TUR for systems with discrete states, since continuous systems can be described by a suitable fine discretization scheme, we now show derivations for both, discrete and continuous systems.

### 4.2.1 *Continuous systems*

First, we prove the TUR for systems in a NESS obeying a one-dimensional overdamped Langevin equation (2.1) with a constant protocol $\lambda_t = \lambda$.

We denote the force of the original system as $F(x_t) \equiv F(x_t, \lambda)$, where $x_t$ is the continuous trajectory of the particle. We assume that the auxiliary dynamics describes a perturbed system with force $F^\dagger(x_t;\epsilon) = F(x_t) + \epsilon F_{\text{pert}}(x_t)$, where $F_{\text{pert}}(x_t)$ is an arbitrary perturbing force. We further assume that the original system and the perturbed system are in the stationary states $p^{\text{s}}(x)$ and $p^{\text{s},\dagger}(x;\epsilon)$, respectively. Obviously, when setting $\epsilon = 0$ the force is given by $F^\dagger(x_t;\epsilon = 0) = F(x_t)$ and the densities coincide, i.e., $p^{\text{s},\dagger}(x;\epsilon = 0) = p^{\text{s}}(x)$.

The mean value of a generalized time-integrated current in the auxiliary dynamics reads

$$\langle J[x_t]\rangle^\dagger \equiv \int \mathrm{d}x\, d(x) \left[\mu F^\dagger(x;\epsilon) - D\partial_x\right] p^{\text{s},\dagger}(x;\epsilon) \equiv \int \mathrm{d}x\, d(x) j^{\text{s},\dagger}(x;\epsilon), \tag{4.8}$$

where $d(x)$ is an arbitrary increment and $j^{\text{s},\dagger}(x;\epsilon)$ is the probability current in the auxiliary dynamics. For $\epsilon = 0$, the current in Eq. (4.8) coincides with the current in the original dynamics, which is given by

$$\langle J[x_t]\rangle \equiv \int \mathrm{d}x\, d(x) \left[\mu F(x) - D\partial_x\right] p^{\text{s}}(x) \equiv \int \mathrm{d}x\, d(x) j^{\text{s}}(x) \tag{4.9}$$

with $j^{\text{s}}(x)$ the probability current in the original dynamics. We now choose the perturbing force

$$F_{\text{pert}}(x) = j^{\text{s}}(x)/p^{\text{s}}(x), \tag{4.10}$$

which leads to a time-rescaled process with $t \to (1+\epsilon)t$. This perturbation leaves the stationary state unchanged, i.e., $p^{\text{s},\dagger}(x;\epsilon) = p^{\text{s}}(x)$ and scales the current like $j^{\text{s},\dagger}(x;\epsilon) = (1+\epsilon) j^{\text{s}}(x)$. Consequently, the generalized current in Eq. (4.8) becomes $\langle J[x_t]\rangle^\dagger = (1+\epsilon)\langle J[x_t]\rangle$. Hence, the response in Eq. (4.5) is given by

$$\Delta J = \langle J[x_t]\rangle \equiv J \tag{4.11}$$

and coincides with the mean value in the original dynamics.

To evaluate the cost term (4.7), we use the path weight (2.22) with an action defined in Eq. (2.23) to build the Radon-Nikodým derivative

$$\frac{\mathcal{P}^\dagger[x_t;\epsilon]}{\mathcal{P}[x_t]} = \exp(\Phi[x_t;\epsilon]), \tag{4.12}$$

with

$$\Phi[x_t;\epsilon] \equiv -\frac{1}{4D}\int_0^T \mathrm{d}t \Big[\{\dot{x}_t - \mu F^\dagger(x_t)\}^2 - \{\dot{x}_t - \mu F(x_t)\}^2 + 2D\mu\{\partial_x F^\dagger(x) - \partial_x F(x)\}|_{x=x_t}\Big]. \tag{4.13}$$

Inserting Eq. (4.13) into Eq. (4.7), using Itô's Lemma and Itô's Isometry [47] yields the cost term

$$\mathcal{C}(T) = \int \mathrm{d}x\, p^{\text{s}}(x) F_{\text{pert}}(x)^2/D = \int \mathrm{d}x\, \frac{j^{\text{s}}(x)^2}{D p^{\text{s}}(x)} = \sigma. \tag{4.14}$$

Finally, inserting Eqs. (4.11) and (4.14) into the inequality (4.6) leads to the TUR in Eq. (4.1).

We note that the TUR holds not only for one-dimensional systems but also for multi-dimensional systems with multiple interacting degrees of freedom. Proving the TUR for these systems is achieved by following the same steps as for one-dimensional systems (see also, e.g., Ref. [74]). Alternatively, a proof of the TUR for discrete Markovian systems suffices to prove the TUR for multi-dimensional Langevin systems as well since, as already mentioned above, a continuous system can be modeled as a discrete system by discretizing the coordinates.

### 4.2.2 *Discrete systems*

We consider a system with discrete states obeying a Markovian dynamics described by the master equation (2.62). We denote the transition rates of the original dynamics as $k_{ij} \equiv k_{ij}(\lambda)$ and the ones of the auxiliary dynamics as $k_{ij}^\dagger(\epsilon)$, where $k_{ij}^\dagger(\epsilon = 0) = k_{ij}$. The path weight for a discrete Markovian system is given by the expression in Eq. (2.88). We assume that the original dynamics and the auxiliary dynamics are both prepared in their stationary states $p_i^{\mathrm{s}}$ and $p_i^{\mathrm{s},\dagger}(\epsilon)$, respectively. Since $k_{ij}^\dagger(\epsilon = 0) = k_{ij}$, it holds $p_i^{\mathrm{s},\dagger}(\epsilon = 0) = p_i^{\mathrm{s}}$.

The mean value of a generalized current in the auxiliary dynamics reads

$$\langle J[n_t]\rangle^\dagger \equiv \sum_{i>j} d_{ij}\left(p_i^{\mathrm{s},\dagger}(\epsilon)k_{ij}^\dagger(\epsilon) - p_j^{\mathrm{s},\dagger}(\epsilon)k_{ji}^\dagger(\epsilon)\right) \equiv \sum_{i>j} d_{ij} j_{ij}^{\mathrm{s},\dagger}(\epsilon) \quad (4.15)$$

with arbitrary anti-symmetric increments $d_{ij} = -d_{ji}$ and the probability current $j_{ij}^{\mathrm{s},\dagger}$ in the auxiliary dynamics. Obviously, for $\epsilon = 0$ the current in Eq. (4.15) coincides with the current in the original dynamics given by

$$\langle J[n_t]\rangle \equiv \sum_{i>j} d_{ij}\left(p_i^{\mathrm{s}}k_{ij} - p_j^{\mathrm{s}}k_{ji}\right) \equiv \sum_{i>j} d_{ij} j_{ij}^{\mathrm{s}}, \quad (4.16)$$

where $j_{ij}^{\mathrm{s}}$ denotes the probability current in the original dynamics. To derive the TUR, we choose the auxiliary rates as

$$k_{ij}^\dagger(\epsilon) = k_{ij}\left(1 + \epsilon\left[1 + \frac{\nu_{ji}}{t_{ij}^{\mathrm{s}}}\left(-2 \pm \sqrt{4 - f_{ij}}\right)\right]\right) \quad (4.17)$$

with

$$f_{ij} \equiv \frac{t_{ij}^{\mathrm{s}}}{\nu_{ij}\nu_{ji}}\left[t_{ij}^{\mathrm{s}} - j_{ij}^{\mathrm{s}} \ln\left(\frac{\nu_{ij}}{\nu_{ji}}\right)\right], \quad (4.18)$$

$\nu_{ij} \equiv p_i^{\mathrm{s}}k_{ij}$ and the steady-state traffic $t_{ij}^{\mathrm{s}} \equiv p_i^{\mathrm{s}}k_{ij} + p_j^{\mathrm{s}}k_{ji}$. This choice describes a time-rescaled process with $t \to (1+\epsilon)t$, leaves the stationary state unchanged, i.e., $p_i^{\mathrm{s},\dagger}(\epsilon) = p_i^{\mathrm{s}}$, and scales the current like

$j_{ij}^{\mathrm{s},\dagger}(\epsilon) = (1+\epsilon) j_{ij}^{\mathrm{s}}$. Thus, the generalized current in Eq. (4.15) is given by $\langle J[n_t] \rangle^{\dagger} = (1+\epsilon) \langle J[n_t] \rangle$ and, consequently, the response in Eq. (4.5) is given by

$$\Delta J = \langle J[n_t] \rangle \equiv J, \tag{4.19}$$

i.e., the response of the current coincides with the mean value of the current.

Next, we evaluate the cost term in Eq. (4.7) for the choice of rates in Eq. (4.17). Using the path weight for a discrete Markovian system in Eq. (2.88), the Radon-Nikodým derivative can be written as

$$\frac{\mathcal{P}^{\dagger}[n_t;\epsilon]}{\mathcal{P}[n_t]} = \exp(\Phi[n_t;\epsilon]) \tag{4.20}$$

with

$$\Phi[n_t;\epsilon] \equiv \int_0^T \mathrm{d}t \sum_{ij} \left[ \dot{m}_{ij}(t) \ln\left( \frac{k_{ij}^{\dagger}(\epsilon)}{k_{ij}} \right) - \delta_{i,n_t} \{ k_{ij}^{\dagger}(\epsilon) - k_{ij} \} \right]. \tag{4.21}$$

To calculate the cost term in Eq. (4.7), we either have to evaluate the correlations $\left\langle \left( \partial_\epsilon \Phi[n_t;\epsilon]|_{\epsilon=0} \right)^2 \right\rangle$ by using the discrete noise variable

$$\zeta_{ij}(t) \equiv \dot{m}_{ij}(t) - k_{ij} \delta_{i,n_t} \tag{4.22}$$

with zero mean $\langle \zeta_{ij}(t) \rangle = 0$ and correlations

$$\langle \zeta_{ij}(t) \zeta_{kl}(t') \rangle = p_i^{\mathrm{s}} k_{ij} \delta_{i,k} \delta_{j,l} \delta(t-t') \tag{4.23}$$

or we have to use the relation

$$\left\langle \left( \partial_\epsilon \Phi[n_t;\epsilon]|_{\epsilon=0} \right)^2 \right\rangle = - \left\langle \partial_\epsilon^2 \Phi[n_t;\epsilon]|_{\epsilon=0} \right\rangle, \tag{4.24}$$

which follows from the normalization of the path weights. The latter method only requires to evaluate mean values of the quantities $\dot{m}_{ij}(t)$ and $\delta_{i,n_t}$ via Eqs. (2.80) and (2.81). Both methods yield

$$\mathcal{C}(T) = \sum_{ij} j_{ij}^{\mathrm{s}} \ln\left( \frac{p_i^{\mathrm{s}} k_{ij}}{p_j^{\mathrm{s}} k_{ji}} \right) = \sigma \tag{4.25}$$

from which together with Eqs. (4.6) and (4.19) follows the TUR in Eq. (4.1).

### 4.2.3 *Overview*

The mathematical method used above yields a lower bound on entropy production in terms of a current and its fluctuations and, hence, directly proves the TUR. Originally, the TUR has been proven by deriving an upper global quadratic bound on the LDF in the long-time limit [28],

which is equivalent to a lower quadratic bound on the SCGF [129]. From these bounds, the lower bound on entropy production follows immediately. Thus, it has been shown that rare fluctuations in a steady-state can be bounded by Gaussian processes. Equality in the quadratic bounds and, consequently, in the TUR can be achieved in the linear response regime, where fluctuations become Gaussian [27, 86]. Recently, it has been shown that in the short-time limit, Gaussian fluctuations in the entropy production lead to equality as well [89].

After its proof in the long-time limit, the TUR has been proven for finite observation times in a steady state using large deviation techniques and assuming virtual copies of the system of interest. Here, the same global quadratic bound on the LDF in the long-time limit holds for finite observation times as well [72, 73]. Subsequently, it has been shown in Refs. [74, 75] that the corresponding quadratic bound on the SCGF can be directly derived for finite observation times without the introduction of virtual copies. Moreover, recent works have used information theoretic bounds like the Cramèr-Rao inequality to derive the TUR [77, 124, 126], which are equivalent to the method used in this section. In principle, these bounds can be applied to an arbitrary dynamics and have the advantage that the TUR can be easily derived by a proper choice of an auxiliary dynamics without further knowledge about the mathematical framework of large deviation theory. Thus, these information theoretic bounds are easier accessible to physicists. However, they are not able to prove the quadratic global bounds on the LDF or SCGF.

To summarize, recent works found simplified proofs of the TUR and introduced new methods providing the ability to derive further thermodynamic bounds for various types of dynamics by using a proper choice of auxiliary dynamics.

## 4.3 BOUND ON THE EFFICIENCY OF STEADY-STATE HEAT ENGINES

We now focus on one important application of the TUR: a bound on the efficiency of heat engines [29, 78]. A steady-state heat engine consists of a system simultaneously coupled to a hot reservoir and to a cold reservoir as sketched in Fig. 4.1. Steady-state heat engines should be clearly distinguished from cyclic heat engines, where the system is driven by the periodic modulation of a protocol and/or coupled to reservoirs in an alternating manner. Examples for steady-state heat engines are a model for a solar cell consisting of a two-state quantum dot, where the two heat baths are coupled through different transition channels [130] and the Brownian gyrator model, where two heat baths are coupled through the strength of the noise [131–133].

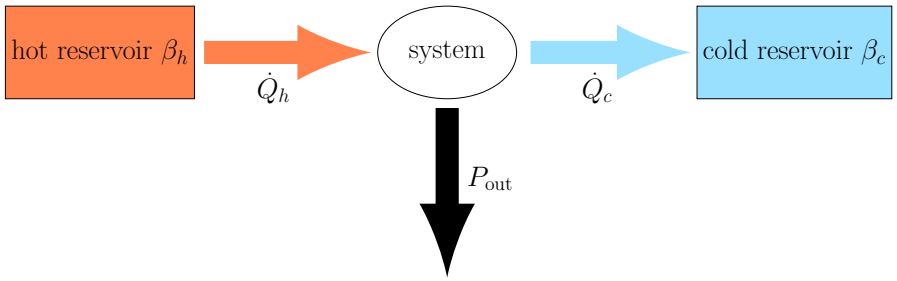


Figure 4.1: Schematic of a steady-state heat engine coupled to a hot reservoir with inverse temperature $\beta_h$ and to a cold reservoir with inverse temperature $\beta_c$.

For a generic heat engine, a heat flux $\dot{Q}_h$ is flowing from the hot reservoir into the system and another heat flux $\dot{Q}_c$ is flowing from the system into a cold reservoir. In this process, heat is converted into useful work quantified by the output power $P_{\text{out}}$. From the second law of thermodynamics it follows that the efficiency $\eta$ of any heat engine is bounded from above by the Carnot efficiency $\eta_{\text{C}}$, i.e.,

$$\eta \equiv P_{\text{out}}/\dot{Q}_h \leq \eta_{\text{C}} \equiv 1 - \beta_h/\beta_c. \tag{4.26}$$

Since the TUR provides a stronger bound on the entropy production than the second law does, it must also yield a stronger bound on the efficiency. In a steady state, the entropy production reads $\sigma = \beta_h \dot{Q}_h + \beta_c \dot{Q}_c$ and can be rewritten as $\sigma = P_{\text{out}}(\eta_{\text{C}}/\eta - 1)\beta_c$ by using the first law of thermodynamics. Using this expression for the entropy production and choosing as a current the output power $J = P_{\text{out}}$ in Eq. (4.1) leads to the stronger bound

$$\eta \leq \frac{\eta_{\text{C}}}{1 + P_{\text{out}}/[\beta_c D_{P_{\text{out}}}(T)]} \leq \eta_{\text{C}}, \tag{4.27}$$

where $D_{P_{\text{out}}}(T)$ denotes the diffusion coefficient of the output power. The bound on the efficiency in Eq. (4.27) shows that Carnot efficiency can only be reached for vanishing output power or at finite power if the power fluctuations diverge. The latter condition is a direct consequence of the TUR and is unique for steady-state systems. In the special case of isothermal engines like a molecular motor or a work-to-work converter ($\beta_h = \beta_c = 1$), the bound on the efficiency yields similar implications, where we formally can set $\eta_{\text{C}} = \beta_c = 1$ in Eq. (4.27). Lastly, the bound on the efficiency is only valid for steady-state engines and not for cyclic heat engines. It has been shown in Ref. [31] that the steady-state TUR and, thus, also the bound on the efficiency (4.27), can be violated strongly for periodically driven systems. The generalization of the thermodynamic uncertainty relation to periodically driven systems with meaningful implications for efficiencies of cyclic heat engines is one substantial part of this thesis and discussed in the next Chapter 5.

# Part III

# GENERALIZATIONS OF THE THERMODYNAMIC UNCERTAINTY RELATION

# 5

# PERIODIC DRIVING

Periodically driven systems will typically reach a PSS in the long-time limit. Such a PSS is relevant for mesoscopic cyclic processes under periodic mechanical, optical or chemical stimuli [43, 134] such as stochastic pumps [44, 120, 135, 136] or most prominently microscopic heat engines [41, 137–143]. Analogously to a NESS, the PSS is the periodic stationary solution of the underlying equations of motion and has the same period as the driving. In contrast, it is time-dependent and leads to time-dependent probability currents, which are the arguably most important property that clearly separates a PSS from a NESS.

Since the discovery of the TUR for a NESS in 2015, finding a generalization to periodically driven systems that includes only operationally accessible quantities has been one of the most intriguing problems of stochastic thermodynamics. Especially for cyclic heat engines, such a generalization has the ability to clarify whether or not reaching Carnot efficiency at finite power causes diverging power fluctuations [29, 97, 98, 144, 145].

An early counter-example has shown that a naive extension of the thermodynamic uncertainty relation from steady-state systems to periodically driven ones is not admissible [31]. Subsequent attempts to find an analog for periodically driven systems comprise Proesman and van den Broeck's bound valid for *time-symmetric* driving that, however, for a small frequency of driving leads to a rather weak bound [30]. Barato *et al.* replace $\sigma$ in Eq. (4.1) by a modified entropy production rate that requires detailed knowledge of dynamical properties of the whole system [100]. In a follow up [146], a whole class of such modified entropy production rates were discussed that, from an operational perspective, are arguably not that useful since they require input that is typically not available in experiments. The same holds for our generalization introducing an effective entropy production for further types of currents [4] and for a further scheme [147]. Recently, Proesmans and Horowitz introduced a modified uncertainty relation for hysteretic currents that overcomes some of the above mentioned short-comings [101]. However, from the perspective of thermodynamic inference [10], an operationally accessible relation, which allows one to bound entropy production and which becomes the TUR for steady-state systems, is still missing for periodically driven systems.

## 5.1 THERMODYNAMIC UNCERTAINTY RELATION FOR PERIODIC DRIVING

As a main result of this chapter, for systems driven with a period $\mathcal{T} \equiv 2\pi/\Omega$, we will derive a family of universal bounds that relate, *inter alia*, the entropy production with fluctuations of observables. Applied to current fluctuations, we get specifically

$$\sigma(\Omega) D_J(\Omega) / J(\Omega)^2 \geq [1 - \Omega J'(\Omega)/J(\Omega)]^2. \tag{5.1}$$

The left-hand side involves the same combination of variables as the ordinary TUR does, where we make the dependence on $\Omega$ explicit. The right-hand side additionally contains the derivative of the current with respect to the driving frequency, i.e., the response of the current to a slight change of the period of driving. In the special case of constant driving, this bound becomes the ordinary TUR, Eq. (4.1), since then the current is formally independent of the driving frequency. Thus, the entropy production in a periodically driven system can be bounded using experimental data for the mean of any current, its fluctuations and its response to a slight change of driving frequency.

One consequence of this relation is that it provides a generic condition for (almost) dissipation-less precision. If the current is proportional to the frequency of driving, the right-hand side vanishes. This insight rationalizes the earlier construction of a dissipation-less Brownian clock [31].

Applied to the efficiency $\eta \equiv P_{\text{out}}/P_{\text{in}}$ of isothermal cyclic engines that convert an input source of energy with mean $P_{\text{in}}$ to an output power with mean $P_{\text{out}} = P_{\text{in}} - \sigma$, the relation implies

$$P_{\text{out}} \leq \frac{1-\eta}{\eta} \frac{D_{P_{\text{out}}}}{[1 - \Omega P'_{\text{out}}(\Omega)/P_{\text{out}}(\Omega)]^2}. \tag{5.2}$$

Hence, in general, the power of a cyclic engine vanishes at least linearly as its efficiency approaches the maximum value of 1. A finite power in this limit is, in principle, possible only if the current fluctuations diverge or if the output power is proportional to the cycling frequency of the engine. While the first option has been previously been derived for steady-state engines from the TUR [78], the second one is genuine for periodically driven engines.

These results and the further ones derived and discussed below hold for systems described by a Markov dynamics on a discrete set of states. The transition rate $k_{ij}(\tau)$ from state $i$ to state $j$ at time $\tau$ is time-periodic with $k_{ij}(\tau + \mathcal{T}) = k_{ij}(\tau)$ and $0 \leq \tau \leq \mathcal{T}$. In the long-time limit, the probability to find the system in state $i$ becomes periodic as well and will be denoted by $p_i^{\text{ps}}(\tau; \Omega)$, where the corresponding driving frequency $\Omega$ is explicitly introduced through the second argument.

## 5.2 SETUP AND OBSERVABLES

One class of fluctuating time-integrated current depends on the number of transitions between states

$$J_T^d \equiv \frac{1}{T}\int_0^T \mathrm{d}t \sum_{ij} \dot{m}_{ij}(t) d_{ij}(t) \tag{5.3}$$

with periodic increments $d_{ij}(t) = -d_{ji}(t)$ and $0 \leq t \leq T$. Here, $m_{ij}(t)$ is the number of transitions from $i$ to $j$ up to time $t$ along a trajectory $n_t$ of length $T$. In the long-time limit $T \to \infty$, the current in Eq. (5.3) reaches the mean value

$$J^d(\Omega) \equiv \left\langle J_T^d \right\rangle = \frac{1}{\mathcal{T}}\int_0^{\mathcal{T}} \mathrm{d}\tau \sum_{i>j} j_{ij}^{\mathrm{ps}}(\tau;\Omega) d_{ij}(\tau), \tag{5.4}$$

where $j_{ij}^{\mathrm{ps}}(\tau;\Omega) \equiv p_i^{\mathrm{ps}}(\tau;\Omega)k_{ij}(\tau) - p_j^{\mathrm{ps}}(\tau;\Omega)k_{ji}(\tau)$. One example for the mean value of a current in Eq. (5.3) is the entropy production

$$\sigma(\Omega) = \frac{1}{\mathcal{T}}\int_0^{\mathcal{T}} \mathrm{d}\tau \sum_{i>j} j_{ij}^{\mathrm{ps}}(\tau;\Omega) \ln\left(\frac{p_i^{\mathrm{ps}}(\tau;\Omega)k_{ij}(\tau)}{p_j^{\mathrm{ps}}(\tau;\Omega)k_{ji}(\tau)}\right). \tag{5.5}$$

A second class of current can be derived from the residence time in certain states as

$$J_T^a \equiv \frac{1}{T}\int_0^T \mathrm{d}t \sum_i \delta_{n_t,i}\dot{a}_i(t), \tag{5.6}$$

where $\delta_{n_t,i}$ is 1 if state $i$ is occupied at time $t$ and 0, otherwise. Here, the periodic increment can be written as a time-derivative of a state variable, e.g., for power input $\dot{a}_i(t) = \dot{E}_i(t)$, where $E_i(t)$ is the energy of state $i$. The mean value of Eq. (5.6) is denoted by $J^a(\Omega) \equiv \langle J_T^a \rangle$. An arbitrary average current consists of a superposition of the two types of currents defined in Eqs. (5.3) and (5.6), i.e., $J(\Omega) \equiv J^d(\Omega) + J^a(\Omega)$.

A further type of observable is called residence quantity that is defined as

$$A_T \equiv \frac{1}{T}\int_0^T \mathrm{d}t \sum_i \delta_{n_t,i} A_i(t) \tag{5.7}$$

with time-dependent periodic state variables $A_i(t)$ that cannot be written as time-derivatives. Simple examples of such a quantity are the average fraction of time $\tau_k$ spent in state $k$ during one cycle with increment $A_i(t) = \delta_{i,k}$ or the average energy with $A_i(t) = E_i(t)$. For long times, their mean value is given by

$$A(\Omega) \equiv \langle A_T \rangle = \frac{1}{\mathcal{T}}\int_0^{\mathcal{T}} \mathrm{d}\tau \sum_i p_i^{\mathrm{ps}}(\tau;\Omega) A_i(\tau). \tag{5.8}$$

Fluctuations of residence and current observables can be quantified via the diffusion coefficient

$$D_X(\Omega) \equiv \lim_{T\to\infty} T\left\langle \left(X_T - \langle X_T \rangle\right)^2 \right\rangle / 2 \tag{5.9}$$

with $X_T \in \{J_T^d, J_T^a, A_T\}$.

For the residence variable $A_T$ in Eq. (5.7), we will show that the mean value $A(\Omega)$ and the fluctuations $D_A$ obey

$$\sigma(\Omega) D_A(\Omega) \geq [\Omega A'(\Omega)]^2. \tag{5.10}$$

Thus, by measuring how the mean value of this observable changes with driving frequency, a lower bound on the entropy production can be obtained without knowing further details of the system. It is quite remarkable that by observing a variable that is even under time-reversal a bound on entropy production, which is a hallmark of broken time-reversal symmetry, can be inferred. There is no analog of this relation in the case of constant driving, since then the right-hand side vanishes.

## 5.3 INFERENCE OF ENTROPY PRODUCTION IN A THREE-STATE MODEL

As a first example, we illustrate relation (5.10) via an isothermal three-state model with the following energy levels

$$\begin{aligned} E_1(t) &= E_1^c \cos \Omega t + E_1^s \sin \Omega t + E_1^0, \\ E_2(t) &= E_2^0, \quad \text{and} \quad E_3(t) = E_3^0. \end{aligned} \tag{5.11}$$

The rates $k_{ij}(\tau)$

$$k_{ij}(t) = k_{ij}^0 \exp\left[-\alpha(E_j(t) - E_i(t))\right], \tag{5.12}$$

$$k_{ji}(t) = k_{ij}^0 \exp\left[(1-\alpha)(E_j(t) - E_i(t))\right] \tag{5.13}$$

fulfill the local detailed balance condition for any $\alpha$, where $i > j$. Here, we have set $\beta = 1$ and introduced a rate amplitude $k_{ij}^0$ for each link $(i, j)$.

We vary the driving frequency $\Omega$ for different energy amplitudes $E_1^c$ and fix all other parameters. The total entropy production can be estimated via Eq. (5.10): the frequency-dependent fraction of residence time $\tau_1(\Omega)$ in state 1 and its diffusion coefficient $D_{\tau_1}(\Omega)$ are sufficient to obtain the estimator

$$\sigma_{\text{est}} \equiv \left[\Omega \tau_1'(\Omega)\right]^2 / D_{\tau_1}(\Omega) \leq \sigma, \tag{5.14}$$

plotted in Fig. 5.1 as a function of the driving frequency $\Omega$ for different amplitudes $E_1^c$. Hence, this simple estimate yields already up to 40% of the total entropy production.

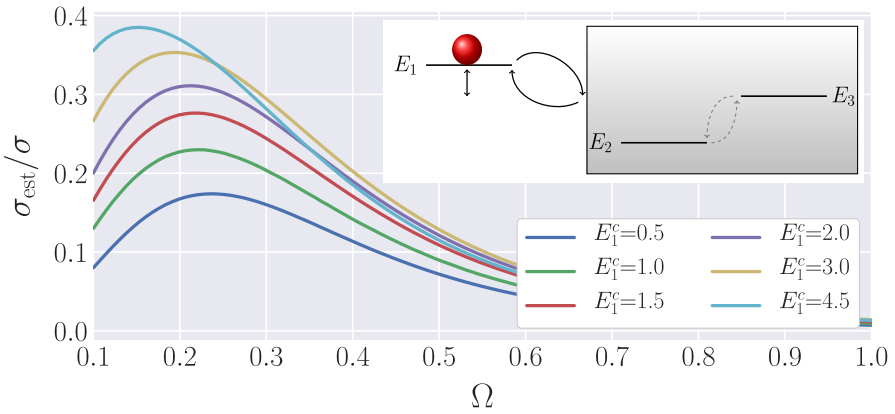


Figure 5.1: Ratio of estimator (5.14) and total entropy production (5.5) as a function of the driving frequency $\Omega$ for different energy amplitudes $E_1^c$ for the driven three-state system (inset). The parameters $E_1^s = 1.0, E_1^0 = 8.0, E_2^0 = 2.3, E_3^0 = 4.1, k_{12}^0 = 0.01, k_{23}^0 = 0.2, k_{13}^0 = 10.0$, and $\alpha = 0.1$ are kept fixed.

## 5.4 DERIVATION

The derivation of our main results (5.1) and (5.10) exploits a strategy introduced by Dechant and Sasa [74] and can be sketched as follows. The diffusion coefficient $D_G(\Omega)$ for a quantity

$$G_T \equiv A_T + J_T^a + J_T^d \tag{5.15}$$

with mean $G(\Omega) \equiv \langle G_T \rangle$ can be bounded by dynamical quantities of an auxiliary process as shown in Section A.1. The auxiliary process is the original one except that its external driving frequency $\tilde{\Omega}$ differs from the original frequency $\Omega$. Thus, we can bound the diffusion coefficient by

$$2D_G(\Omega) \geq (G(\Omega) - G(\Omega, \tilde{\Omega}))^2 / [(\Omega/\tilde{\Omega} - 1)^2 \mathcal{S}(\Omega, \tilde{\Omega})] \tag{5.16}$$

with dynamical quantities depending on the chosen frequency $\tilde{\Omega}$ of the auxiliary process

$$\mathcal{S}(\Omega, \tilde{\Omega}) \equiv \frac{1}{\mathcal{T}} \int_0^{\mathcal{T}} \mathrm{d}\tau \sum_{i>j} \left[ j_{ij}^{\rm ps}(\Omega\tau/\tilde{\Omega}; \tilde{\Omega}) \right]^2 / t_{ij}^{\rm ps}(\tau; \Omega), \tag{5.17}$$

$$G(\Omega, \tilde{\Omega}) \equiv A(\tilde{\Omega}) + (\Omega/\tilde{\Omega}) J(\tilde{\Omega}) \tag{5.18}$$

and the current $J(\tilde{\Omega}) \equiv J^a(\tilde{\Omega}) + J^d(\tilde{\Omega})$ of the auxiliary process. Here, we introduced the probability current at frequency $\tilde{\Omega}$

$$j_{ij}^{\rm ps}(\Omega\tau/\tilde{\Omega}; \tilde{\Omega}) \equiv p_i^{\rm ps}(\Omega\tau/\tilde{\Omega}; \tilde{\Omega}) k_{ij}(\tau) - p_j^{\rm ps}(\Omega\tau/\tilde{\Omega}; \tilde{\Omega}) k_{ji}(\tau) \tag{5.19}$$

and the activity at link $(i, j)$

$$t_{ij}^{\rm ps}(\tau; \Omega) \equiv p_i^{\rm ps}(\tau; \Omega) k_{ij}(\tau) + p_j^{\rm ps}(\tau; \Omega) k_{ji}(\tau) \tag{5.20}$$

at the original frequency $\Omega$.

We choose either the increments $d_{ij} = \dot{a}_i = 0$ or $A_i = 0$ such that $G(\Omega) = J(\Omega)$ for currents and $G(\Omega) = A(\Omega)$ for residence quantities and take the limit $\tilde{\Omega} \to \Omega$. This leads to the following two inequalities

$$D_J(\Omega)C(\Omega)/J(\Omega)^2 \geq (1 - \Omega J'(\Omega)/J(\Omega))^2, \tag{5.21}$$
$$D_A(\Omega)C(\Omega)/A(\Omega)^2 \geq (\Omega A'(\Omega)/A(\Omega))^2. \tag{5.22}$$

Here, $C(\Omega) \in \{2\mathcal{S}(\Omega), 2\mathcal{A}(\Omega), \sigma(\Omega)\}$ can be chosen as one of three cost terms with $\mathcal{S}(\Omega) \equiv \mathcal{S}(\Omega, \tilde{\Omega} = \Omega)$ and the average dynamical activity $\mathcal{A}(\Omega) \equiv 1/\mathcal{T} \int_0^{\mathcal{T}} \mathrm{d}\tau \sum_{i>j} t_{ij}^{\mathrm{ps}}(\tau; \Omega)$. These two inequalities (5.21) and (5.22) are our most general results, from which our main results (5.1) and (5.10) are obtained with $C(\Omega) = \sigma(\Omega)$. These inequalities are valid in the long-time limit. For a finite number of periods an additional cost term arises (see Section A.2).

By choosing $C(\Omega) = \mathcal{A}(\Omega)$, the average dynamical activity can be bounded via Eq. (5.21) by current observables and their fluctuations. The steady-state analog of this relation was proven in [129] and extended to more general observables in [108]. Our generalization of the latter one for periodic driving is derived in Section A.3. These bounds on activity can be generalized to residence observables through Eq. (5.22). They have no steady-state analog.

## 5.5 HEAT ENGINES

Finally, we investigate the implications of our results for heat engines operating cyclically between two baths of inverse temperature $\beta_h < \beta_c$ with efficiency

$$\eta(\Omega) \equiv P_{\mathrm{out}}(\Omega)/\dot{Q}_h(\Omega) \leq \eta_C \equiv 1 - \beta_h/\beta_c, \tag{5.23}$$

where $P_{\mathrm{out}} > 0$ is the output power and $\dot{Q}_h$ the heat current flowing into the system from the hot reservoir. The inequality (5.1) implies the bound

$$\eta(\Omega) \leq \hat{\eta}(\Omega) \equiv \eta_C \left(1 + \frac{[P_{\mathrm{out}}(\Omega) - \Omega P'_{\mathrm{out}}(\Omega)]^2}{\beta_c D_{P_{\mathrm{out}}}(\Omega) P_{\mathrm{out}}(\Omega)}\right)^{-1}. \tag{5.24}$$

Carnot efficiency at finite power can thus be reached only if the power fluctuations diverge or if the power increases linearly with the driving frequency. The latter condition is typical for quasi-static driving [98]. For maximal output power ($P'_{\mathrm{out}}(\Omega_{\mathrm{max}}) = 0$), Eq. (5.24) reduces to the established bound for steady-state systems [29] thus showing a universal trade-off between efficiency, power and constancy at maximum power.

So far we discussed systems with a discrete set of states. We now illustrate the new bound on efficiency (5.24) for a system obeying an overdamped Langevin equation. Specifically, we consider a Stirling

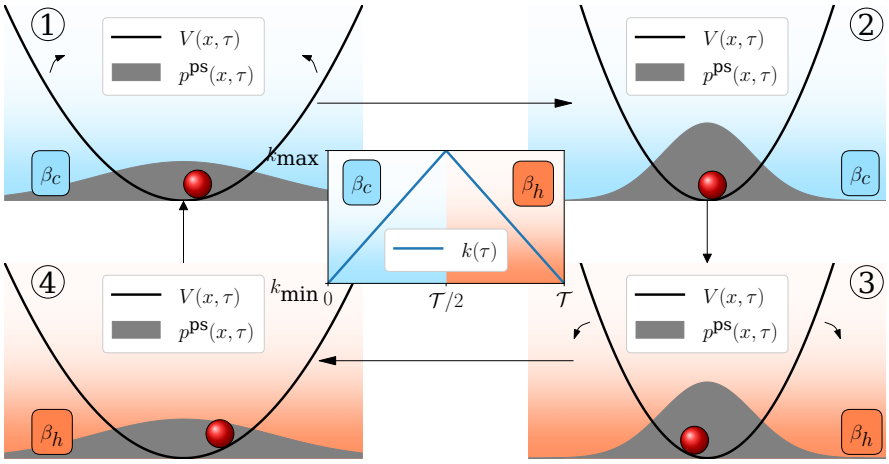


Figure 5.2: Particle in a harmonic trap with time-dependent stiffness $k(\tau)$ operating as a Stirling heat engine between temperatures $\beta_c > \beta_h$.

heat engine model inspired by [41, 137]. The engine consists of a colloid in a one-dimensional harmonic potential with a time-dependent stiffness $k(\tau)$

$$V(x, k(\tau)) \equiv V(x,\tau) \equiv k(\tau)x^2/2 \geq 0. \tag{5.25}$$

The position $x$ follows the Langevin equation

$$\dot{x}(t) = -\mu k(t)x(t) + \zeta(t). \tag{5.26}$$

Here, $\mu$ denotes the mobility, and $\zeta(t)$ is zero-mean Gaussian noise with correlation $\langle \zeta(t)\zeta(\tilde{t})\rangle = 2\mu\delta(t-\tilde{t})/\beta(t)$ and a periodic inverse temperature $\beta(t) = \beta(t+\mathcal{T})$. The corresponding Fokker-Planck equation for the probability distribution $p(x,t)$ reads

$$\partial_t p(x,t) = \mu\partial_x \left(\partial_x V(x,t) + \beta^{-1}(t)\partial_x\right) p(x,t). \tag{5.27}$$

The periodic stationary solution $p^{\mathrm{ps}}(x,\tau)$ of (5.27) is a Gaussian with zero mean.

As a protocol for the stiffness, we use the one from the experiment in [41], which increases and decreases linearly in time according to

$$k(\tau) = \begin{cases} 2\Delta k\tau/\mathcal{T} + k_{\min}, & 0 \leq \tau < \mathcal{T}/2 \\ -2\Delta k(\tau/\mathcal{T} - 1/2) + k_{\max}, & \mathcal{T}/2 \leq \tau < \mathcal{T} \end{cases} \tag{5.28}$$

with $\Delta k \equiv k_{\max} - k_{\min}$, see Fig. 5.2. The coupling to two different heat baths leads to a time-dependent temperature that is piecewise constant, i.e., $\beta(\tau) = \beta_c$ for $0 \leq \tau < \mathcal{T}/2$ and $\beta(\tau) = \beta_h$ for $\mathcal{T}/2 \leq \tau < \mathcal{T}$.

Currents of interest are power, entropy production and heat. Their explicit expressions and the diffusion coefficient for the output power

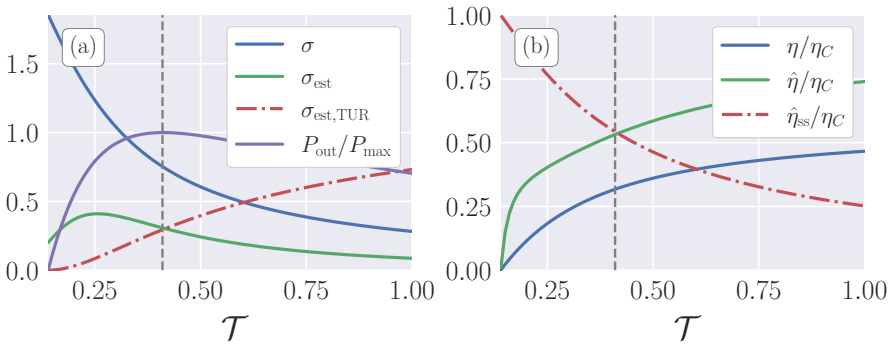


Figure 5.3: (a) Entropy production $\sigma$, its corresponding estimator $\sigma_{\rm est}$ (5.29), estimator for steady-state systems $\sigma_{\rm est,TUR}$ and output power $P_{\rm out}$ divided by its maximum $P_{\rm max}$ and (b) efficiency $\eta$, bound on the efficiency $\hat{\eta}$ (5.24), and its steady-state analog $\hat{\eta}_{\rm ss}$ as function of the cycle duration $\mathcal{T}$ with $\mu = 10.0$, $k_{\rm max} = 2.0$, $k_{\rm min} = 1.0$, $\beta_c = 2.0$ and $\beta_h = 1.0$. For $\mathcal{T} \lesssim 0.2$, the machine no longer generates power.

are given in Section A.4. In order to illustrate Eq. (5.1) and (5.24), we define the estimator

$$\sigma_{\rm est} \equiv \left(P_{\rm out}(\Omega) - \Omega P'_{\rm out}(\Omega)\right)^2 / D_{P_{\rm out}}(\Omega) \leq \sigma \tag{5.29}$$

for entropy production and vary the cycle duration $\mathcal{T}$. The output power, the estimator (5.29) and the bound on efficiency (5.24) are shown in Fig. 5.3. With increasing $\mathcal{T}$, the output power increases for small $\mathcal{T}$. According to Eq. (5.1) the ordinary TUR, Eq. (4.1), is still valid. At maximum power (vertical dotted line) Eq. (5.1) is equivalent to the TUR and the estimator $\sigma_{\rm est,TUR} \equiv P_{\rm out}^2/D_{P_{\rm out}}$ intersects $\sigma_{\rm est}$. After reaching the maximum value, the power decreases with increasing $\mathcal{T}$ with the TUR violated for $\mathcal{T} \gtrsim 0.6$.

## 5.6 CONCLUSION

In summary, for periodically driven systems, we have derived a class of inequalities that relate, *inter alia*, entropy production with the mean of an observable, its dependence on driving frequency and its variance. Remarkably, apart from the more familiar currents, such observables can also be even under time-reversal like residence times are. For cyclic heat engines and cyclically driven isothermal engines, the thermodynamic efficiency can now be bounded using data only for the input or output current. Since our results have been obtained for a Markov dynamics on a discrete set of states, they trivially hold as well for overdamped Langevin dynamics.

Recently, our results have been generalized to underdamped Langevin systems in Refs. [94, 95]. However, these generalizations require to measure a response of the current that is operationally inaccessible,

which obviously does not allow one to infer entropy production. Moreover, for two-dimensional underdamped systems driven into a NESS, a violation of the TUR in the long-time limit has been reported in Ref. [34]. While this observation suggests that our main results for periodic driving cannot be applied to arbitrary underdamped systems, investigating these results specifically in one dimension deserves future work. Arguably even more exciting is to explore periodically driven open quantum systems for which coherences are relevant. In this context, violations of our results have been observed in, e.g., Refs. [118, 119]. Thus, finding universally applicable and operationally accessible bounds on entropy production in underdamped Langevin systems or in open quantum systems remains an intriguing open problem for future research.

# 6 ARBITRARY TIME-DEPENDENT DRIVING

The arguably most striking feature of the thermodynamic uncertainty relation is its ability to infer entropy production by measuring currents and their fluctuations. Since the TUR in its original form is restricted to systems driven into a NESS, several attempts have been made to generalize the TUR to more complex setups.

For systems relaxing either to equilibrium or to a NESS, entropy production can be bounded by measuring the fluctuations of a current and its mean value at the end of the observation time [74, 128].

For periodically driven systems, inferring the entropy production, or at least a lower bound for it, is somewhat more complex. There exist variants that either require time-symmetric driving [30] or need input from the time-reversed protocol [101]. In addition, there are a number of more formal versions that cannot easily be applied under experimentally realistic conditions [4, 100, 146]. An operationally accessible version for arbitrary periodic driving has been derived in Chapter 5 that requires the response of the current to a change of the driving frequency as an additional input (see also Ref. [1]).

Finally, it has been an open problem so far whether related bounds on entropy production can be derived for the generic class of arbitrary time-dependently driven systems including applications like bit erasure processes [148–151] or stochastic pumps [135, 136, 147, 152, 153].

In this chapter, we present the thermodynamic uncertainty relation for the remaining huge class of time-dependently driven systems. We will show how by measuring an observable, its fluctuations and its change under speeding up the driving parameter(s) a lower bound on the entropy production can be obtained. The observable needs not to be a current; it could also be, e.g., a binary variable characterizing the state of the system at the final time or the integrated time spent in a subset of states. As a paradigmatic illustration, we analyze in a numerical experiment the dynamical unfolding of a small peptide for which all relevant parameters have been previously determined experimentally [26]. We show how a bound on the associated entropy production can be extracted from the observation of fluctuations without any further input.

## 6.1 MAIN RESULT FOR A CURRENT

We consider a system prepared in an arbitrary initial state. This system is then driven through an arbitrary control $\lambda(vt)$ with speed parameter $v$ from $t = 0$ to a final time $t = T$. As a consequence, the system exhibits a mean current $J(T, v)$ and corresponding current fluctuations characterized by a diffusion coefficient $D_J(T, v)$, both defined more precisely below. Our first main result relates these quantities with the mean total entropy production rate $\sigma(T, v)$ in the interval $T$ through

$$[J(T, v) + \Delta J(T, v)]^2 / D_J(T, v) \leq \sigma(T, v). \tag{6.1}$$

In comparison with the ordinary TUR for NESSs [27, 28], there is first the dependence on the speed parameter $v$, and, second, the crucial additional term $\Delta J(T, v)$ with differential operator

$$\Delta \equiv T\partial_T - v\partial_v \tag{6.2}$$

that describes the response of the current with respect to a slight change of the speed of driving $v$ as well as with respect to the observation time $T$. Consequently, all quantities entering the left-hand side of Eq. (6.1) are physically transparent and thus provide an operationally accessible lower bound on entropy production. This result is valid for driven overdamped Langevin dynamics of an arbitrary number of coupled degrees of freedom and for driven Markovian systems on a discrete set of states (see Sections B.1 and B.2, respectively) [1].

## 6.2 A FIRST ILLUSTRATION: MOVING TRAP

The role of the additional response term can be illustrated with an overdamped particle with mobility $\mu$, which is dragged by a harmonic trap with stiffness $k$. The system is initially prepared in equilibrium. The center of the trap is moved from $x_0 \equiv \lambda_0 = 0$ to $x_f \equiv \lambda_T = vT$ in time $t = T$ with a constant velocity $v$ leading to a potential

$$V(x, \lambda(vt)) = k\,[x - \lambda(vt)]^2 / 2 \tag{6.3}$$

with protocol $\lambda(vt) \equiv vt$.

One current of interest in this system is the time-averaged velocity $\nu_T \equiv [x(T) - x(0)]/T$, which is still a stochastic quantity. Its mean, $\nu(T, v) \equiv \langle \nu_T \rangle$, depends obviously on the observation time $T$ and on the speed of the protocol $v$ which yields the response $\Delta\nu(T, v)$ (see Section B.3 for details).

For a generic current $J$, the quality of bounds like (6.1) will be quantified throughout this chapter by plotting the quality factor

$$\mathcal{Q}_J \equiv \frac{[J(T, v) + \Delta J(T, v)]^2}{D_J(T, v)\sigma(T, v)} \leq 1. \tag{6.4}$$

1 Coloured noise and memory can arise from integrating out degrees of freedom from an underlying Markovian model. In such a case, our results will apply to the corresponding non-Markovian dynamics as well.

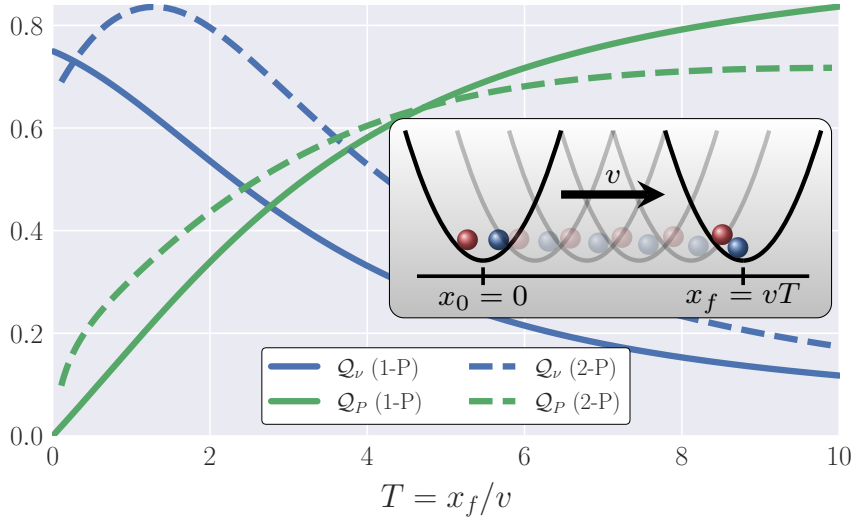


Figure 6.1: Quality factors $\mathcal{Q}_v$ and $\mathcal{Q}_P$ for velocity and power, respectively, as a function of inverse driving speed $T = x_f/v$ for a moving trap. Solid lines (1-P): One particle, $\beta = 10.0$, $\mu = 1.0$ and $x_f = vT = 10.0$. Dashed lines (2-P): Two interacting particles as shown in the inset. The parameters are given in Section B.4.

For the particle in a moving trap, the quality factor for velocity, $\mathcal{Q}_v$, is shown in Fig. 6.1 as a function of observation time $T$, or, equivalently, of driving speed $v$. The bound (6.1) becomes strongest for $T \ll 1/(\mu k)$, i.e., for observation times smaller than the relaxation time. Remarkably, an estimate that yields up to $\sim 80\%$ of the total entropy production is obtained by just observing the traveled distance of the particle without knowing the strength of the trap. In the slow-driving limit, the dispersion of the velocity becomes negligible, while heat is continuously dissipated into the surrounding medium. As a consequence, the original TUR for a NESS is violated while relation (6.1) holds due to the additional response term.

Another current to which relation (6.1) can be applied to is the time-averaged power

$$P(T,v) = \frac{1}{T}\int_0^T \mathrm{d}t \int \mathrm{d}x\, p(x,t;v)\partial_t V(x,\lambda(vt)). \tag{6.5}$$

Due to the Gaussian nature of the work fluctuations, it follows that $D_P(T,v) = P(T,v)/\beta$. Moreover, the entropy production is bounded from above as $\beta P(T,v)/\sigma(T,v) \geq 1$ (see Section B.3.4). Consequently, the TUR for steady-state systems [27, 28] is always violated except in the long-time limit, where the mean power converges to the mean total entropy production rate. In contrast, our result (6.1) provides a lower bound on the mean total entropy production rate, which, in this case, is obviously quite different from the ordinary TUR.

To illustrate the inequality (6.1) for a more complex system, we investigate two interacting particles trapped in the harmonic potential (6.3). We choose a Lennard-Jones interaction between the particles (see Section B.4 for details) and analyze the quality factors for the sum of both particle velocities, i.e., the total traveled distance, and for the power applied to the particles. As shown in Fig. 6.1, the quality factors are similar compared to the ones for the non-interacting model and reach also about 80%.

## 6.3 GENERAL SETUP FOR OVERDAMPED LANGEVIN DYNAMICS

We consider a system described by an overdamped Langevin equation for the position $x(t)$ in a thermal environment with inverse temperature $\beta$,

$$\partial_t x(t) = \mu F(x(t), \lambda(vt)) + \zeta(t), \tag{6.6}$$

where $\mu$ denotes the mobility and $\zeta(t)$ is Gaussian white noise with strength $2D \equiv 2\mu/\beta$. The system is driven by a force $F(x, \lambda(vt))$, which depends on an external protocol $\lambda(vt)$ that contains a speed parameter $v$. The driving starts at $t = 0$ with arbitrary initial distribution $p(x, 0)$ and runs until $t = T$. The time evolution of the probability density $p(x, t; v)$ follows the Fokker-Planck equation $\partial_t p(x, t; v) = -\partial_x j(x, t; v)$ with the probability current

$$j(x, t; v) \equiv [\mu F(x, \lambda(vt)) - D\partial_x]\, p(x, t; v). \tag{6.7}$$

On the level of individual trajectories, we distinguish *state variables* from (still fluctuating) *currents*. Specifically, given a function $a(x, \lambda)$, we define an instantaneous state variable as

$$a_T \equiv a(x(T), \lambda(vT)), \tag{6.8}$$

which depends on the final value of position and control. A further observable is its time-averaged variant given by

$$A_T \equiv \frac{1}{T} \int_0^T \mathrm{d}t\, a(x(t), \lambda(vt)). \tag{6.9}$$

The ensemble average of these stochastic quantities will be denoted by $a(T, v) \equiv \langle a_T \rangle$ and $A(T, v) \equiv \langle A_T \rangle$, where we make the dependence on the two crucial parameters explicit.

For time-dependently driven systems there exist two kinds of currents. Both are odd under time-reversal. The first type of current is called a *jump current* and is of the form

$$J_T^{\mathrm{I}} = \frac{1}{T} \int_0^T \mathrm{d}t\, d^{\mathrm{I}}(x(t), \lambda(vt)) \circ \dot{x}(t). \tag{6.10}$$

Here, $\circ$ denotes the Stratonovich product. The second type is a *state* current given by

$$J_T^{\mathrm{II}} = \frac{1}{T}\int_0^T \mathrm{d}t\, d^{\mathrm{II}}(x(t),\lambda(vt)). \tag{6.11}$$

For jump currents, $d^{\mathrm{I}}(x(t),\lambda(vt))$ is an arbitrary increment, whereas for state currents the increment

$$d^{\mathrm{II}}(x(t),\lambda(vt)) \equiv \partial_t\lambda(vt)\partial_\lambda b(x(t),\lambda)|_{\lambda=\lambda(vt)} \tag{6.12}$$

involves the derivative of a state function $b(x,\lambda_t)$ with respect to the time-dependent driving. We denote the mean values of these observables by $J^{\mathrm{I}}(T,v) \equiv \langle J_T^{\mathrm{I}}\rangle$ and $J^{\mathrm{II}}(T,v) \equiv \langle J_T^{\mathrm{II}}\rangle$. A prominent example for the first type is the mean rate of entropy production in the medium [8]

$$\sigma_m(T,v) \equiv \frac{1}{T}\int_0^T \mathrm{d}t \int \mathrm{d}x\, \beta F(x,\lambda(vt))j(x,t;v) \tag{6.13}$$

with increment $d^{\mathrm{I}}(x,\lambda_t) = \beta F(x,\lambda_t)$. The mean total entropy production rate

$$\sigma(T,v) \equiv \frac{1}{T}\int_0^T \mathrm{d}t \int \mathrm{d}x\, \frac{j^2(x,t;v)}{Dp(x,t;v)} \tag{6.14}$$

additionally contains the entropy production rate of the system [8]. The power applied to a system as given in Eq. (6.5) belongs to the second type of currents and is obtained by choosing $b(x,\lambda) = V(x,\lambda_t)$, where $V(x,\lambda_t)$ is an external potential.

Fluctuations of all these observables can be quantified by the effective *diffusion coefficient*

$$D_X(T,v) \equiv T\left(\langle X_T^2\rangle - \langle X_T\rangle^2\right)/2 \tag{6.15}$$

and $X_T \in \{a_T, A_T, J_T^{\mathrm{I,II}}\}$. For both types of current observables as defined in Eqs. (6.10) and (6.11), the TUR (6.1) holds true (see Section B.1).

## 6.4 UNCERTAINTY RELATION FOR STATE VARIABLES

Our second main result is a thermodynamic uncertainty relation for end-point and time-integrated state observables as defined in Eqs. (6.8) and (6.9). For both types of observables, it reads (see Section B.1)

$$[\Delta\mathcal{A}(T,v)]^2/D_{\mathcal{A}}(T,v) \leq \sigma(T,v), \tag{6.16}$$

where $\mathcal{A}(T,v) \in \{a(T,v), A(T,v)\}$. For $a(T,v)$, this relation shows that a lower bound for the mean total entropy production rate can be obtained by just observing the final state of the system. There is neither information required about the initial distribution nor information about the forces acting on the particle. This bound is especially useful for finite-time or relaxation processes where the total entropy production is not necessarily time-extensive.

## 6.5 SKETCH OF THE PROOF

To sketch the derivation of our main results (6.1) and (6.16) (see Section B.1 for a full proof), we use a recently obtained inequality, called the FRI, which relates the fluctuations of an observable with its response to an external perturbation [75]. Specifically, for this perturbation we choose the additional force $\epsilon Y(x,t;\epsilon)$ with a parameter $\epsilon$. Averages in the perturbed dynamics are denoted by $\langle\cdot\rangle^\dagger$. For a small force, i.e., for $\epsilon \to 0$, the FRI bounds the diffusion coefficient (6.15) for each choice of $X_T$ as [75]

$$D_X(T,v) \geq \frac{\left(\partial_\epsilon \langle X_T\rangle^\dagger|_{\epsilon=0}\right)^2}{1/T\int_0^T \mathrm{d}t\,\langle Y(x(t),t;\epsilon)^2/D\rangle^\dagger|_{\epsilon=0}}. \tag{6.17}$$

We choose $Y(x,t;\epsilon) = j(x,t';v^\dagger)/p(x,t';v^\dagger)$, scale time $t' = (1+\epsilon)t$ as in Refs. [76, 128], and additionally modify the speed parameter $v^\dagger = v/(1+\epsilon)$. The perturbed dynamics then corresponds to a system that evolves slightly slower or faster in time. The denominator in (6.17) becomes the total entropy production rate $\sigma(T,v)$. The nominator simplifies to $\Delta\mathcal{A}(T,v)$ for state variables and to $J^{\mathrm{I,II}}(T,v) + \Delta J^{\mathrm{I,II}}(T,v)$ for currents leading to our main results (6.1) and (6.16).

## 6.6 GENERALIZATION TO DISCRETE STATES: PROTEIN FOLDING

Our two main results (6.1) and (6.16) hold not only for overdamped Langevin systems but also for systems with discrete states. A paradigm for such a system is a protein undergoing conformational transitions. Experimental studies aim to infer the structure of the underlying Markovian network that possibly contains hidden folded states. For the protein Calmodulin, the transition rates between various folded and unfolded states have been measured as a function of an external force generated by optical tweezers in Ref. [26].

We apply our bounds to this system by using these experimental data. In Fig. 6.2(a), the topology of the network consisting of six different conformational states (denoted as in the original paper) is shown. Starting in the stationary state at a constant external force of $f_0 = 9.0$ pN, we drive the system in a force ramp according to the driving protocol $\lambda(vt) \equiv f_0 + vt(f_1 - f_0)$ with $f_1 = 11.0\,\mathrm{pN}$ and $vT = 1.0$.

For three different observables, we consider the quality factor of the resulting bound on the entropy production associated with this dynamical unfolding. One estimate according to Eq. (6.1) is obtained by observing the current between the unfolded state $U$ and any of the adjacent states $F \in \{F_{12}, F_{23}, F_{34}\}$,

$$\nu_T^{UF} \equiv [m_{UF}(T) - m_{FU}(T)]/T. \tag{6.18}$$

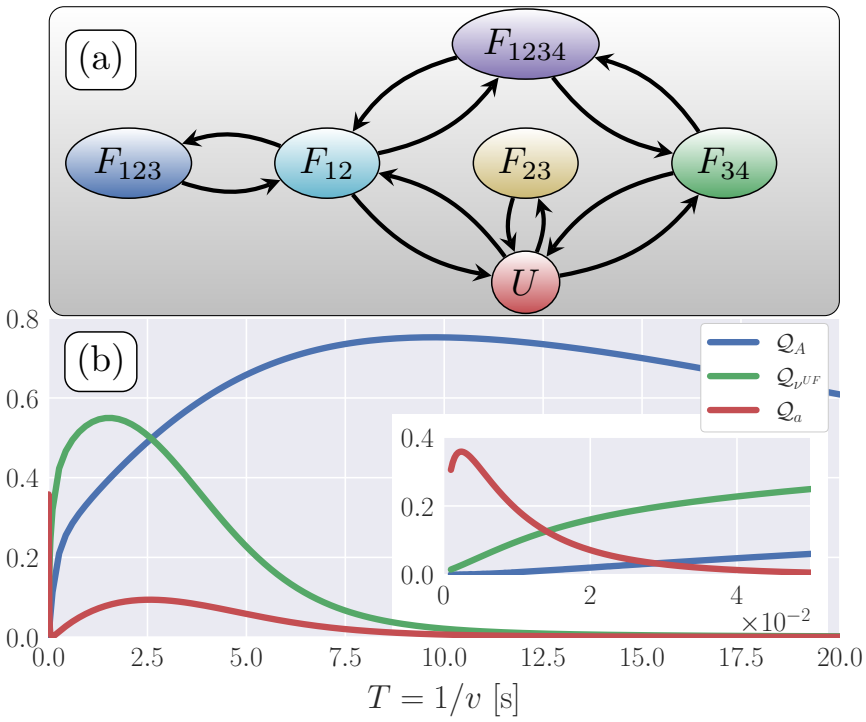


Figure 6.2: Dynamical unfolding of Calmodulin. (a) Network of its six states, comprising an unfolded state $U$, two partially folded states $F_{12}$ and $F_{34}$, a folded state $F_{1234}$, and two misfolded states $F_{23}$ and $F_{123}$. The force-dependent transition rates between the six states as extracted from Ref. [26] are given in Section B.5. (b) Three quality factors as defined in the main text as a function of the inverse driving speed $T = 1/v$. Inset shows data for fast driving.

The variable $m_{UF}$ counts the total number of transitions from the unfolded state $U$ to any of these states $F$ and $m_{FU}$ is the number of reverse transitions. Two further bounds are obtained using $a(i,\lambda) = \delta_{i,F_{12}}$ in Eq. (6.8) and $a(i,\lambda) = \delta_{i,U}$ in Eq. (6.9), which corresponds to the characteristic function of state $F_{12}$ and $U$, respectively [2]. The first choice corresponds to the probability for the protein to be in state $F_{12}$ at the end of the observation time and the latter one to the overall fraction of time the system has spent in the unfolded state $U$. We denote the corresponding quality factors by $\mathcal{Q}_a$ and $\mathcal{Q}_A$, respectively. The quality factors obtained from monitoring the mean, the fluctuations and the response of these three observables are shown in Fig. 6.2(b). The quality factor $\mathcal{Q}_A$ becomes best at slower driving, $T \simeq 10$, where it yields about 75% of the total entropy production rate. The estimate $\mathcal{Q}_{v^{UF}}$ through the current observable is especially strong for intermediate times $1.0 \leq T \leq 2.0$. The quality factor $\mathcal{Q}_a$ based on the observation of the final state is always weaker than the other two except for fast driving speeds $T = 1/v \sim 10^{-2}$, where it reaches a maximal value of about 40% as shown in the inset of Fig. 6.2(b). Obviously, in future experiments, one should explore the bounds resulting from as many experimentally accessible state and current observables as possible since we do not yet have a criterion for selecting *a priori* the observable that will yield the strongest bound.

## 6.7 GENERALIZATION TO MULTIPLE CONTROL PARAMETERS: TWO-STATE SYSTEM

Our two main results, Eqs. (6.1) and (6.16) can be generalized to systems that are driven by a set of control parameters $\{\lambda_\alpha(v_\alpha t)\}$ (see Sections B.1 and B.2). In this case, the operator defined in Eq. (6.2) must be replaced by $\Delta \equiv T\partial_T - \sum_\alpha v_\alpha \partial_{v_\alpha}$, i.e., Eq. (B.36).

For a simple illustration, we consider a two-state system shown in Fig. 6.3 (inset), which is initially prepared in equilibrium and driven through time-dependent energy levels

$$E_i(\boldsymbol{\lambda}_t) \equiv E_0^i \left[1 - \exp(-v_\alpha t)\right], \tag{6.19}$$

with $v_\alpha$ the speed control parameter, where $\alpha = i$ and $E_0^i$ the amplitude of driving for state $i \in \{1,2\}$. We choose the rates between two state $i$ and $j$ as

$$k_{ij}(\boldsymbol{\lambda}_t) = k_0 \exp\{-0.5\beta[E_j(\boldsymbol{\lambda}_t) - E_i(\boldsymbol{\lambda}_t)]\}, \tag{6.20}$$

with $k_0$ as basic timescale. In this model, the protocol depends on two speed parameter, i.e., $\boldsymbol{\lambda}_t \equiv \{\lambda_1(v_1 t), \lambda_2(v_2 t)\}$. We keep the final value of the protocol fixed, i.e., $v_1 T = \text{const}$ and $v_2 T = \text{const}$.

2 Note that $a(i,\lambda)$ is a straightforward generalization of the state variable $a(x,\lambda)$ defined in Eq. (6.8) to systems with discrete degrees of freedom, where the continuous state $x$ is replaced by the discrete state $i$ and the integral $\int \mathrm{d}x$ becomes a sum $\sum_i$.

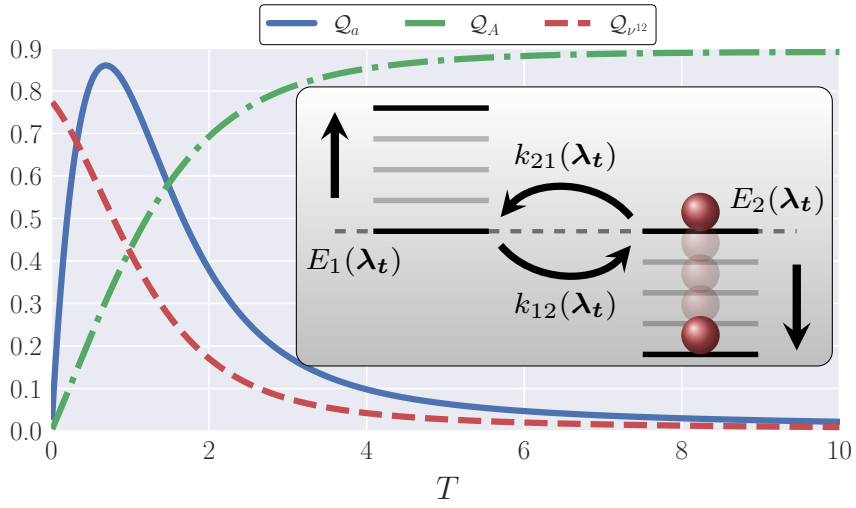


Figure 6.3: Quality factors in the two-state system (inset) for three different classes of observables as a function of observation time $T$. The parameters $k_0 = 1.0, E_0^1 = -1.0, E_0^2 = 1.0, \beta = 1.0, v_1 T = 0.5$, and $v_2 T = 1.5$ are kept fixed.

For three different observables, we consider the quality of the resulting bound. One estimate for the total entropy production using Eq. (6.1) is obtained by observing the current between state 1 and 2

$$v_T^{12} \equiv [m_{12}(T) - m_{21}(T)]/T, \tag{6.21}$$

where the variable $m_{ij}(T)$ counts the total number of transitions from state $i$ to state $j$. Two more bounds are obtained using $a(n_t, \lambda) = \delta_{n_t,2}$ in Eqs. (6.8) and (6.9), which corresponds to the characteristic function of state 2 either at the end of the observation time or time-averaged. The first choice corresponds to the probability to be in state 2 and the latter one to the fraction of time the system spends in this state. We denote the corresponding quality factors by $\mathcal{Q}_a$ and $\mathcal{Q}_A$, respectively. The quality factors obtained from monitoring the mean, the fluctuation and the response of these three observables are shown in Fig. 6.3. For fast driving $T \ll 1$, the current observable $v_T^{12}$ yields the best estimate for the total entropy production, whereas for intermediate speeds of driving $T \sim 1/k_0$, the observable based on the final state yields the best bound. In the limit of quasi-static driving, the fraction of time spent in state 2 yields up to 90% of the total entropy production rate. Throughout the whole range of driving speeds, the bounds based on these three observables yield at least 60% of the total entropy production rate.

Table 6.1: Unification of TURs with their range of applicability (y=yes, n=no). The factor $\Delta J(T, v)$ in Eq. (6.1) specialized to NESSs, PSSs and relaxation processes (RELs) towards equilibrium states or NESSs leads to the terms shown on the right-hand sides in the first column. Beyond these known cases, the new relation (6.1) is applicable for relaxation towards a PSS and for arbitrary time-dependent driving (TDD).

| $D_J\sigma/J^2 \geq \Xi$ | Ref. | NESS | PSS | REL | TDD |
|---|---|---|---|---|---|
| $\Xi = 1$ | [27, 28] | y | n | n | n |
| $\Xi = [1 + T\partial_T J/J]^2$ | [74, 128] | y | n | y[3] | n |
| $\Xi = [1 - \Omega\partial_\Omega J/J]^2$ | Eq. (5.1), [1] | y | y | n | n |
| $\Xi = [1 + \Delta J/J]^2$ | Eq. (6.1), [2] | y | y | y | y |

## 6.8 CONCLUDING PERSPECTIVE

We have derived a universal thermodynamic uncertainty relation that holds for current and state variables in systems that are time-dependently driven from an arbitrary initial state over a finite time-interval. The mean and fluctuations of any such observable yields a lower bound on the overall entropy production. Depending on the conditions the observables leading to the relative best bound may change. For observables based on currents, our relation becomes the established ones for the very special cases of time-independent driving, of periodic driving and of relaxation at constant control parameters as summarized in Table 6.1. In this sense, our work presents a unifying perspective on extant TURs.

With these relations we have provided universally applicable tools that will allow thermodynamic inference in time-dependently driven systems. We emphasize that it is neither necessary to know the precise coupling between the system and the control nor to know the interactions within the system. It suffices that the experimentalist can change the overall speed of the control slightly and measure the resulting response of an observable. These rather weak demands should facilitate the application to systems beyond colloidal particles and single molecules manipulated with time-dependent optical traps.

3 only valid for time-independent driving

Part IV

# QUALITY OF THE THERMODYNAMIC UNCERTAINTY RELATION

# 7 FAST AND SLOW DRIVING

So far we derived *inter alia* bounds on the total entropy production rate for periodically driven and arbitrary time-dependently driven systems. Due to their universality and operational accessibility, these bounds provide useful tools to infer entropy production and unify the TURs in Refs. [27, 28, 72, 73, 76, 128]. Since these lower bounds are valid for various types of observables, a crucial question is which observable yields the best estimate for entropy production and how sharp these bounds typically are. Furthermore, it is *a priori* not clear under which conditions they can be saturated. A first step to answer these questions is to analyze limiting cases in which analytical calculations are feasible.

In this chapter, we analyze the quality of the TUR for time-dependent driving (6.1) in the limiting cases of fast and slow driving for overdamped Langevin systems. These theoretically interesting and analytically accessible limiting cases are especially relevant for heat engines [41, 42, 137, 154] and bit erasure protocols [148–150]. The slow driving limit is essential for heat engines since they typically reach maximum efficiency when driven quasistatically, whereas the fast driving limit is important for bit erasure as practical information processing can require fast erasure. We show that in each limiting case at least one optimal class of observable exists that generically yields an estimate of order one for the total entropy production rate. Furthermore, we show that the time-dependent uncertainty relation in Eq. (6.1) simplifies to the conventional form of the steady-state TUR in Refs. [27, 28] in the fast-driving limit. In this limiting case, we demonstrate that a current proportional to the total entropy production rate can saturate the TUR. For the slow-driving limit, we show that the choice of the optimal observable depends on whether or not a non-conservative force is applied. Moreover, we show that these results hold not only for systems with continuous degrees of freedom, but also for systems with a discrete set of states as we illustrate for a driven three-state model.

## 7.1 SETUP

### 7.1.1 *Dynamics*

We consider a system with one continuous degree of freedom $x(t)$. The dynamics is given by an overdamped Langevin equation

$$\dot{x}(t) = \mu F(x(t), \lambda_t) + \zeta(t), \tag{7.1}$$

where $\zeta(t)$ is a zero-mean Gaussian white noise satisfying

$$\langle \zeta(t) \rangle = 0, \tag{7.2}$$
$$\langle \zeta(t)\zeta(t') \rangle = 2D\delta(t-t'). \tag{7.3}$$

The system is driven by a time-dependent force

$$F(x,\lambda_t) \equiv f(\lambda_t) - \partial_x V(x,\lambda_t), \tag{7.4}$$

which consists of a non-conservative force $f(\lambda_t)$ and a conservative part $-\partial_x V(x,\lambda_t)$. Both contributions depend on a time-dependent protocol $\lambda_t \equiv \lambda(vt)$. Here, $v$ denotes the speed of driving and $D \equiv \mu/\beta$ is the diffusion constant, where $\mu$ is the mobility and $\beta$ is the inverse temperature. Equivalently, we can use a Fokker-Planck equation

$$\partial_t p(x,t) = -\partial_x(\mu F(x,\lambda_t) - D\partial_x)p(x,t) \tag{7.5}$$

describing the dynamics for the probability $p(x,t)$ to find the system in state $x$ at time $t$. The system is observed up to time $T$, where the protocol $\lambda_t$ evolves from value $\lambda(0)$ to $\lambda(\tau_f \equiv vT)$. In the following, we keep the final value $\tau_f$ of the protocol fixed, i.e., the observation time $T = \tau_f/v$ is coupled to the speed of driving. Equation (7.5) describes probability conservation and, hence, is a continuity equation for the probability current

$$j(x,t) \equiv (\mu F(x,\lambda_t) - D\partial_x)p(x,t). \tag{7.6}$$

In this chapter, we derive our main results for systems with a single continuous degree of freedom. These results can generically be adapted to systems with multiple time-dependently driven degrees of freedom, in principle. A discussion about possible deviations in special cases is given in a concluding perspective at the end of this chapter.

### 7.1.2 *Observables*

The framework of stochastic thermodynamics allows us to define several types of observables for arbitrary time-dependently driven systems [2, 8]. These observables depend on the state $x(t)$ of the system or the velocity $\dot{x}(t) \equiv \partial_t x(t)$. The first type of observable we are focusing on is called a state variable $a(x,\lambda_t)$. This variable can be either observed at a fixed observation time

$$a_T \equiv a(x_T,\lambda_T) \tag{7.7}$$

or it can be time-averaged over a finite-time $T$

$$A_T \equiv \frac{1}{T}\int_0^T \mathrm{d}t\, a(x_t,\lambda_t), \tag{7.8}$$

where $x_t \equiv x(t)$. The second kind of observable is a current, which is odd under time reversal. Here, we distinguish between a current depending on the time spent in a certain state

$$J_T^b \equiv \frac{1}{T}\int_0^T \mathrm{d}t\, \dot{b}(x_t, \lambda_t), \tag{7.9}$$

which depends on the time-derivative of a state variable $\dot{b}(x_t, \lambda_t) \equiv (\partial_t \lambda_t)\partial_\lambda b(x_t, \lambda)|_{\lambda=\lambda_t}$ and a current depending on the velocity, i.e.,

$$J_T^d \equiv \frac{1}{T}\int_0^T \mathrm{d}t\, d(x_t, \lambda_t) \circ \dot{x}_t, \tag{7.10}$$

where $d(x_t, \lambda_t)$ is a function of the state and $\circ$ denotes the Stratonovich product. Examples for the currents defined in Eqs. (7.9) and (7.10) are the power by choosing $b(x_t, \lambda_t) = V(x_t, \lambda_t)$ and the heat flux by choosing $d(x_t, \lambda_t) = \beta F(x_t, \lambda_t)$, respectively. A further important observable of interest is the mean total entropy production rate

$$\sigma(T, v) \equiv \frac{1}{T}\int_0^T \mathrm{d}t \int \mathrm{d}x\, \frac{j^2(x,t)}{Dp(x,t)}. \tag{7.11}$$

The fluctuations around the mean value $\langle X_T \rangle$ of any of the above introduced observables $X_T \in \{a_T, A_T, J_T^{b,d}\}$ are quantified by the diffusion coefficient

$$D_X(T, v) \equiv T\left(\langle X_T^2 \rangle - \langle X_T \rangle^2\right)/2, \tag{7.12}$$

where $\langle \cdot \rangle$ denotes the mean value.

### 7.1.3 *Quality factors and the thermodynamic uncertainty relation*

The generalization of the thermodynamic uncertainty relation to arbitrary time-dependent driving in Chapter 6 (see also Ref. [2]) can be applied to all types of observables defined in Eqs. (7.7)–(7.10). For current-type observables $J_T \in \{J_T^d, J_T^b\}$ the uncertainty relation

$$1 \geq \frac{\mathcal{R}_J(T, v)}{D_J(T, v)\sigma(T, v)} \tag{7.13}$$

imposes a bound in terms of the response term

$$\mathcal{R}_J(T, v) \equiv [J(T, v) + \Delta J(T, v)]^2 \tag{7.14}$$

with mean value $J(T, v) \equiv \langle J_T \rangle$ and operator $\Delta \equiv T\partial_T - v\partial_v$. The term $\Delta J(T, v)$ describes the change of the current with respect to a slight change of the observation time $T$ and the speed of driving $v$. For state variables $\mathcal{A}_T \in \{a_T, A_T\}$ the uncertainty relation

$$1 \geq \frac{\mathcal{R}_\mathcal{A}(T, v)}{D_\mathcal{A}(T, v)\sigma(T, v)} \tag{7.15}$$

involves a modified response term

$$\mathcal{R}_{\mathcal{A}}(T,v) \equiv [\Delta\mathcal{A}(T,v)]^2, \tag{7.16}$$

where $\mathcal{A}(T,v) \equiv \langle \mathcal{A}_T \rangle$ denotes the mean value of a state variable.

For both relations Eqs. (7.13) and (7.15) we define the quality factors as

$$\mathcal{Q}_J \equiv \frac{\mathcal{R}_J(T,v)}{D_J(T,v)\sigma(T,v)} \tag{7.17}$$

and

$$\mathcal{Q}_{\mathcal{A}} \equiv \frac{\mathcal{R}_{\mathcal{A}}(T,v)}{D_{\mathcal{A}}(T,v)\sigma(T,v)}, \tag{7.18}$$

respectively. Both quality factors are always larger than zero and smaller than one. If a quality factor is zero, no information can be inferred about the entropy production by observing the response and fluctuations of an observable. However, if a quality factor is one, the uncertainty relation is saturated and we can determine the total entropy production exactly.

### 7.1.4 *Timescale separation*

The aim of this chapter is to analyze the limits of fast driving and slow driving. Hence, it is useful to introduce a timescale separation between the timescale of the system $t_{\text{sys}}$ and the timescale of the driving $v^{-1}$. If the relaxation timescales in the system are approximately of the same order of magnitude, we can choose the basic timescale of the system $t_{\text{sys}}$ as this order of magnitude. However, if the relaxation timescales have different orders of magnitudes, e.g., due to a complex topology like energy barriers in the system, we have to distinguish between the limiting cases of fast driving and slow driving: for the fast-driving limit the basic timescale of the system $t_{\text{sys}}$ has to be chosen as the relaxation timescale describing the fastest relaxation. In contrast, for the limit of slow driving we have to chose $t_{\text{sys}}$ as the timescale that describes the slowest relaxation. Depending on the above discussed cases, the fastest or slowest relaxation timescale in the system is proportional to the inverse of the mobility $\mu$. Hence, the mobility is proportional to the inverse of the timescale $t_{\text{sys}}$ of the system. This circumstance allows us to define a scaled mobility

$$\tilde{\mu} \equiv \mu t_{\text{sys}}. \tag{7.19}$$

Plugging Eq. (7.19) into Eq. (7.5) and using the substitution $\tau \equiv vt = \tau_f t/T$ leads to the scaled Fokker-Planck equation

$$\partial_\tau \tilde{p}(x,\tau) = -\left(\frac{T}{\tau_f t_{\text{sys}}}\right) \partial_x(\tilde{\mu}F(x,\lambda_\tau) - \tilde{D}\partial_x)\tilde{p}(x,\tau) \tag{7.20}$$

with a scaled diffusion constant $\tilde{D} \equiv \tilde{\mu}/\beta$. The density $\tilde{p}(x,\tau) \equiv p(x,\tau/v)$ depends on the speed of driving $v$, i.e.,

$$\tilde{p}(x,\tau) = \tilde{p}(x,\tau;v). \tag{7.21}$$

We further define the scaled probability current as

$$\tilde{j}(x,\tau;v) \equiv (\tilde{\mu}F(x,\lambda_\tau) - \tilde{D}\partial_x)\tilde{p}(x,\tau;v). \tag{7.22}$$

For the sake of simplicity, we change the notation $\tilde{p}(x,\tau;v) \to p(x,\tau;v)$ and $\tilde{j}(x,\tau;v) \to j(x,\tau;v)$ in the following. The scaled Fokker-Planck equation (7.20) then reads

$$\partial_\tau p(x,\tau;v) = (vt_{\mathrm{sys}})^{-1}\hat{\mathcal{L}}_{\mathrm{FP}}\,(x,\lambda_\tau)\,p(x,\tau;v), \tag{7.23}$$

with the scaled Fokker-Planck operator

$$\hat{\mathcal{L}}_{\mathrm{FP}}\,(x,\lambda_\tau) \equiv -\partial_x(\tilde{\mu}F(x,\lambda_\tau) - \tilde{D}\partial_x). \tag{7.24}$$

The general solution of Eq. (7.23) for a given initial distribution $p(x,0)$ reads

$$p(x,\tau;v) = \hat{U}\,(x,\tau,0)\,p(x,0), \tag{7.25}$$

where

$$\hat{U}\,(x,\tau_2,\tau_1) \equiv \overrightarrow{\exp}\left(\int_{\tau_1}^{\tau_2} \mathrm{d}\tau\,(vt_{\mathrm{sys}})^{-1}\hat{\mathcal{L}}_{\mathrm{FP}}\,(x,\lambda_\tau)\right) \tag{7.26}$$

is the time evolution operator and $\overrightarrow{\exp}\,(\cdot)$ denotes a time-ordered exponential. Via Eq. (7.26) we can define the propagator as

$$p(x_2,\tau_2|x_1,\tau_1) \equiv \hat{U}\,(x_2,\tau_2,\tau_1)\,\delta(x_2-x_1), \tag{7.27}$$

where $\tau_2 \geq \tau_1$ and $\delta(\cdot)$ denotes a Dirac delta.

The mean values of the state variables (7.7) and (7.8) in terms of the scaled time $\tau = vt = \tau_f t/T$ are given by

$$a(T,v) \equiv \int \mathrm{d}x\,a(x,\lambda_{\tau_f})p(x,\tau_f;v) \tag{7.28}$$

and

$$A(T,v) \equiv \frac{1}{\tau_f}\int_0^{\tau_f}\mathrm{d}\tau\int \mathrm{d}x\,a(x,\lambda_\tau)p(x,\tau;v), \tag{7.29}$$

respectively, whereas the mean values of the currents (7.9) and (7.10) are given by

$$J_b(T,v) \equiv \frac{v}{\tau_f}\int_0^{\tau_f}\mathrm{d}\tau\int \mathrm{d}x\,\dot{b}(x,\lambda_\tau)p(x,\tau;v) \tag{7.30}$$

and

$$J_d(T,v) \equiv \frac{1}{t_{\mathrm{sys}}\tau_f}\int_0^{\tau_f}\mathrm{d}\tau\int \mathrm{d}x\,d(x,\lambda_\tau)j(x,\tau;v), \tag{7.31}$$

respectively. Here, $\dot{b}(x,\lambda_\tau) \equiv \partial_\tau b(x,\lambda_\tau)$ is the time-derivative in terms of timescale $\tau$ and

$$j(x,\tau;v) \equiv (\tilde{\mu}F(x,\lambda_\tau) - \tilde{D}\partial_x)p(x,\tau;v) \tag{7.32}$$

is the scaled probability current. Moreover, the mean total entropy production rate (7.11) in terms of the scaled quantities is given by

$$\sigma(T,v) \equiv \frac{1}{t_{\text{sys}}\tau_f}\int_0^{\tau_f} \mathrm{d}\tau \int \mathrm{d}x\, \frac{j^2(x,\tau;v)}{\tilde{D}p(x,\tau;v)}. \tag{7.33}$$

The diffusion coefficients of the quantities defined in Eqs. (7.7)–(7.10) can be written in terms of correlation functions between state variables and, hence, depend on the propagator (7.27). Their explicit expressions in terms of the scaled time $\tau$ can be found in Section C.1.1.

## 7.2 FAST DRIVING

We first consider the limit of fast driving, where the driving is much faster than the fastest relaxation timescale of the system. The limit of fast driving requires the parameter

$$\epsilon_f \equiv \frac{1}{vt_{\text{sys}}} \ll 1 \tag{7.34}$$

to be small, i.e., $v^{-1} \ll t_{\text{sys}}$ or equivalently, $T \ll \tau_f t_{\text{sys}}$. This means that the timescale of the driving $v^{-1} = T/\tau_f$ is much shorter than the timescale $t_{\text{sys}}$ on which the fastest relaxation of the system takes place. The time evolution operator in Eq. (7.26) can be expanded in terms of $\epsilon_f$, i.e.,

$$\hat{U}(x,\tau_2,\tau_1) = 1 + \epsilon_f \int_{\tau_1}^{\tau_2} \mathrm{d}\tau\, \hat{\mathcal{L}}_{\text{FP}}(x,\lambda_\tau) + \mathcal{O}\left(\epsilon_f^2\right). \tag{7.35}$$

Via Eq. (7.25) the density is given by

$$p(x,\tau;v) = p^{(0)}(x,\tau) + \epsilon_f p^{(1)}(x,\tau) + \mathcal{O}\left(\epsilon_f^2\right) \tag{7.36}$$

with zeroth and first order

$$p^{(0)}(x,\tau) = p(x,0), \tag{7.37}$$
$$p^{(1)}(x,\tau) = \hat{\mathcal{L}}_{\text{eff}}(x,\tau,0)\, p(x,0), \tag{7.38}$$

respectively, and

$$\hat{\mathcal{L}}_{\text{eff}}(x,\tau,0) \equiv \int_0^{\tau} \mathrm{d}\tau'\, \hat{\mathcal{L}}_{\text{FP}}(x,\lambda_{\tau'}) \tag{7.39}$$

being the time-averaged Fokker-Planck operator. The probability current is analogously given by

$$j(x,\tau;v) = j^{(0)}(x,\tau) + \epsilon_f j^{(1)}(x,\tau) + \mathcal{O}\left(\epsilon_f^2\right) \tag{7.40}$$

with zeroth and first order

$$j^{(0)}(x,\tau) = (\tilde{\mu}F(x,\lambda_\tau) - \tilde{D}\partial_x)p(x,0), \tag{7.41}$$
$$j^{(1)}(x,\tau) = (\tilde{\mu}F(x,\lambda_\tau) - \tilde{D}\partial_x)\hat{\mathcal{L}}_{\text{eff}}(x,\tau,0)\,p(x,0), \tag{7.42}$$

respectively. The leading order of the density (7.37) shows that the fast driving leaves the initial distribution over the observation time unchanged. The density can then approximately be described by the time-independent initial condition. As a consequence, the leading order of the probability current (7.41) depends only on the protocol. Furthermore, we can use (7.35) to get the leading orders of the propagator (7.27), i.e.,

$$p(x_2,\tau_2|x_1,\tau_1) = p^{(0)}(x_2,\tau_2|x_1,\tau_1) + \epsilon_f p^{(1)}(x_2,\tau_2|x_1,\tau_1) + \mathcal{O}\left(\epsilon_f^2\right). \tag{7.43}$$

with zeroth and first order

$$p^{(0)}(x_2,\tau_2|x_1,\tau_1) = \delta(x_2 - x_1), \tag{7.44}$$
$$p^{(1)}(x_2,\tau_2|x_1,\tau_1) = \hat{\mathcal{L}}_{\text{eff}}(x_2,\tau_2,\tau_1)\,\delta(x_2 - x_1), \tag{7.45}$$

respectively.

To determine the leading orders of the quality factors for the different types of observables, we use Eqs. (7.36), (7.40) as well as (7.43) to determine the leading orders of the scaled mean values, Eqs. (7.28)–(7.31), their response terms, their corresponding diffusion coefficients, Eqs. (C.1)–(C.4), as well as the scaled total entropy production rate (7.33). Here, all mean values and diffusion coefficients can be written as

$$X(T,v) \equiv \sum_{n=0} \left(\epsilon_f\right)^n X^{(n)}(T,v) \tag{7.46}$$

and

$$D_X(T,v) \equiv \sum_{n=0} \left(\epsilon_f\right)^n D_X^{(n)}(T,v), \tag{7.47}$$

respectively with mean values $X(T,v) \in \{a(T,v), A(T,v), \epsilon_f J_b(T,v), J_d(T,v)\}$ and diffusion coefficients $D_X(T,v) \in \{D_a(T,v), D_A(T,v), \epsilon_f D_{J_b}(T,v), D_{J_d}(T,v)\}$. Their leading orders and the resulting quality factors are shown in Table 7.1 (see Section C.2 for details of the derivation). The response terms of the state variables vanish like $\epsilon_f^2$, whereas the response terms of the current observables are of $\mathcal{O}(1)$. The diffusion coefficients of the state variables vanish like $\epsilon_f$ because their variances are of $\mathcal{O}(1)$. This circumstance is a consequence of the fact that the fast driving conserves the initial distribution. In contrast to the state variables $a(T,v)$ and $A(T,v)$ the diffusion coefficient for currents depending on the residence time $D_{J_b}$ diverges proportional

Table 7.1: Leading orders of the total entropy production rate $\sigma(T,v)$, the response terms $\mathcal{R}_X$ of observables $X$, the diffusion coefficents $D_X$ and the quality factors $\mathcal{Q}_X$ of the observables in the limit of fast driving.

| $X$ | $\mathcal{R}_X$ | $D_X$ | $\sigma(T,v)$ | $\mathcal{Q}_X$ |
|---|---|---|---|---|
| $a(T,v)$ | $[\Delta a(T,v)]^2 = \mathcal{O}\left(\epsilon_f^2\right)$ | $\mathcal{O}(\epsilon_f)$ | $\mathcal{O}(1)$ | $\mathcal{O}(\epsilon_f)$ |
| $A(T,v)$ | $[\Delta A(T,v)]^2 = \mathcal{O}\left(\epsilon_f^2\right)$ | $\mathcal{O}(\epsilon_f)$ | $\mathcal{O}(1)$ | $\mathcal{O}(\epsilon_f)$ |
| $J_b(T,v)$ | $[J_b(T,v) + \Delta J_b(T,v)]^2 = \mathcal{O}(1)$ | $\mathcal{O}\left(\epsilon_f^{-1}\right)$ | $\mathcal{O}(1)$ | $\mathcal{O}(\epsilon_f)$ |
| $J_d(T,v)$ | $[J_d(T,v) + \Delta J_d(T,v)]^2 = \mathcal{O}(1)$ | $\mathcal{O}(1)$ | $\mathcal{O}(1)$ | $\mathcal{O}(1)$ |

to $\epsilon_f^{-1}$ due to the additional time-derivative of the increment. Together with the fact that the mean total entropy production rate is of $\mathcal{O}(1)$ these results imply quality factors that vanish linearly with $\epsilon_f$ for all observables except for the quality factor $\mathcal{Q}_{J_d}$, which is of $\mathcal{O}(1)$.

To summarize, in the limit of fast driving generically only the current observable $J_d(T,v)$ yields an useful estimate for entropy production. Moreover, the explicit expression for quality factor reads (see Section C.2)

$$\mathcal{Q}_{J_d} \approx \frac{\left[\int_0^{\tau_f} \mathrm{d}\tau \int \mathrm{d}x\, d(x,\lambda_\tau) j^{(0)}(x,\tau)\right]^2}{\left[\int_0^{\tau_f} \mathrm{d}\tau \int \mathrm{d}x\, d^2(x,\lambda_\tau) p(x,0)\right] \left[\int_0^{\tau_f} \mathrm{d}\tau \int \mathrm{d}x\, \frac{\left(j^{(0)}(x,\tau)\right)^2}{\tilde{D} p(x,0)}\right]}. \tag{7.48}$$

Here, the term $\Delta J_d(T,v)$ vanishes, which implies that Eq. (7.13) simplifies to the conventional form of the steady-state uncertainty relation in Refs. [27, 28]. Furthermore, Eq. (7.48) shows that the TUR for time-dependent driving can be saturated for the choice

$$\begin{aligned} d(x,\lambda_\tau) &= (\tilde{\mu} F(x,\lambda_\tau) - D[\partial_x p(x,0)]/p(x,0))/\tilde{D} \\ &= j^{(0)}(x,\tau)/(\tilde{D} p(x,0)), \end{aligned} \tag{7.49}$$

i.e., when the current is chosen to be the total entropy production rate. We remark that choosing the total entropy production as a current in Eq. (7.13) is in general not allowed due to the fact that the increment for the entropy production $d_\sigma \equiv j(x,\tau;v)/p(x,\tau;v)$ is not a function of the protocol, i.e., $d_\sigma \neq d_\sigma(x,\lambda_\tau)$ (see derivation in Section B.1). However, in the fast-driving limit the probability current becomes a function of the protocol, i.e., $j(x,\tau;v) = j^{(0)}(x,\lambda_\tau) + \mathcal{O}(\epsilon_f)$ and, thus, the total entropy production rate fulfills the uncertainty relation (7.13). Moreover, for a constant protocol the result in Eq. (7.48) for fast driving reduces to the result for steady-states in Refs. [88, 89] in the limit of short observation times. As a consequence, we have generalized this

result to arbitrary time-dependent driving and have shown that the total entropy production rate can always saturate the TUR in the short-time limit beyond steady-states for arbitrary driving.

## 7.3 SLOW DRIVING

As the second limiting case we consider the limit of slow driving, where the time-dependent driving is much slower than the slowest relaxation time of the system. In this limit, the parameter

$$\epsilon_s \equiv v t_{\mathrm{sys}} \ll 1 \tag{7.50}$$

is assumed to be small. Here, the timescale of the driving $v^{-1} = T/\tau_f$ is large compared to the timescale of the system $t_{\mathrm{sys}}$ describing the slowest relaxation in the system. If the system is initially prepared in an arbitrary distribution $p(x,0)$ it will relax into the stationary state at fixed $\lambda_0$. This relaxation process occurs on a timescale that is much faster than the timescale of the external driving. In the following, we focus on the slow timescale on which the protocol is changing. Therefore, we assume that the system has already relaxed into the stationary state at $\lambda_0$.

The density depending only on the slow timescale

$$p(x,\tau;v) = p^{(0)}(x,\tau) + \epsilon_s p^{(1)}(x,\tau) + \mathcal{O}(\epsilon_s^2) \tag{7.51}$$

relaxes instantaneously into the stationary state

$$p^{(0)}(x,\tau) = p^s(x,\lambda_\tau) \tag{7.52}$$

at fixed $\lambda_\tau$, i.e., it fulfills

$$\hat{\mathcal{L}}_{\mathrm{FP}}(x,\lambda_\tau)\, p^{(0)}(x,\tau) = 0. \tag{7.53}$$

Equation (7.53) follows by inserting Eq. (7.51) into (7.23) and by comparing the zeroth orders in $\epsilon_s$. The time dependence of the density (7.52) is given through the protocol $\lambda_\tau$. The density corresponds either to a NESS or an equilibrium state at a fixed protocol $\lambda_\tau$. If the density is that of a NESS at fixed $\lambda_\tau$, the probability current

$$j(x,\tau;v) = j^{(0)}(x,\tau) + \epsilon_s j^{(1)}(x,\tau) + \mathcal{O}(\epsilon_s^2) \tag{7.54}$$

converges to a finite value

$$j^{(0)}(x,\tau) = (\tilde{\mu} F(x,\lambda_\tau) - \tilde{D}\partial_x) p^s(x,\lambda_\tau). \tag{7.55}$$

In contrast, if the density is an equilibrium state at fixed $\lambda_\tau$, the driving is quasi-static and the probability current vanishes such that $j^{(0)}(x,\tau) = 0$ and

$$j(x,\tau;v) = \epsilon_s j^{(1)}(x,\tau) + \mathcal{O}(\epsilon_s^2). \tag{7.56}$$

The time evolution operator (7.26) converges to the leading order

$$\hat{U}^{(0)}(x,\tau_2,\tau_1) \equiv \lim_{\epsilon_s\to 0} \overrightarrow{\exp}\left(\int_{\tau_1}^{\tau_2} \mathrm{d}\tau\, \epsilon_s^{-1} \hat{\mathcal{L}}_{\mathrm{FP}}(x,\lambda_\tau)\right), \tag{7.57}$$

which satisfies

$$\hat{U}^{(0)}(x,\tau_2,\tau_1)\,\rho(x,\tau_1) = p^s(x,\lambda_{\tau_2}) \tag{7.58}$$

for an arbitrary density $\rho(x,\tau)$. Equation (7.58) shows that the time evolution operator transforms any density into the stationary state at fixed $\lambda_\tau$. As a consequence, the leading order of the propagator is given by

$$p(x_2,\tau_2|x_1,\tau_1) = p(x_2,\lambda_{\tau_2}) + \mathcal{O}(\epsilon_s). \tag{7.59}$$

We now use Eqs. (7.51), (7.54) and (7.59) to determine the leading orders of the scaled mean values, Eqs. (7.28)–(7.31), their response terms, their corresponding diffusion coefficients, Eqs. (C.1)–(C.4), as well as the scaled total entropy production rate (7.33). We assume that all mean values and diffusion coefficients can be written as

$$X(T,v) \equiv \sum_{n=0} (\epsilon_s)^n\, X^{(n)}(T,v) \tag{7.60}$$

and

$$D_X(T,v) \equiv \sum_{n=0} (\epsilon_s)^n\, D_X^{(n)}(T,v) \tag{7.61}$$

respectively, with mean values $X(T,v) \in \{a(T,v), A(T,v), J_{b,d}(T,v)\}$ and diffusion coefficients $D_X(T,v) \in \{\epsilon_s D_a(T,v), D_A(T,v), D_{J_{b,d}}(T,v)\}$. Their leading orders and the resulting quality factors are shown in Table 7.2 (see Section C.3 for details of the derivation).

The response terms of the state variables vanish like $\epsilon_s^2$ due to the fact that in the stationary state at fixed $\lambda_\tau$ the state variables are invariant under a perturbation that scales the time [2, 75, 155]. The same argument holds for the response term of the current $J_b(T,v)$, which vanishes like $\epsilon_s^4$. The additional power of two comes from the time-derivative of the increment. If a non-conservative force is applied, the system is driven into a NESS at fixed $\lambda_\tau$. In this case, the current $J_d(T,v)$ gets rescaled after applying the latter mentioned perturbation of rescaling the time. Hence, the response term of this current is equal to its squared mean value up to order $\epsilon_s$ which implies a response term of $\mathcal{O}(1)$. However, if only a conservative force is applied, this symmetry does no longer hold because the current vanishes as the system is in an equilibrium state at fixed $\lambda_\tau$. Consequently, the response term vanishes like $\epsilon_s^2$.

The diffusion coefficient of the state variable $A(T,v)$ and the current $J_d(T,v)$ are of $\mathcal{O}(1)$ because their fluctuations are finite in the

Table 7.2: Leading orders of the total entropy production rate $\sigma(T,v)$, the response terms $\mathcal{R}_X$ of observables $X$, the diffusion coefficents $D_X$ and the quality factors $\mathcal{Q}_X$ of the observables in the limit of slow driving. In this limit, we have to distinguish whether a non-conservative force $f(\lambda_t)$ is applied to the system or not: if a non-conservative force is applied the system is in a NESS at fixed $\lambda_\tau$ (NESS). However, if only a conservative force is applied, the system is in an equilibrium state (EQ) for a fixed $\lambda_\tau$.

| $X$ | $\mathcal{R}_X$ | | $D_X$ | $\sigma(T,v)$ | | $\mathcal{Q}_X$ | |
|---|---|---|---|---|---|---|---|
| | NESS | EQ | | NESS | EQ | NESS | EQ |
| $a(T,v)$ | $\mathcal{O}(\epsilon_s^2)$ | $\mathcal{O}(\epsilon_s^2)$ | $\mathcal{O}(\epsilon_s^{-1})$ | $\mathcal{O}(1)$ | $\mathcal{O}(\epsilon_s^2)$ | $\mathcal{O}(\epsilon_s^3)$ | $\mathcal{O}(\epsilon_s)$ |
| $A(T,v)$ | $\mathcal{O}(\epsilon_s^2)$ | $\mathcal{O}(\epsilon_s^2)$ | $\mathcal{O}(1)$ | $\mathcal{O}(1)$ | $\mathcal{O}(\epsilon_s^2)$ | $\mathcal{O}(\epsilon_s^2)$ | $\mathcal{O}(1)$ |
| $J_b(T,v)$ | $\mathcal{O}(\epsilon_s^4)$ | $\mathcal{O}(\epsilon_s^4)$ | $\mathcal{O}(\epsilon_s^2)$ | $\mathcal{O}(1)$ | $\mathcal{O}(\epsilon_s^2)$ | $\mathcal{O}(\epsilon_s^2)$ | $\mathcal{O}(1)$ |
| $J_d(T,v)$ | $\mathcal{O}(1)$ | $\mathcal{O}(\epsilon_s^4)$ | $\mathcal{O}(1)$ | $\mathcal{O}(1)$ | $\mathcal{O}(\epsilon_s^2)$ | $\mathcal{O}(1)$ | $\mathcal{O}(\epsilon_s^2)$ |

stationary state at fixed $\lambda_\tau$. The instantaneous state variable diverges proportional to $\epsilon_s^{-1}$ due to the factor of $T$ in the definition of its diffusion constant. The diffusion coefficient of the current $J_b(T,v)$ vanishes like $\epsilon_s$ due to the time-derivative of its increment. The total entropy production rate is of $\mathcal{O}(1)$, if a non-conservative force is applied. In this case the probability currents do not vanish and are of $\mathcal{O}(1)$. In contrast, if the system is only driven by a conservative force, the total entropy production rate is of $\mathcal{O}(\epsilon_s^2)$. In this case, the system is in an equilibrium state at fixed $\lambda_\tau$ and, hence, the probability currents vanish like $\epsilon_s$. Combining these results yields the leading orders of the quality factors: if a non-conservative force is applied, all quality factors except the quality factor for the current $J_d(T,v)$ vanish. In contrast, if only a conservative force is applied, the quality factors of the state variable $A(T,v)$ and of the current $J_b(T,v)$ are of $\mathcal{O}(1)$. The other quality factors vanish asymptotically. To summarize, a useful estimate for the entropy production rate is only possible for the current $J_d(T,v)$, if a non-conservative force is applied or for both, the state variable $A(T,v)$ and the current $J_b(T,v)$, if the system is driven by a conservative force only.

## 7.4 SYSTEMS WITH DISCRETE STATES

### 7.4.1 *General approach*

For a system with discrete degrees of freedom, the dynamics for the probability to find the system in a discrete state $i$ is described by the master equation

$$\partial_t p_i(t;v) = -\sum_j j_{ij}(t;v) \tag{7.62}$$

with probability current

$$j_{ij}(t;v) \equiv p_i(t;v)k_{ij}(\lambda_t) - p_j(t;v)k_{ji}(\lambda_t), \tag{7.63}$$

where we introduced the dependence with respect to the speed parameter $v$ as the second argument for both, the probability $p_i(t;v)$ to find the system in a state $i$ and the probability current $j_{ij}(t;v)$ between two states $i$ and $j$. The transition rates $k_{ij}(\lambda_t)$ between two states $i$ and $j$ are time-dependent through the protocol $\lambda_t$ and fulfill the local detailed balance condition

$$\frac{k_{ij}(\lambda_t)}{k_{ji}(\lambda_t)} = \exp\{-\beta\left[E_j(\lambda_t) - E_i(\lambda_t)\right] - \mathcal{A}_{ij}(\lambda_t)\}, \tag{7.64}$$

where $\beta$ denotes the inverse temperature, $E_i(\lambda_t)$ denotes the time-dependent energy of state $i$ and $\mathcal{A}_{ij}(\lambda_t)$ is a driving affinity, which drives the system additionally to the time-dependent energies into a non-equilibrium state.

In the following, we are interested in the discrete counterparts of the several types of observables discussed in Section 7.1.2. As an example for the instantaneous state variable, we consider the variable

$$a_T^i = \delta_{i,n_T}. \tag{7.65}$$

Its mean value is the probability to find the system in state $i$ at the end of the observation time $T$. Here, $\delta_{i,n_t}$ is one, if the trajectory $n_t$ is in state $i$ and zero, otherwise. We are further interested in the time-average over this variable

$$A_T^i = \frac{1}{T}\int_0^T \mathrm{d}t\, \delta_{i,n_t}, \tag{7.66}$$

which is the overall fraction of time the system has spent in state $i$ up to the finite observation time $T$. For the current observables, we consider the power

$$P_T^i \equiv \frac{1}{T}\int_0^T \mathrm{d}t\, \dot{E}_i(\lambda_t)\delta_{i,n_t} \tag{7.67}$$

exerted at energy level $i$, which is an example for the current $J_T^b$ and the rate of directed number of transitions between state $i$ and $j$

$$J_T^{ij} \equiv \frac{1}{T}\int_0^T \mathrm{d}t\, \left[\dot{m}_{ij}(t) - \dot{m}_{ji}(t)\right], \tag{7.68}$$

which is an example for the current $J_T^d$. Here, $m_{ij}(t)$ denotes the number of transitions between states $i$ and $j$ up to time $t$ along a trajectory $n_t$. The average value of Eq. (7.68) is the time-averaged probability current between state $i$ and $j$. Furthermore, the total entropy production rate for a discrete system is defined as

$$\sigma(T,v) \equiv \frac{1}{T}\int_0^T \mathrm{d}t \sum_{i>j} j_{ij}(t;v) \ln\left(\frac{p_i(t;v)k_{ij}(\lambda_t)}{p_j(t;v)k_{ji}(\lambda_t)}\right). \tag{7.69}$$

The master equation (7.62) can be written in terms of a generator matrix $L_{ij}(\lambda_t) \equiv k_{ji}(\lambda_t) - \sum_j k_{ij}(\lambda_t)\delta_{i,j}$ and the density, i.e., it has the same structure as the Fokker-Planck equation (7.23). As a consequence, the analysis of the limiting cases of fast and slow driving is straightforward after defining an appropriate timescale describing the fastest or slowest relaxation in the system. It thus leads to the same scaling behavior of the mean values as for the continuous systems. For evaluating the fluctuations, the propagator in Eq. (7.27) can be defined similarly for discrete systems by using the generator matrix $L_{ij}(\lambda_t)$. Hence, the calculation of the correlation functions follows essentially the same steps as for systems with continuous degrees of freedom. Therefore, the quality factors of discrete systems have the same scaling behavior as for systems with continuous degrees of freedom. While the scaling behavior of the total entropy production rate is also similar, the logarithm entering in Eq. (7.69) prevents the uncertainty relation to be saturated in the limit of fast driving far away from equilibrium. Only for discrete systems close to equilibrium the TUR can be saturated [28, 86].

### 7.4.2 *Three-state system*

We illustrate our main results by using a system with three discrete states, where the energy levels of the states are driven time-dependently through a protocol $\lambda_t$. The topology of this network is shown in Fig. 7.1(a). We distinguish between two models: model A contains a link between state 1 and 3. In addition to the time-dependent driving of the energy levels, the system is driven by a constant non-conservative force $f$. In model B there is no link between state 1 and 3. As a consequence the net number of transitions between two states is zero or $\pm 1$, which implies that their fluctuations are not time-extensive. The energy levels of the three states

$$E_i(\lambda_t) \equiv -E_i^0 \lambda_t, \tag{7.70}$$

are driven by a quadratic protocol

$$\lambda_t \equiv (vt)^2, \tag{7.71}$$

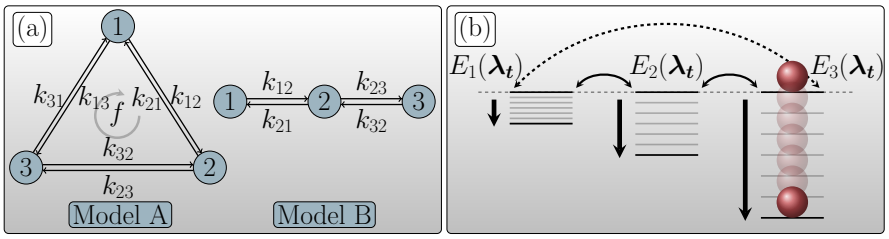


Figure 7.1: Topology of the two models A and B for the three-state system (a) and schematic of the three-state system with time-dependent energy levels (b). In model A there is a link between state 1 and 3 such that a NESS can be reached by applying a non-conservative force $f$. In model B there is no link between states 1 and 3, which limits the net number of transitions up to a finite observation time $T$ between two states. The three energy levels have initially the same value $E_i(0) = 0$ and are decreased over time to a fixed final value $E_i(\lambda_{\tau_f}) = -E_i^0 \tau_f^2$.

where $E_i^0$ is the amplitude of the driving and $v$ is the speed parameter. The rates are chosen according to the local detailed balance condition (7.64) and read

$$k_{ij}(\lambda_t) \equiv k_0^{ij} \exp\left(-\beta \left[E_j(\lambda_t) - E_j(\lambda_t)\right]/2 - f/6\right), \tag{7.72}$$

$$k_{ji}(\lambda_t) \equiv k_0^{ij} \exp\left(\beta \left[E_j(\lambda_t) - E_j(\lambda_t)\right]/2 + f/6\right), \tag{7.73}$$

where we have chosen the driving affinity as a constant $\mathcal{A}_{ij}(\lambda_t) = -\mathcal{A}_{ji}(\lambda_t) = f/3$ with $i > j$. The rate amplitudes $k_0^{ij}$ determine time scale of the system $t_{\text{sys}}$. In the following, we set all the rate amplitudes to the same value $k_0^{ij} \equiv k_0 = 1$ and choose all other parameters $\beta$, $E_i(\lambda_t)$ and $f$ of $\mathcal{O}(1)$. As a consequence all relaxation times in system are of the same order of magnitude and, hence, we are able to choose $t_{\text{sys}} \equiv 1/k_0 = 1$ as outlined in Section 7.1.4. Moreover, we choose the initial distribution $p_i(0)$ as the stationary state at fixed $\lambda_0$ at the beginning of the driving.

In the following, we plot *inter alia* $\mathcal{Q}_X/\epsilon_{s,f}^n$ against $\epsilon_{s,f}^{-1}$ to analyze the scaling of the quality factor for an observable $X$. Here, $\mathcal{Q}_X/\epsilon_{s,f}^n$ converges to a constant value for the correct power $n$ (see Tables 7.1 and 7.2) in the limit of fast-driving $\epsilon_f^{-1} \to \infty$ and slow-driving $\epsilon_s^{-1} \to \infty$, i.e., $\epsilon_f \to 0$ and $\epsilon_s \to 0$, respectively.

### 7.4.3 *Model A*

The topology of model A in Fig. 7.1(a) allows the system to reach a NESS by applying a non-conservative force $f$ or to converge to an equilibrium system by applying only a conservative force. These distinct two cases are especially relevant for the limit of slow driving.

Figure 7.2 shows the quality factors of the different types of observables defined in Eqs. (7.65)–(7.68) for a finite non-conservative force

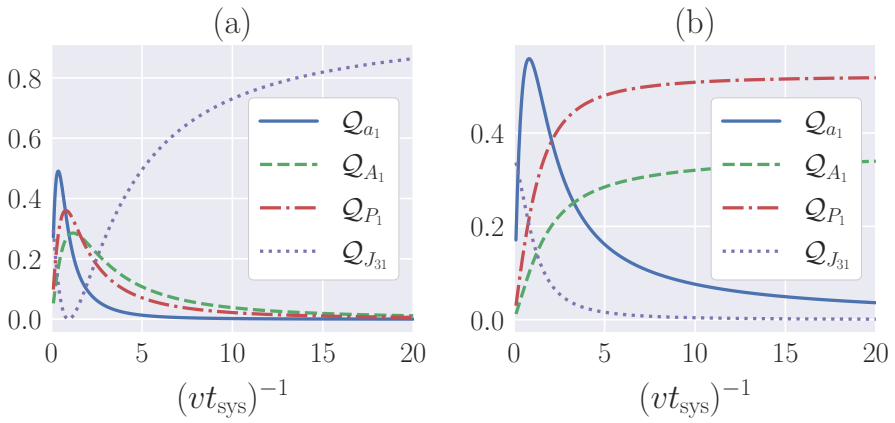


Figure 7.2: Quality factors of the probability $a_1(T,v)$ to find the system in state 1, of the fraction of time $A_1(T,v)$ the system has spent in state 1, of the power $P_1(T,v)$ applied to state 1 and of the current $J_{31}(T,v)$ between state 3 and 1. The quality factors are plotted against $(vt_{\mathrm{sys}})^{-1}$ for $f = 1.5$ (a) and for $f = 0$ (b). Here, we have set $\beta = 1.0$, $E_1^0 = 0.5$, $E_2^0 = 1.0$ and $E_3^0 = 2$.

$f \geq 0$ (a) and for a vanishing non-conservative force $f = 0$ (b). Comparing the results for fast driving in Table 7.1 and for slow driving in Table 7.2 for the three-state model let us conclude that either the current $J_{31}(T,v) \equiv \langle J_T^{31} \rangle$ between state 3 and 1 or the time-averaged state variable $A_1(T,v) \equiv \langle A_T^1 \rangle$ as well as the power $P_1(T,v) \equiv \langle P_T^1 \rangle$ are the best choice to infer the total entropy production in the respective limiting cases. However, the instantaneous state variable, the probability $a_1(T,v) \equiv \langle a_T^1 \rangle$ to find the system in state 1, is not an optimal choice for both limiting cases as its quality factor vanishes as shown in Fig. 7.2(a) and (b). In contrast, we expect that the quality factor for the instantaneous state variable has a maximum and is of $\mathcal{O}(1)$ for a speed of driving comparable with the timescale of the system, i.e., $(vt_{\mathrm{sys}})^{-1} \sim 1$. This can be seen for the three-state model in Fig. 7.2(a) and (b), where the instantaneous state variable yields about 50% of the total entropy production rate.

Next, we analyze the quality factors for the observables defined in Eqs. (7.65)–(7.68) in the limit of fast driving. The quality factors for the power, for the fraction of time the system has spent in a certain state, for the probability to find the system in a state and for the time-averaged current between two states are shown in Fig. 7.3(a)–(d). As predicted by Table 7.1, the quality factors for the state variables $A_i(T,v)$ and $a_i(T,v)$ and the current depending on the residence time $P_i(T,v)$ are proportional to $\epsilon_f$ as their quality factors divided by $\epsilon_f$ converge to a constant value in the limit $\epsilon_f^{-1} \to \infty$ (see Fig. 7.3(a)–(c)). The quality factor for the current $J_{ij}(T,v)$ converges to a constant value

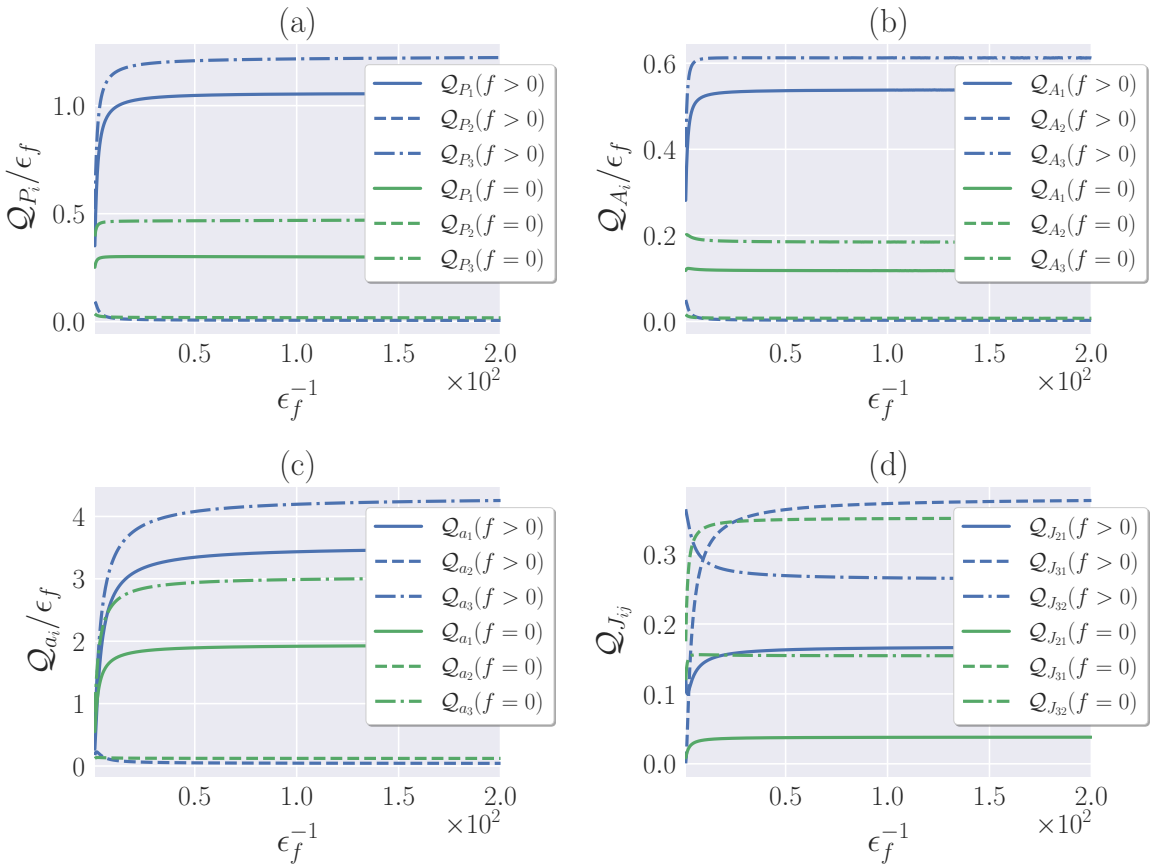


Figure 7.3: Quality factors in the limit of fast driving for the power (a), for the fraction of time spent in a certain state (b), for the probability to find the system in a certain state (c) and for the time-averaged probability current between two states (d). The quality factors are plotted against the parameter $\epsilon_f^{-1}$ and shown for a finite non-conservative force $f = 1.5 > 0$ and for a vanishing force $f = 0$. Here, we have set $\beta = 1.0$, $E_1^0 = 0.5$, $E_2^0 = 1.0$ and $E_3^0 = 2$.

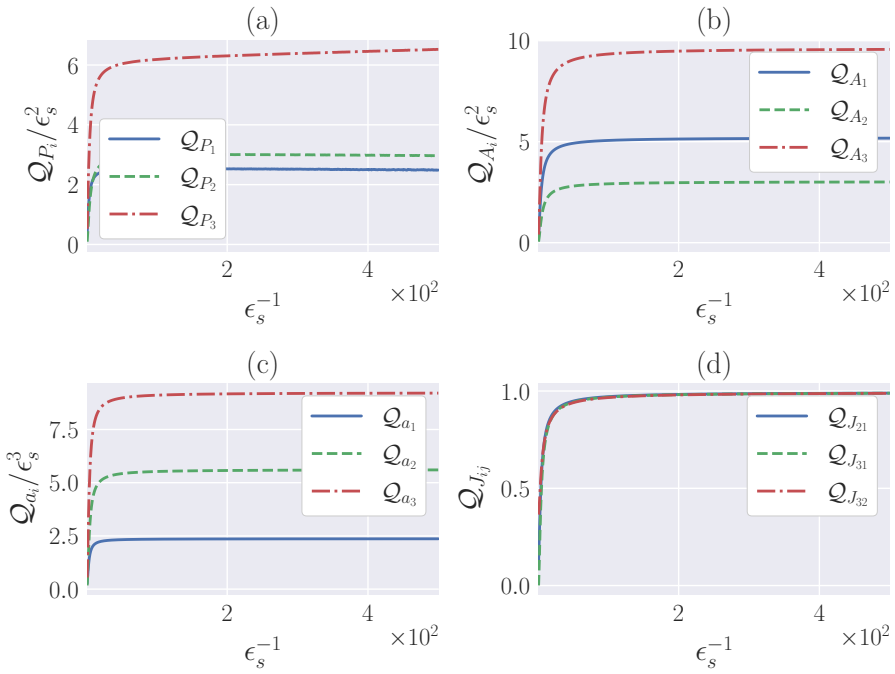


Figure 7.4: Quality factors in the limit of slow driving for the power (a), for the fraction of time spent in a certain state (b), for the probability to find the system in a certain state (c) and for the time-averaged probability current between two states (d). The quality factors are plotted against the parameter $\epsilon_s^{-1}$ and shown for a finite force $f = 1.5 > 0$. Here, we have set $\beta = 1.0$, $E_1^0 = 0.5$, $E_2^0 = 1.0$ and $E_3^0 = 2$.

and is of $\mathcal{O}(1)$ as shown in Fig 7.3(d). The scaling of these quality factors are independent of the force $f$.

In contrast, in the limit of slow driving the scaling of the quality factors depend on the non-conservative force $f$. For $f > 0$, the system converges to a NESS at a constant $\lambda_t$, whereas for a vanishing force $f = 0$ the system converges to an equilibrium state at constant $\lambda_t$. We first focus on the case of a non-vanishing force $f > 0$. The quality factors for the power, for the fraction of time the system has spent in a certain state, for the probability to find the system in a state and for the time-averaged current between two states are shown in Fig. 7.4(a)–(d). The quality factors for the current $P_i(T, v)$ and the time-averaged state variable $A_i(T, v)$ scale like $\epsilon_s^2$, whereas it scales for the instantaneous state variable like $\epsilon_s^3$. In contrast, only the quality factor of the current $J_{ij}(T, v)$ yields to a quality factor of $\mathcal{O}(1)$. There are three quality factors of the time-averaged probability current for each link: $\mathcal{Q}_{J_{21}}$, $\mathcal{Q}_{J_{31}}$ and $\mathcal{Q}_{J_{31}}$. While all three of the quality factors are different in the region of small $\epsilon_s^{-1}$, where the slow-driving limit is not yet reached, they converge asymptotically identical to the same value in the limit of slow driving ($\epsilon_s^{-1} \to \infty$). This can be understood as follows. When the system is driven slowly enough, it passes different NESSs in the course

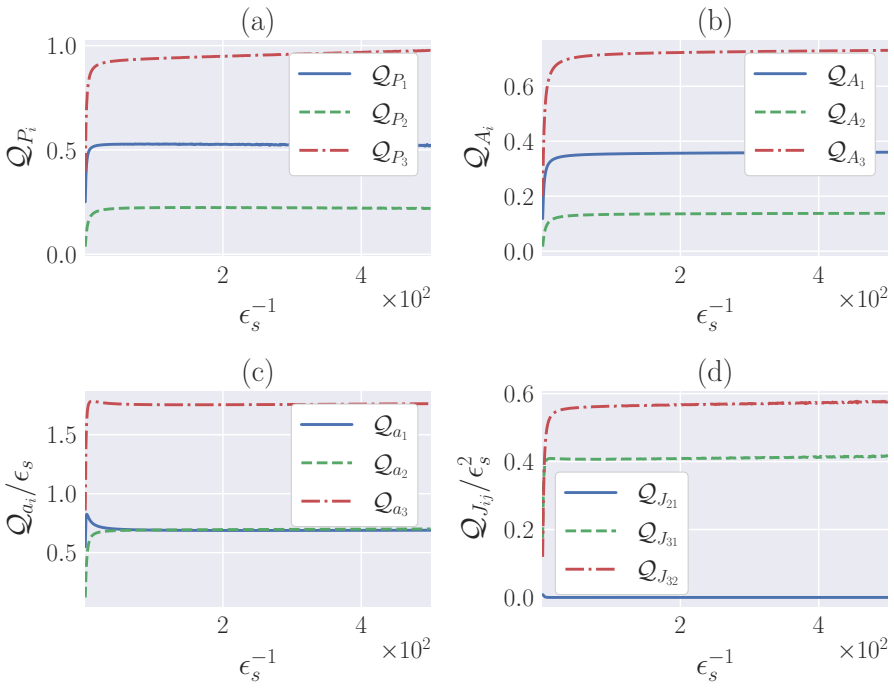


Figure 7.5: Quality factors in the limit of slow driving for the power (a), for the fraction of time spent in a certain state (b), for the probability to find the system in a certain state (c) and for the time-averaged probability current between two states (d). The quality factors are plotted against the parameter $\epsilon_s^{-1}$ and shown for a vanishing force $f = 0$. Here, we have set $\beta = 1.0$, $E_1^0 = 0.5$, $E_2^0 = 1.0$ and $E_3^0 = 2$.

of time. In each NESS all three currents are identical. As a consequence the quality factors must also be identical. To summarize, the optimal observable leading to a useful estimate for the total entropy production rate is a current $J_d(T, v)$ depending on the velocity or, equivalently, depending on the number of transitions between two discrete states. All other observables yield a quality factor that vanishes at least of order $\epsilon_s^2$ as predicted in Table 7.2.

Next, we consider the limit of slow driving for a vanishing force $f = 0$, where the system is in an equilibrium state at fixed $\lambda_t$. The quality factors for the power, for the fraction of time the system has spent in a certain state, for the probability to find the system in a certain state and for the time-averaged current between two states are shown in Fig. 7.5(a)–(d). In contrast to the case with $f > 0$, where the quality factors of the current $P_i(T, v)$ and the state variable $A_i(T, v)$ vanish like $\epsilon_s^2$ (see Fig. 7.4(a) and (b)), they both converge to a value of $\mathcal{O}(1)$ as shown in Fig. 7.5(a) and (b). In the latter case, the time-averaged state variable $A_3(T, v)$ yields over 60% of the total entropy production rate. The quality factor for the power $P_3(T, v)$ even nearly saturates due to the fact that the total power $P_{\text{tot}}(T, v) \equiv \sum_i P_i(T, v)$

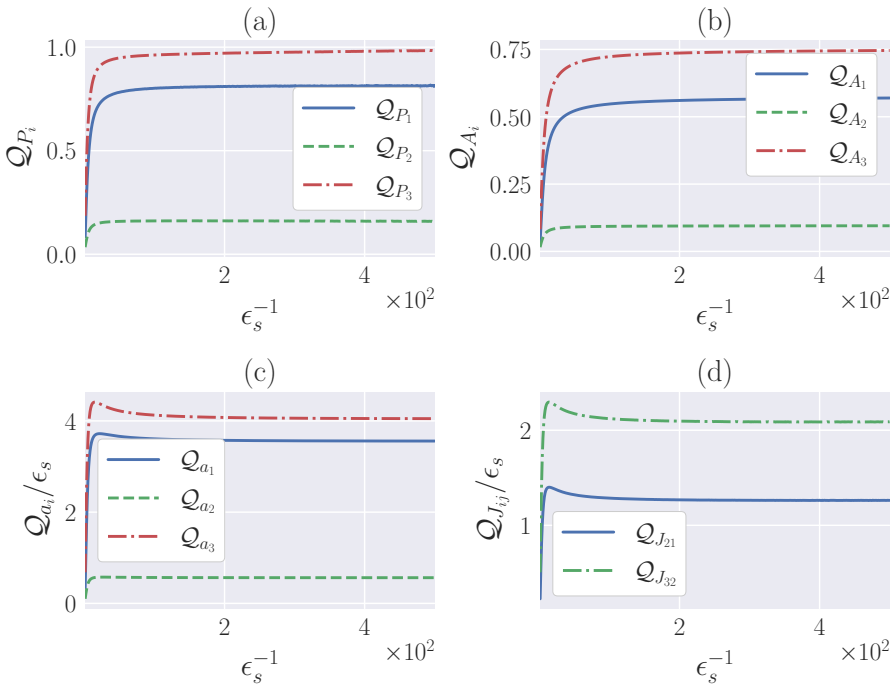


Figure 7.6: Quality factors in the limit of slow driving for the power (a), for the fraction of time spent in a certain state (b), for the probability to find the system in a certain state (c) and for the time-averaged probability current between two states (d). The quality factors are plotted against the parameter $\epsilon_s^{-1}$. Here, we have set $\beta = 1.0$, $E_1^0 = 0.5$, $E_2^0 = 1.0$ and $E_3^0 = 2$.

converges to the entropy production rate in the limit of slow driving. The power $P_3(T, v)$ contributes the most to the total power (due to $E_3^0 > E_2^0 > E_1^0$ as sketched in Fig. 7.1(b)) and, hence, yields to the best estimate for the total entropy production rate. As shown in Fig. 7.5(c) and (d) the quality factors for the state variable $a_i(T, v)$ and the for the current $J_{ij}(T, v)$ vanish like $\epsilon_s$ and $\epsilon_s^2$, respectively. This is an important contrast to the case $f > 0$, where the quality factor for the current $J_{ij}(T, v)$ is of $\mathcal{O}(1)$.

### 7.4.4 *Model B*

Model B cannot be driven into a NESS due to its topology depicted in Fig. 7.1(a). Hence, the system can only reach an equilibrium state, which leads to the generic scaling for the quality factors in the limit of slow driving as shown in Table 7.2 (second columns). However, in this system the topology of the network leads to deviations of the predicted scaling behavior of these quality factors, which are shown in Fig. 7.6(a)–(d). Only the state variable $A_i(T, v)$ and the current $P_i(T, v)$ yield an estimate for the entropy production of $\mathcal{O}(1)$ as shown in Fig. 7.6(a) and (b). The quality factors for the instantaneous variable $a_i(T, v)$ and for

the current $J_{ij}(T, v)$ vanish. However, the quality factor of the current $J_{ij}(T, v)$ does not vanish like $\epsilon_s^2$ as generically predicted in Table 7.2 but scales like $\epsilon_s$. This circumstance follows from the fact that the net number of transitions between two states and, consequently, also their fluctuations cannot become arbitrary large. As a consequence, the diffusion coefficient of the current is not of $\mathcal{O}(1)$ but vanishes proportional to $\epsilon_s$. This leads to the modified scaling of $\mathcal{O}(\epsilon_s)$ as shown in Fig 7.6(d).

## 7.5 CONCLUSION

In this chapter, we have analyzed the quality of the thermodynamic uncertainty relation for the limiting cases of fast and slow driving.

For a one-dimensional Langevin dynamics, we have reached a fairly comprehensive classification. In the limit of fast driving, the generic optimal observable is the current observable that depends on the velocity. The quality factors of all other observables vanish asymptotically. We have further shown that in the limit of fast driving a current proportional to the total entropy production rate can saturate the uncertainty relation. In the limit of slow driving, one has to distinguish whether a driving affinity is additionally applied to the system or not in order to choose the optimal observable. If the system is driven by a driving affinity the optimal observable is the current that depends on the velocity. However, if there is no driving affinity, only the current that depends on the residence time or the time-averaged state variable yields a useful estimate for the total entropy production rate. All other quality factors vanish generically with a power law in the ratio of the relevant timescales. The quality factor of the instantaneous state variable vanishes in both limiting cases.

For multi-dimensional Langevin systems, we expect the behavior for the one-dimensional case to remain generic if the driving affects all degrees of freedom in a qualitatively similar manner. Deviations from this generically predicted scaling may occur if some degrees of freedom of the system are not driven. As an example, consider two interacting particles initially prepared in equilibrium, where one particle is time-dependently driven by an external force. In the limit of fast driving the current of the externally driven particle is finite whereas the current of the other one vanishes. As the leading order of the current of the externally driven particle is finite we get the scaling behavior for the quality factor predicted in this chapter. However, since the leading order of the current of the second particle vanishes, for this current deviations of the predicted scaling behavior occur. An exhaustive listing of all cases is impossible. Still, for any specific system an analysis following the methods developed in this chapter should allow one to extract the behavior of the quality factor for the observable of interest.

In systems with discrete degrees of freedom, the quality factors will generically show also power law behavior in the limits of slow and fast driving. Again, a systematic analysis for all kind of network topologies is prohibitive. For two simple three-state networks, we have illustrated the fact that the results derived for the one-dimensional Langevin system can be applied as well. The first model, model A, shows that although the quality factors of the instantaneous state variable vanishes generically for fast and slow driving it still yields a useful estimate when the speed of driving is comparable with the relaxation timescales in the system. For the second three-state model, model B, we have shown that depending on the topology of the system deviations of the generic scaling of the quality factors can occur.

With these results we have introduced first steps for optimizing inference schemes using the thermodynamic uncertainty relation for time-dependent driving. Optimizing these schemes is especially relevant for biophysical systems with possibly hidden states, e.g., the folding and unfolding process of a protein driven by a time-dependent force [156]. An example for such a folding process has been observed for Calmodulin, which has been experimentally investigated in Ref. [26]. This system has a complex topology with multiple relaxation timescales. In Section 6.6, we have analyzed the quality factors for various types of observables in this system. The results for fast and slow driving coincide with our predictions, e.g., for the instantaneous state variable in Fig. 6.2(b) in Section 6.6. However, especially in the limiting case of fast driving in more complex systems where the leading orders strongly depend on the initial condition one can construct currents for which the leading order vanishes implying a potentially different scaling behavior.

In this chapter, we have focused on the scaling behavior of various classes of observables. In a next step, one could investigate which observable is optimal within each class. Moreover, it would be possible to use a superposition of two observables or to involve correlations between them in order to optimize the bounds on entropy production [157].

# Part V

# CONCLUSION

# CONCLUSION

Despite its universality, the TUR and its various applications are restricted to systems driven into a NESS. Since it is desirable to profit from its concepts and applications beyond steady-state systems, we have generalized the TUR to time-dependently driven systems in Part iii.

In Chapter 5, we have derived a generalization of the TUR to periodically driven systems that involves solely operationally accessible observables and the total rate of entropy production. As a new ingredient, this relation involves the response of a current with respect to the driving frequency. An important application is the bound on the efficiency of cyclic heat engines, which involves the response and the fluctuations of the output power. This inequality is stronger than the bound imposed by the Carnot efficiency and implies a trade-off between power, efficiency and constancy for an engine operating at maximum power. It gives valuable insights into how the driving frequency influences the efficiency in relation to fluctuations and provides general design principles for heat engines. As a next step for future research the influence of the protocol on fluctuations can be further analyzed. For example, in Ref. [158] the authors found protocols, which minimize work fluctuations. Other generalizations of the TUR require symmetries in the protocol [30, 101]. However, a systematic picture to what extent the choice of the protocol influences fluctuations in relation to efficiencies of heat engines is still missing.

By deriving the most general form of the TUR in Chapter 6, we have unified various earlier derived uncertainty relations for different types of dynamics including steady-state systems, relaxation processes and periodically driven systems. Thus, we have bundled them into one single universal applicable and operationally accessible relation valid for arbitrary time-dependent driving and from arbitrary initial states. The crucial step to derive this relation is to identify a speed parameter associated with the protocol and to refine the ansatz for periodically driven systems. Moreover, we have generalized the TUR to instantaneous and time-averaged state variables, which clearly extends the possibilities to infer entropy production. These bounds are especially useful for finite-time processes like the erasure of a bit [148–150]. In such processes the Landauer bound predicts a minimum amount of cost to erase a bit [159]. This bound follows from the second law and, hence, analogously to the bound on the efficiency of heat engines, the TUR must predict a tighter bound possibly implying a further trade-off relation since it is a stronger statement than the second law. The key step to find such a physical transparent relation is a proper choice of the observable entering the TUR. Thus, identifying

the consequences of the TUR for bit erasure processes is an interesting open question for future research.

The new possibility to get an estimate for entropy production via state variables through the time-dependent TURs raises the questions which observable yields the best estimate and how sharp the bounds typically are. We have discussed these questions in Part iv, where we have analyzed the TUR for fast and slow driving in Chapter 7. In the limit of fast driving, we have shown that a current observable yields the best estimate, which can even saturate the TUR if it is proportional to the entropy production. In the limit of slow driving, the observable yielding the best estimate depends on whether or not a driving affinity is applied. If there is a finite driving affinity, only a current observable leads to an estimate of order 1. In contrast, for a vanishing driving affinity, a current observable as well as a state variable yield a useful estimate. Possible next steps can deal with the optimization of increments within a certain class of observables. For example, the authors in Ref. [121] optimized a state-dependent increment to obtain an observable that yields the tightest possible TUR in a NESS. Interestingly, this observable does not coincide with the total entropy production. Whether a similar observable can be found for time-dependent TURs is an open question. Moreover, one could adapt the multidimensional thermodynamic uncertainty relation (MTUR) [126] to time-dependently driven systems, which yields the tightest possible bound over a linear combination of available current observables and/or state variables. Here, one could determine which combination of different types of observables improve the quality of the estimate for entropy production. Last but not least, the MTUR provides the ability to analyze time-dependently driven interacting many-body systems. A recent systematic study about applying the MTUR to interacting many-body systems in a steady state can be found in Ref. [6].

The TURs for time-dependent driving derived in this thesis are based on an ansatz for an auxiliary dynamics, which describes a time-rescaled dynamics. One might expect that a similar ansatz would prove the TUR in a NESS for underdamped Langevin systems as well. However, it has been shown in Ref. [90] that such an ansatz leads to a cost term that does not coincide with entropy production. Since the time rescaling in overdamped systems can be interpreted as a rescaling of friction, a similar approach for underdamped systems admittedly yields a cost term identical to entropy production, but also a response of the current that is operationally inaccessible [94, 95]. While a violation of the TUR for particles in a magnetic field has been reported in Ref. [32], violations for systems without a magnetic field have been observed so far only for finite-times [33]. Therefore, the authors in Ref. [33] have conjectured a time-dependent bound imposed by the free diffusion process, which converges to the original TUR in the

long-time limit. Very recently, it has been shown that this conjecture is violated for two-dimensional systems even in the long-time limit [34]. While this result rules out the existence of a TUR valid for multiple interacting degrees of freedom, there has been no evidence for the violation of the TUR for one-dimensional underdamped steady-state systems in the long-time limit, which suggests a bound depending on the dimension of the system.

To summarize, at a first glance, one might expect that the TUR can be derived for underdamped Langevin systems in a straightforward manner. However, recent research shows that the additional timescale describing the relaxation of the momenta makes a generalization of the TUR somewhat more complicated. Thus, generalizing the TUR for underdamped steady-state systems remains an intriguing and challenging open question and certainly deserves future work.

All in all, we have derived universal applicable bounds on the total entropy production for time-dependently driven systems. While in the recent years a vast amount of different TURs have been derived [51], which are valid in a limited region, we have provided a systematic unifying picture by deriving the most general form of the TUR for arbitrary time-dependently driven systems.

# Part VI

# APPENDIX

# A

# PERIODIC DRIVING

This appendix contains three sections. In the first section, we provide detailed derivations of the main results discussed in Chapter 5. In the second section, we generalize these main results to finite observation times. In the third section, we prove further bounds on the average dynamical activity introduced in Section 5.4. In the fourth section, we calculate the total output power and its diffusion coefficient for the Stirling heat engine discussed in Section 5.5.

## A.1 DERIVATION OF THE MAIN RESULTS

We derive our main results in Section 5.1 by using a lower bound on the SCGF.

$$\lambda_T(z) \equiv \frac{1}{T} \ln \left\langle e^{zTX_T} \right\rangle . \tag{A.1}$$

Here, $X_T = X_T[n_t]$ is an arbitrary observable defined along a trajectory $n_t$ of length $T$. The bound on the generating function can be expressed in terms of a Kullback-Leibler divergence between two path weights [74]. This can be derived as follows. The expectation value in Eq. (A.1) can be written as a path integral over all trajectories $n_t$ of length $T$

$$\left\langle e^{zTX_T} \right\rangle = \sum_{n_t} \mathcal{P}[n_t] e^{zTX_T[n_t]}. \tag{A.2}$$

Here, the summation indicates the path integral and $\mathcal{P}[n_t]$ is the path weight in the original dynamics of interest. By introducing an auxiliary process with path weight $\widetilde{\mathcal{P}}[n_t]$, we can write Eq. (A.1) as

$$\lambda_T(z) = \frac{1}{T} \ln \left\langle \exp \left[ zTX_T[n_t] - \ln \left( \frac{\widetilde{\mathcal{P}}[n_t]}{\mathcal{P}[n_t]} \right) \right] \right\rangle^{\text{aux}}, \tag{A.3}$$

where the average with respect to the auxiliary dynamics is denoted by $\langle \cdot \rangle^{\text{aux}}$. Using Jensen's inequality leads to

$$\lambda_T(z) \geq z \langle X_T \rangle^{\text{aux}} - \frac{1}{T} \left\langle \ln \left( \frac{\widetilde{\mathcal{P}}[n_t|i_0]}{\mathcal{P}[n_t|i_0]} \right) + \ln \left( \frac{\tilde{p}_{i_0}(0)}{p_{i_0}(0)} \right) \right\rangle^{\text{aux}}, \tag{A.4}$$

where we used $\mathcal{P}[n_t] = \mathcal{P}[n_t|i_0] p_{i_0}(0)$ and $\widetilde{\mathcal{P}}[n_t] = \widetilde{\mathcal{P}}[n_t|i_0] \tilde{p}_{i_0}(0)$ with the initial distribution $p_{i_0}(0)$ of the process of interest and an *a priori* arbitrary initial distribution $\tilde{p}_{i_0}(0)$.

In the following, we assume that the original process of interest with path weight $\mathcal{P}[n_t]$ is in a periodic stationary state with rates $k_{ij}(\tau)$ leading to densities $p_i^{\rm ps}(\tau;\Omega)$ at frequency $\Omega = 2\pi/\mathcal{T}$. Also, we assume that the auxiliary process with path weight $\widetilde{\mathcal{P}}[n_t]$ is described by periodic rates $\tilde{\mathbf{k}}(\tau) \equiv \{\tilde{k}_{ij}(\tau)\}$ leading to periodic densities $\tilde{\mathbf{p}}(\tau) \equiv \{\tilde{p}_i(\tau)\}$ with period $\mathcal{T}$.

The first term in Eq. (A.4) is the mean value of observable $X_T$ in the auxiliary dynamics. The second term in Eq. (A.4) is given by the ratio of the two path weights for the same trajectory $n_t$

$$\frac{\widetilde{\mathcal{P}}[n_t|i_0]}{\mathcal{P}[n_t|i_0]} = \exp\left(\int_0^T \mathrm{d}t \sum_{ij}\left[\dot{m}_{ij}(t)\ln\left(\frac{\tilde{k}_{ij}(t)}{k_{ij}(t)}\right) - \delta_{n_t,i}\left(\tilde{k}_{ij}(t) - k_{ij}(t)\right)\right]\right). \tag{A.5}$$

The third term in Eq. (A.4) is the Kullback-Leibler divergence between $\tilde{p}_i(0)$ and $p^{\rm ps}(0;\Omega)$, i.e.,

$$\left\langle \ln\left(\frac{\tilde{p}_{i_0}(0)}{p_{i_0}(0)}\right)\right\rangle^{\rm aux} = \sum_i \tilde{p}_i(0)\ln\left(\frac{\tilde{p}_i(0)}{p_i^{\rm ps}(0;\Omega)}\right). \tag{A.6}$$

Inserting Eqs. (A.5) and (A.6) into (A.4), using $\langle \dot{m}_{ij}(t)\rangle^{\rm aux} = \tilde{p}_i(t)\tilde{k}_{ij}(t)$ and $\langle \delta_{n_t,i}\rangle^{\rm aux} = \tilde{p}_i(t)$ leads to a general bound on the SCGF at time $T = n\mathcal{T}$, which is given by [4]

$$\lambda_{n\mathcal{T}}(z) \geq z\langle X_T\rangle^{\rm aux} - F[\tilde{\mathbf{p}}(\tau),\tilde{\mathbf{k}}(\tau)] - \frac{1}{n\mathcal{T}} D\left(\tilde{\mathbf{p}}(0)||\mathbf{p}^{\rm ps}(0;\Omega)\right), \tag{A.7}$$

with

$$F[\tilde{\mathbf{p}}(\tau),\tilde{\mathbf{k}}(\tau)] \equiv \frac{1}{\mathcal{T}}\int_0^{\mathcal{T}} \mathrm{d}\tau \sum_{ij}\left(\tilde{p}_i(\tau)\tilde{k}_{ij}(\tau)\ln\left(\frac{\tilde{k}_{ij}(\tau)}{k_{ij}(\tau)}\right) - \tilde{p}_i(\tau)[\tilde{k}_{ij}(\tau) - k_{ij}(\tau)]\right) \tag{A.8}$$

and the Kullback-Leibler divergence

$$D\left(\tilde{\mathbf{p}}(0)||\mathbf{p}^{\rm ps}(0;\Omega)\right) \equiv \sum_i \tilde{p}_i(0)\ln[\tilde{p}_i(0)/p_i^{\rm ps}(0;\Omega)], \tag{A.9}$$

where $\mathbf{p}^{\rm ps}(0;\Omega) \equiv \{p_i^{\rm ps}(0;\Omega)\}$.

Furthermore, we can optimize the bound (A.7) with respect to the activity of the auxiliary dynamics [4]. For this purpose, we express the rates

$$\tilde{k}_{ij}(\tau) = \left(\tilde{j}_{ij}(\tau) + \tilde{t}_{ij}(\tau)\right)/[2\tilde{p}_i(\tau)] \tag{A.10}$$

in terms of the probability current

$$\tilde{j}_{ij}(\tau) \equiv \tilde{p}_i(\tau)\tilde{k}_{ij}(\tau) - \tilde{p}_j(\tau)\tilde{k}_{ji}(\tau) \tag{A.11}$$

and the activity

$$\tilde{t}_{ij}(\tau) \equiv \tilde{p}_i(\tau)\tilde{k}_{ij}(\tau) + \tilde{p}_j(\tau)\tilde{k}_{ji}(\tau). \tag{A.12}$$

After optimizing Eq. (A.8) with respect to the activity, we get the optimal rates

$$\tilde{k}^*_{ij}(\tau) = \left(\tilde{j}_{ij}(\tau) + \sqrt{[\tilde{j}_{ij}(\tau)]^2 + 4\tilde{p}_i(\tau)\tilde{p}_j(\tau)\tilde{k}_{ij}(\tau)\tilde{k}_{ji}(\tau)}\right) / [2\tilde{p}_i(\tau)]. \tag{A.13}$$

Inserting Eq. (A.13) into (A.7) leads to a bound expressed in terms of densities $\tilde{\mathbf{p}}(\tau) \equiv \{\tilde{p}_i(\tau)\}$ and currents $\tilde{\mathbf{j}}(\tau) \equiv \{\tilde{j}_{ij}(\tau)\}$. For choosing $X_T = G_T$ this bound is given by

$$\lambda_{n\mathcal{T}}(z) \geq z \langle G_T \rangle^{\text{aux}} - \frac{1}{\mathcal{T}} \int_0^{\mathcal{T}} \mathrm{d}\tau\, L\left(\tilde{\mathbf{p}}(\tau), \tilde{\mathbf{j}}(\tau)\right) - \frac{1}{n\mathcal{T}} D\left(\tilde{\mathbf{p}}(0) || \mathbf{p}^{\text{ps}}(0;\Omega)\right), \tag{A.14}$$

where the integrand $L\left(\tilde{\mathbf{p}}(\tau), \tilde{\mathbf{j}}(\tau)\right)$ is defined as

$$\begin{aligned} L\left(\tilde{\mathbf{p}}(\tau), \tilde{\mathbf{j}}(\tau)\right) \equiv & \sum_{i>j} \tilde{j}_{ij}(\tau) \left[\operatorname{arsinh}\left(\frac{\tilde{j}_{ij}(\tau)}{a^{\tilde{p}}_{ij}(\tau)}\right) - \operatorname{arsinh}\left(\frac{j^{\tilde{p}}_{ij}(\tau)}{a^{\tilde{p}}_{ij}(\tau)}\right)\right] \\ & - \left(\sqrt{[\tilde{j}_{ij}(\tau)]^2 + [a^{\tilde{p}}_{ij}(\tau)]^2} - \sqrt{[j^{\tilde{p}}_{ij}(\tau)]^2 + [a^{\tilde{p}}_{ij}(\tau)]^2}\right), \end{aligned} \tag{A.15}$$

with

$$j^{\tilde{p}}_{ij}(\tau) \equiv \tilde{p}_i(\tau)k_{ij}(\tau) - \tilde{p}_j(\tau)k_{ji}(\tau), \quad a^{\tilde{p}}_{ij}(\tau) \equiv \sqrt{4\tilde{p}_i(\tau)\tilde{p}_j(\tau)k_{ij}(\tau)k_{ji}(\tau)}. \tag{A.16}$$

The above introduced auxiliary dynamics has to describe a physical process and, hence, it has to obey the following conditions

$$\sum_i \tilde{p}_i(\tau) = 1, \qquad 0 < \tilde{p}_i(\tau) < 1, \tag{A.17}$$

$$\tilde{p}_i(0) = \tilde{p}_i(\mathcal{T}), \qquad \dot{\tilde{p}}_i(\tau) = -\sum_j \tilde{j}_{ij}(\tau). \tag{A.18}$$

The first condition in (A.18) guarantees that the chosen density $\tilde{p}_i(\tau)$ has the same cycle duration $\mathcal{T}$ as the original periodic stationary state. The latter one can be written as

$$\begin{aligned} p^{\text{ps}}_i(\tau;\Omega) \equiv a_0(\Omega) + \sum_{n=1} \Big(& a_n(\Omega)\cos(n\Omega\tau) \\ & + b_n(\Omega)\sin(n\Omega\tau)\Big). \end{aligned} \tag{A.19}$$

For every frequency $\Omega$ there exists a corresponding set of Fourier coefficients $\{a_n(\Omega), b_n(\Omega)\}$ defining the unique periodic stationary state $p^{\text{ps}}_i(\tau;\Omega)$.

We choose the following ansatz for the auxiliary dynamics

$$\begin{aligned}\tilde{p}_i(\tau) &= p_i^{\mathrm{ps}}(\tau;\Omega) + \epsilon\left(p_i^{\mathrm{ps}}(\tau;\Omega) - p_i^{\mathrm{ps}}(\Omega\tau/\tilde{\Omega};\tilde{\Omega})\right),\\ \tilde{j}_{ij}(\tau) &= j_{ij}^{\mathrm{ps}}(\tau;\Omega) + \epsilon\left(j_{ij}^{\mathrm{ps}}(\tau;\Omega) - \Omega/\tilde{\Omega} j_{ij}^{\mathrm{ps}}(\Omega\tau/\tilde{\Omega};\tilde{\Omega})\right)\end{aligned} \tag{A.20}$$

with small $\epsilon = \mathcal{O}(z)$, where the density

$$\begin{aligned}p_i^{\mathrm{ps}}(\Omega\tau/\tilde{\Omega};\tilde{\Omega}) \equiv a_0(\tilde{\Omega}) + \sum_{n=1}\Big(&a_n(\tilde{\Omega})\cos(n\Omega\tau)\\ &+ b_n(\tilde{\Omega})\sin(n\Omega\tau)\Big)\end{aligned} \tag{A.21}$$

has the same cycle duration $\mathcal{T} = 2\pi/\Omega$ as the original process. The Fourier coefficients $\{a_n(\tilde{\Omega}), b_n(\tilde{\Omega})\}$ correspond to a periodic stationary process with frequency $\tilde{\Omega}$.

Inserting ansatz (A.20) into (A.14), taking the long time limit $n \to \infty$, choosing small $\epsilon = \mathcal{O}(z)$, and optimizing with respect to this parameter leads to a local quadratic bound on the generating function, which implies the inequality

$$2D_G(\Omega) \geq \frac{(G(\Omega) - G(\Omega,\tilde{\Omega}))^2}{(\Omega/\tilde{\Omega} - 1)^2 \mathcal{S}(\Omega,\tilde{\Omega})} \tag{A.22}$$

with

$$\begin{aligned}\mathcal{S}(\Omega,\tilde{\Omega}) &\equiv \frac{1}{\mathcal{T}}\int_0^{\mathcal{T}} \mathrm{d}\tau \left(\sum_{i>j}\frac{\left(j_{ij}^{\mathrm{ps}}(\Omega\tau/\tilde{\Omega};\tilde{\Omega})\right)^2}{t_{ij}^{\mathrm{ps}}(\tau;\Omega)}\right),\\ G(\Omega,\tilde{\Omega}) &\equiv \Omega/\tilde{\Omega} J(\tilde{\Omega}) + A(\tilde{\Omega}),\\ G(\Omega) &\equiv G(\Omega,\tilde{\Omega}=\Omega) = J(\Omega) + A(\Omega)\end{aligned}$$

as quoted in the main text. The nominator in (A.22) follows from the first term in (A.14), i.e., the average of observable $G_T$ in the auxiliary dynamics. Here, we used the substitution $\tilde{\tau} = \Omega\tau/\tilde{\Omega}$ and the following properties of the increments

$$\begin{aligned}d_{ij}(\tau;\Omega) &= d_{ij}(\tilde{\Omega}\tilde{\tau}/\Omega;\Omega) = d_{ij}(\tilde{\tau};\tilde{\Omega}),\\ \dot{a}_i(\tau;\Omega) &= (\Omega/\tilde{\Omega})\dot{a}_i(\tilde{\Omega}\tilde{\tau}/\Omega;\Omega) = (\Omega/\tilde{\Omega})\dot{a}_i(\tilde{\tau};\tilde{\Omega}),\\ A_i(\tau;\Omega) &= A_i(\tilde{\Omega}\tilde{\tau}/\Omega;\Omega) = A_i(\tilde{\tau};\tilde{\Omega}),\end{aligned}$$

where we introduced the second argument to denote the corresponding frequency. The denominator in (A.22), i.e., the cost term, follows from the second term in Eq. (A.14). After taking the long-time limit, the third term in Eq. (A.14), i.e., the Kullback-Leibler divergence, vanishes. Moreover, we note that for $\tilde{\Omega} \to \infty$ and $A_i(\tau;\Omega) = 0$ in Eq. (A.22) the generalized thermodynamic uncertainty relation (GTUR) in [4] is recovered.

Next, we choose $\tilde{\Omega} = \alpha\Omega$ and take the limit $\alpha \to 1$. Both, nominator and denominator on the right-hand side in Eq. (A.22) approach zero in this limit. Hence, we expand both around $\alpha = 1$ leading to

$$D_G(\Omega) \geq \frac{x^2 \left(J(\Omega) - \Omega J'(\Omega) - \Omega A'(\Omega) + \mathcal{O}(x)\right)^2}{\left(x^2 + \mathcal{O}(x^3)\right)\left(\mathcal{S}(\Omega) + \mathcal{O}(x)\right)} \tag{A.23}$$

with $x \equiv \alpha - 1$ and

$$\mathcal{S}(\Omega) \equiv \mathcal{S}(\Omega, \tilde{\Omega} = \Omega) = \frac{1}{\mathcal{T}} \int_0^{\mathcal{T}} \mathrm{d}\tau \left( \sum_{i>j} \frac{\left(j_{ij}^{\mathrm{ps}}(\tau;\Omega)\right)^2}{t_{ij}^{\mathrm{ps}}(\tau;\Omega)} \right). \tag{A.24}$$

Here, $'$ denotes the derivative with respect to frequency $\Omega$. Moreover, by setting either $d_{ij}(\tau;\Omega) = \dot{a}_i(\tau;\Omega) = 0$ or $A_i(\tau;\Omega) = 0$ we get the following inequalities for currents $J(\Omega)$ and residence quantities $A(\Omega)$

$$2D_J(\Omega)\mathcal{S}(\Omega)/J(\Omega)^2 \geq (1 - \Omega J'(\Omega)/J(\Omega))^2, \tag{A.25}$$
$$2D_A(\Omega)\mathcal{S}(\Omega)/A(\Omega)^2 \geq (\Omega A'(\Omega)/A(\Omega))^2, \tag{A.26}$$

as quoted in the main text.

Finally, using $2j_{ij}^{\mathrm{ps}}(\tau)^2 \leq t_{ij}^{\mathrm{ps}}(\tau)\sigma_{ij}(\tau)$ and $j_{ij}^{\mathrm{ps}}(\tau)^2 \leq t_{ij}^{\mathrm{ps}}(\tau)^2$ implies our main results

$$D_J(\Omega)C(\Omega)/J(\Omega)^2 \geq (1 - \Omega J'(\Omega)/J(\Omega))^2, \tag{A.27}$$
$$D_A(\Omega)C(\Omega)/A(\Omega)^2 \geq (\Omega A'(\Omega)/A(\Omega))^2, \tag{A.28}$$

where $C(\Omega) \in \{2\mathcal{S}(\Omega), 2\mathcal{A}(\Omega), \sigma(\Omega)\}$ are cost terms and $\mathcal{A}(\Omega) \equiv 1/\mathcal{T} \int_0^{\mathcal{T}} \mathrm{d}\tau \sum_{i>j} t_{ij}^{\mathrm{ps}}(\tau)$ is the average dynamical activity.

## A.2 FINITE-TIME GENERALIZATION

For a finite-time generalization of relation (A.22) and, hence, of our main results (A.27) and (A.28), an additional cost term arises due to the non-vanishing Kullback-Leibler divergence, i.e.,

$$D_J(n\mathcal{T};\Omega)[C(\Omega) + \tilde{C}(\Omega)]/J(\Omega)^2 \geq (1 - \Omega J'(\Omega)/J(\Omega))^2, \tag{A.29}$$
$$D_A(n\mathcal{T};\Omega)[C(\Omega) + \tilde{C}(\Omega)]/A(\Omega)^2 \geq (\Omega A'(\Omega)/A(\Omega))^2, \tag{A.30}$$

where the additional term

$$\tilde{C}(\Omega) \equiv \frac{1}{n\mathcal{T}} \sum_i \Omega^2 [p_i^{\mathrm{ps}}(0;\Omega)']^2 / p_i^{\mathrm{ps}}(0;\Omega) \tag{A.31}$$

is the contribution of the non-vanishing Kullback-Leibler divergence and

$$D_X(n\mathcal{T};\Omega) \equiv n\mathcal{T} \left\langle \left(X_{n\mathcal{T}} - \langle X_{n\mathcal{T}} \rangle\right)^2 \right\rangle /2 = \lambda''_{n\mathcal{T}}(0)/2 \tag{A.32}$$

is the finite-time generalization of the diffusion coefficient for an observable $X_{n\mathcal{T}}$ after $n$ periods. Here, $\lambda''_{n\mathcal{T}}(0)$ denotes the second derivative of the SCGF with respect to $z$ at $z = 0$.

### A.3 BOUNDS ON ACTIVITY

We now generalize the bounds on activity $\mathcal{A}(\Omega)$ in the main text to arbitrary observables depending on the number of transitions

$$\mathcal{X}_T \equiv \frac{1}{T}\int_0^T \mathrm{d}t \sum_{ij} \dot{m}_{ij}(t) g_{ij}(t) \tag{A.33}$$

along a trajectory $n_t$ of length $T$, where $g_{ij}(t)$ are arbitrary time-periodic increments. Note, that we do not restrict $g_{ij}(t)$ to be anti-symmetric or symmetric. For example, $\mathcal{X}_T$ can be the average number of jumps during one period from state $1 \to 2$ with increments $g_{ij}(t) = \delta_{1,i}\delta_{2,j}$. The average of (A.33) is denoted by $\mathcal{X}(\Omega) \equiv \langle \mathcal{X}_T \rangle$.

To derive the bound on the activity, we use the lower bound (A.7) on the generating function $\lambda_{n\mathcal{T}}(z)$ for the quantity $X_T = \mathcal{X}_T$. We choose the ansatz

$$\begin{aligned} \tilde{p}_i(\tau) &= p_i^{\mathrm{ps}}(\Omega\tau/\tilde{\Omega};\tilde{\Omega}), \\ \tilde{k}_{ij}(\tau) &= (\Omega/\tilde{\Omega}) k_{ij}(\tau) - (\Omega/\tilde{\Omega} - 1) k_{ij}(\tau) \alpha_{ij}(\tau)^{\delta}, \end{aligned} \tag{A.34}$$

with

$$\alpha_{ij}(\tau) \equiv \sqrt{\frac{p_j^{\mathrm{ps}}(\Omega\tau/\tilde{\Omega};\tilde{\Omega}) k_{ji}(\tau)}{p_i^{\mathrm{ps}}(\Omega\tau/\tilde{\Omega};\tilde{\Omega}) k_{ij}(\tau)}} \tag{A.35}$$

and $\delta$ will be chosen as 0 or 1. For $\delta = 0$, the first term in (A.7) is given by

$$\langle \mathcal{X}_{\mathcal{T}} \rangle^{\mathrm{aux}} = \frac{(\Omega/\tilde{\Omega})}{\mathcal{T}} \int_0^{\mathcal{T}} \mathrm{d}\tau \sum_{ij} p_i^{\mathrm{ps}}(\Omega\tau/\tilde{\Omega};\tilde{\Omega}) k_{ij}(\tau) g_{ij}(\tau) \tag{A.36}$$

Using the substitution $\tilde{\tau} = \Omega\tau/\tilde{\Omega}$ and the property of the increments

$$g_{ij}(\tau;\Omega) = g_{ij}(\tilde{\Omega}\tilde{\tau}/\Omega;\Omega) = g_{ij}(\tilde{\tau};\tilde{\Omega}), \tag{A.37}$$

where the upper index denotes the corresponding frequency, leads to

$$\langle \mathcal{X}_T \rangle^{\mathrm{aux}} = (\Omega/\tilde{\Omega}) \mathcal{X}(\tilde{\Omega}). \tag{A.38}$$

Inserting (A.34) into Eq. (A.8), choosing $\tilde{\Omega} = (1+\epsilon)\Omega$ with small parameter $\epsilon = \mathcal{O}(z)$ leads to

$$\begin{aligned} F[\tilde{\mathbf{p}}(\tau), \tilde{\mathbf{k}}(\tau)] = \frac{1}{\mathcal{T}} \int_0^{\mathcal{T}} \mathrm{d}\tau \sum_{ij} \Big( &\sqrt{p_i^{\mathrm{ps}}(\tau;\Omega) k_{ij}(\tau)} \\ &- \delta \sqrt{p_j^{\mathrm{ps}}(\tau;\Omega) k_{ji}(\tau)} \Big)^2 \frac{\epsilon^2}{2} + \mathcal{O}(\epsilon^3). \end{aligned} \tag{A.39}$$

Choosing $\delta = 0$, expanding (A.38) for small $\epsilon$ and optimizing with respect to this parameter leads to a quadratic bound on the generating

function. Taking the long-time limit $n \to \infty$, this quadratic bound implies

$$2D_{\mathcal{X}}(\Omega)\mathcal{A}(\Omega)/\mathcal{X}^2(\Omega) \geq (1-\mathcal{X}'(\Omega)/\mathcal{X}(\Omega))^2, \tag{A.40}$$

which is a generalization of the bound on activity in [108] to periodically driven systems. We note, that for $\delta = 1$, the main results for currents $J_T$ and residence quantities $A_T$ can be recovered.

Finally, the finite-time generalization of Eq. (A.40) is given by

$$2D_{\mathcal{X}}(n\mathcal{T};\Omega)[\mathcal{A}(\Omega)+\tilde{C}(\Omega)]/\mathcal{X}^2(\Omega) \geq (1-\mathcal{X}'(\Omega)/\mathcal{X}(\Omega))^2, \tag{A.41}$$

where $\tilde{C}(\Omega)$ is defined in Eq. (A.31).

## A.4 STIRLING HEAT ENGINE

In this section, we calculate currents of interest and the diffusion coefficient for the output power of the Stirling engine discussed in the main text. The periodic stationary solution of the Fokker-Planck equation in the main text is a Gaussian with zero mean

$$p^{\mathrm{ps}}(x,\tau) = \frac{1}{\sqrt{2\pi\left\langle x^2(\tau)\right\rangle}} \exp\left(-\frac{x^2}{2\left\langle x^2(\tau)\right\rangle}\right), \tag{A.42}$$

where the variance can be calculated according to

$$\partial_\tau \left\langle x^2(\tau)\right\rangle = 2\mu\left(\beta^{-1}(\tau) - k(\tau)\left\langle x^2(\tau)\right\rangle\right), \tag{A.43}$$

which follows from the Fokker-Planck equation [137]. Here, the variance has to be periodic in time, i.e.,

$$\left\langle x^2(0)\right\rangle = \left\langle x^2(\mathcal{T})\right\rangle.$$

The output power is defined by

$$P_{\mathrm{out}} \equiv -\frac{1}{\mathcal{T}}\int_0^{\mathcal{T}} \mathrm{d}\tau \int_{-\infty}^{\infty} \mathrm{d}x\, p^{\mathrm{ps}}(x,\tau)\dot{V}(x,\tau). \tag{A.44}$$

The entropy production associated with heat dissipation in the medium given by

$$\sigma_m \equiv \frac{1}{\mathcal{T}}\int_0^{\mathcal{T}} \mathrm{d}\tau \int_{-\infty}^{\infty} \mathrm{d}x\, \beta(\tau) j^{\mathrm{ps}}(x,\tau)F(x,\tau), \tag{A.45}$$

where

$$j^{\mathrm{ps}}(x,\tau) \equiv -\mu\left[\partial_x V(x,\tau) + \beta^{-1}(\tau)\partial_x\right] p^{\mathrm{ps}}(x,\tau) \tag{A.46}$$

is the probability current. If the system has reached the periodic stationary state, the entropy production $\sigma_m$ of the medium averaged over one cycle duration $\mathcal{T}$ is identical to the average total entropy

production of the system. Hence, we use the notation $\sigma \equiv \sigma_m$. The heat current flowing into or out of the system from or into the heat bath is defined by

$$\dot{Q} \equiv \frac{1}{\mathcal{T}} \int \mathrm{d}\tau \int_{-\infty}^{\infty} \mathrm{d}x \, j^{\mathrm{ps}}(x,\tau) F(x,\tau). \tag{A.47}$$

Note that the integration over $\tau$ is performed during the time interval at which the heat bath is connected to the system.

Inserting (A.42) into (A.44), (A.45) and (A.47) yields the following expressions for power

$$P_{\mathrm{out}} = -\frac{1}{\mathcal{T}} \int_0^{\mathcal{T}} \mathrm{d}\tau \, \frac{\dot{k}(\tau)}{2} \left\langle x^2(\tau) \right\rangle, \tag{A.48}$$

entropy production

$$\sigma = \frac{1}{\mathcal{T}} \int_0^{\mathcal{T}} \mathrm{d}\tau \, \frac{\mu k(\tau)}{2} \left( \beta(\tau) k(\tau) \left\langle x^2(\tau) \right\rangle - 1 \right),$$

and the cold heat flux flowing out of the system

$$\dot{Q}_c = \frac{1}{\mathcal{T}} \int_0^{\mathcal{T}/2} \mathrm{d}\tau \, \frac{\mu k(\tau)}{2\beta_c} \left( \beta_c k(\tau) \left\langle x^2(\tau) \right\rangle - 1 \right), \tag{A.49}$$

as well as the hot heat flux flowing into the system

$$\dot{Q}_h = -\frac{1}{\mathcal{T}} \int_{\mathcal{T}/2}^{\mathcal{T}} \mathrm{d}\tau \, \frac{\mu k(\tau)}{2\beta_h} \left( \beta_h k(\tau) \left\langle x^2(\tau) \right\rangle - 1 \right). \tag{A.50}$$

These currents of interest can be calculated by solving (A.43) for the initial condition leading to the periodic stationary state.

The diffusion coefficient of the output power (A.48) after $n$ periods is given by

$$D_{P_{\mathrm{out}}}(n) = \frac{1}{2n\mathcal{T}} \int_0^{n\mathcal{T}} \int_0^{n\mathcal{T}} \mathrm{d}t \, \mathrm{d}t' \left\langle x^2(t) x^2(t') \right\rangle k(t) k(t')/4 - \frac{n\mathcal{T}}{2} P_{\mathrm{out}}^2. \tag{A.51}$$

The the correlation function $\left\langle x^2(t) x^2(t') \right\rangle$ can be written as

$$\left\langle x^2(t) x^2(t') \right\rangle = \int_{-\infty}^{\infty} \int_{-\infty}^{\infty} \mathrm{d}x \, \mathrm{d}x' \, x^2 x'^2 p(x, x', t, t'), \tag{A.52}$$

where $p(x, x', t, t')$ is the joint probability density. Here, $x$ and $x'$ are Gaussian distributed according to (A.42). Due to the linearity of the Langevin equation, every linear combination of $x$ and $x'$ is also Gaussian distributed. Hence, the joint probability density $p(x, x', t, t')$ is a bivariate normal distribution and the expectation value in (A.52) is consequently given by

$$\left\langle x^2(t) x^2(t') \right\rangle = \left\langle x^2(t) \right\rangle \left\langle x^2(t') \right\rangle + 2 \left\langle x(t) x(t') \right\rangle^2. \tag{A.53}$$

By solving the Langevin equation, we can evaluate the correlation function (A.53) and obtain the following expression for the diffusion coefficient in the long-time limit

$$D_{P_{\text{out}}} = \lim_{n\to\infty} \frac{1}{n\mathcal{T}} \int_0^{n\mathcal{T}} \int_0^t \mathrm{d}t\, \mathrm{d}t' \, \frac{1}{2} k(t)k(t') \left\langle x^2(t') \right\rangle^2 e^{2(I(t')-I(t))} \tag{A.54}$$

with

$$I(t) \equiv \mu \int_0^t \mathrm{d}t'\, k(t'). \tag{A.55}$$

# B

# ARBITRARY TIME-DEPENDENT DRIVING

This chapter contains five sections. In Section B.1, we derive the main results in Chapter 6 for current-like observables, Eq. (6.1), and for state variables, Eq. (6.16), in systems with continuous degrees of freedom. Section B.2 contains the derivation of these main results in Chapter 6 for systems with discrete degrees of freedom. Sections B.3 and B.4 provide more details for the case study of the moving trap with one particle and two interacting particles, respectively. In Section B.5, the rates for the protein folding system are given.

## B.1 DERIVATION OF THE MAIN RESULTS: CONTINUOUS DEGREES OF FREEDOM

### B.1.1 *Setup*

We derive the main results for time-dependently driven systems with $N_x$ interacting continuous degrees of freedom. The coordinate vector $\boldsymbol{x} \equiv \{x_1, ..., x_{N_x}\}$ describes the state of the system, which is driven by multiple protocols $\boldsymbol{\lambda}_t \equiv \boldsymbol{\lambda}_t(\{v_\alpha\}) \equiv \{\lambda_1(v_1 t), ..., \lambda_{N_\lambda}(v_{N_\lambda} t)\}$ with $N_\lambda$ speed parameter $v_\alpha$ and $\alpha \in [1, N_\lambda]$. The dynamics obeys the Langevin equation with multiplicative noise

$$\dot{\boldsymbol{x}}(t) = \boldsymbol{B}(\boldsymbol{x}(t), \boldsymbol{\lambda}_t) + \nabla^T \mathbf{D}(\boldsymbol{x}(t), \boldsymbol{\lambda}_t) - [\mathbf{G}^T(\boldsymbol{x}(t), \boldsymbol{\lambda}_t)\nabla]^T \mathbf{G}(\boldsymbol{x}(t), \boldsymbol{\lambda}_t) + \sqrt{2}\mathbf{G}(\boldsymbol{x}(t), \boldsymbol{\lambda}_t) \circ \boldsymbol{\zeta}(t). \tag{B.1}$$

Here, we use the Stratonovich convention, where $\circ$ denotes the Stratonovich product, $(\cdot)^T$ denotes transposition, $\nabla \equiv \{\partial_{x_1}, ..., \partial_{x_{N_x}}\}$ is the Nabla operator and $\boldsymbol{\zeta}(t) \equiv \{\zeta_1(t), ..., \zeta_{N_x}(t)\}$ is a Gaussian white noise vector describing the random forces with mean and correlations

$$\langle \zeta_i(t) \rangle = 0, \tag{B.2}$$

$$\langle \zeta_i(t)\zeta_j(t') \rangle = \delta_{ij}\delta(t - t'). \tag{B.3}$$

Furthermore, using the $N_x \times N_x$ matrix $\mathbf{G}(\boldsymbol{x}, \boldsymbol{\lambda}_t)$, we define the state- and time-dependent diffusion matrix by $\mathbf{D}(\boldsymbol{x}, \boldsymbol{\lambda}_t) \equiv \mathbf{G}(\boldsymbol{x}, \boldsymbol{\lambda}_t)\mathbf{G}^T(\boldsymbol{x}, \boldsymbol{\lambda}_t)$, which is a symmetric matrix. The diffusion matrix obeys the Einstein relation, i.e., $\mathbf{D}(\boldsymbol{x}, \boldsymbol{\lambda}_t) = \boldsymbol{\mu}(\boldsymbol{x}, \boldsymbol{\lambda}_t)/\beta$, where $\boldsymbol{\mu}(\boldsymbol{x}, \boldsymbol{\lambda}_t)$ denotes the $N_x \times N_x$ mobility matrix and $\beta$ is the inverse temperature of the heat bath. The drift vector

$$\boldsymbol{B}(\boldsymbol{x}, \boldsymbol{\lambda}_t) = \boldsymbol{\mu}(\boldsymbol{x}, \boldsymbol{\lambda}_t)\boldsymbol{F}(\boldsymbol{x}, \boldsymbol{\lambda}_t) \equiv \boldsymbol{\mu}(\boldsymbol{x}, \boldsymbol{\lambda}_t)(-\nabla V(\boldsymbol{x}, \boldsymbol{\lambda}_t) + \boldsymbol{f}(\boldsymbol{x}, \boldsymbol{\lambda}_t)) \tag{B.4}$$

contains the forces $\boldsymbol{F}(\boldsymbol{x}, \boldsymbol{\lambda}_t)$ driving the system out of equilibrium. They consist of a conservative force generated by a potential $V(\boldsymbol{x}, \boldsymbol{\lambda}_t)$ and a non-conservative force $\boldsymbol{f}(\boldsymbol{x}, \boldsymbol{\lambda}_t)$. Both, the drift and diffusion term are controlled by the protocol $\boldsymbol{\lambda}_t$. The additional drift term $\nabla^T \mathbf{D}(\boldsymbol{x}, \boldsymbol{\lambda}_t) - [\mathbf{G}^T(\boldsymbol{x}, \boldsymbol{\lambda}_t)\nabla]^T \mathbf{G}(\boldsymbol{x}, \boldsymbol{\lambda}_t)$ arises due to the Stratonovich convention and makes sure that a non-driven system will reach the Boltzmann distribution for $t \to \infty$ [37].

Equivalently to the Langevin equation (B.1), we can describe the dynamics for the probability density $p(\boldsymbol{x}, t; \{v_\alpha\})$ by the Fokker-Planck equation [38]

$$\partial_t p(\boldsymbol{x}, t; \{v_\alpha\}) = -\nabla \boldsymbol{j}(\boldsymbol{x}, t; \{v_\alpha\}) \tag{B.5}$$

with probability current vector

$$\boldsymbol{j}(\boldsymbol{x}, t; \{v_\alpha\}) \equiv (\boldsymbol{B}(\boldsymbol{x}, \boldsymbol{\lambda}_t) - \mathbf{D}(\boldsymbol{x}, \boldsymbol{\lambda}_t)\nabla)\, p(\boldsymbol{x}, t; \{v_\alpha\}). \tag{B.6}$$

The probability density for an individual trajectory $\boldsymbol{x}(t)$ of length $T$ is given by the path weight

$$\mathcal{P}[\boldsymbol{x}(t)] \equiv \mathcal{N} \exp\left(-\mathcal{S}[\boldsymbol{x}(t), \boldsymbol{\lambda}_t]\right) p(\boldsymbol{x}(0), 0) \tag{B.7}$$

with the action

$$\begin{aligned} \mathcal{S}[\boldsymbol{x}(t), \boldsymbol{\lambda}_t] \equiv \frac{1}{4} \int_0^T \mathrm{d}t\, (\dot{\boldsymbol{x}}(t) - \boldsymbol{B}(\boldsymbol{x}(t), \boldsymbol{\lambda}_t))^T\, \mathbf{D}(\boldsymbol{x}(t), \boldsymbol{\lambda}_t)^{-1} \\ \times (\dot{\boldsymbol{x}}(t) - \boldsymbol{B}(\boldsymbol{x}(t), \boldsymbol{\lambda}_t)) \\ + \frac{1}{2} \int_0^T \mathrm{d}t\, \nabla \boldsymbol{B}(\boldsymbol{x}(t), \boldsymbol{\lambda}_t) + \Gamma[\mathbf{G}(\boldsymbol{x}(t), \boldsymbol{\lambda}_t)] \end{aligned} \tag{B.8}$$

for an arbitrary initial condition $p(\boldsymbol{x}(0), 0)$. Here, $\mathbf{D}(\boldsymbol{x}(t), \boldsymbol{\lambda}_t)^{-1}$ denotes the inverse of the diffusion matrix and

$$\mathcal{N} \equiv \left( \prod_{l=1}^{N_t} \frac{1}{\sqrt{4\pi} \det\left[\mathbf{G}(\boldsymbol{x}(t_l), \boldsymbol{\lambda}_{t_l})\right]} \right) \tag{B.9}$$

is a normalization factor with respect to the measure of integration

$$\int \mathrm{d}[\boldsymbol{x}(t)] \equiv \prod_{l=0}^{N_t} \int \mathrm{d}\boldsymbol{x}(t_l)\,, \tag{B.10}$$

i.e., $\int \mathrm{d}[\boldsymbol{x}(t)]\, \mathcal{P}[\boldsymbol{x}(t)] = 1$, where $\det[\cdot]$ denotes the determinant of a matrix. The path weight in Eq. (B.7) is well defined for a suitable discretization in time. The trajectory is sliced into $N_t$ discrete values $\{\boldsymbol{x}(t_0), \boldsymbol{x}(t_1), ..., \boldsymbol{x}(t_{N_t})\}$ with $t_l \equiv l\Delta t$, where $\Delta t$ is a small enough time

step and chosen such that $N_t \Delta t = T$ is fulfilled. The two last terms in Eq. (B.8) with

$$\begin{aligned}\Gamma[\mathbf{G}(\boldsymbol{x},\boldsymbol{\lambda}_t)] \equiv \frac{1}{2}\int_0^T \mathrm{d}t \sum_{ijk}\Big(&\partial_{x_i}\partial_{x_j}\left[G_{ik}(\boldsymbol{x},\boldsymbol{\lambda}_t)G_{jk}(\boldsymbol{x},\boldsymbol{\lambda}_t)\right] \\ &- \partial_{x_i}\left[G_{kj}(\boldsymbol{x},\boldsymbol{\lambda}_t)\partial_{x_k}G_{ij}(\boldsymbol{x},\boldsymbol{\lambda}_t)\right] \\ &+\frac{1}{2}\{[\partial_{x_k}G_{ij}(\boldsymbol{x},\boldsymbol{\lambda}_t)][\partial_{x_i}G_{kj}(\boldsymbol{x},\boldsymbol{\lambda}_t)] \\ &- [\partial_{x_i}G_{ij}(\boldsymbol{x},\boldsymbol{\lambda}_t)][\partial_{x_k}G_{kj}(\boldsymbol{x},\boldsymbol{\lambda}_t)]\}\Big),\end{aligned} \tag{B.11}$$

where $G_{ij}(\boldsymbol{x},\boldsymbol{\lambda}_t) \equiv [\mathbf{G}(\boldsymbol{x},\boldsymbol{\lambda}_t)]_{ij}$ are matrix elements, arise from a Stratonovich discretization scheme [37].

### B.1.2 *Bound on the diffusion coefficient*

For deriving our main result, we use the method introduced by Dechant and Sasa [74, 75] that bounds the scaled cumulant generating function, or short *generating function*,

$$\lambda(z) \equiv \frac{1}{T}\ln\langle \exp(zTX_T)\rangle \equiv \frac{1}{T}\ln\int \mathrm{d}[\boldsymbol{x}(t)]\,\mathcal{P}[\boldsymbol{x}(t)]\exp(zTX_T[\boldsymbol{x}(t)]) \tag{B.12}$$

for a fluctuating observable $X_T = X_T[\boldsymbol{x}(t)] \in \{a_T, A_T, J_T^{\mathrm{I,II}}\}$ by introducing an auxiliary path weight $\mathcal{P}^\dagger[\boldsymbol{x}(t)]$ that describes an auxiliary dynamics obeying a Langevin equation of type (B.1). The first two derivatives of $\lambda(z)$ at $z = 0$ yield the mean and diffusion coefficient of $X_T$, i.e.,

$$\lambda'(z)|_{z=0} = \langle X_T\rangle\,, \tag{B.13}$$

$$\lambda''(z)|_{z=0} = 2D_X(T,\{v_\alpha\}). \tag{B.14}$$

Writing the expectation value in (B.12) in terms of the auxiliary path weight $\mathcal{P}^\dagger[\boldsymbol{x}(t)]$ and using Jensen's inequality, we get the lower bound

$$\begin{aligned}\lambda(z) &= \frac{1}{T}\ln\int \mathrm{d}[\boldsymbol{x}(t)]\,\mathcal{P}^\dagger[\boldsymbol{x}(t)]\frac{\mathcal{P}[\boldsymbol{x}(t)]}{\mathcal{P}^\dagger[\boldsymbol{x}(t)]}\exp(zTX_T[\boldsymbol{x}(t)]) \\ &\geq z\,\langle X_T\rangle^\dagger - \frac{1}{T}\left\langle \ln\left(\frac{\mathcal{P}^\dagger[\boldsymbol{x}(t)]}{\mathcal{P}[\boldsymbol{x}(t)]}\right)\right\rangle^\dagger\end{aligned} \tag{B.15}$$

on the generating function, where $\langle\cdot\rangle^\dagger$ denotes the expectation value in the auxiliary dynamics. For a suitable choice of the path weight $\mathcal{P}^\dagger[\boldsymbol{x}(t)]$, the bound (B.15) implies a bound on the diffusion coefficient as we will show below.

We require the auxiliary path weight $\mathcal{P}^\dagger[\boldsymbol{x}(t)]$ to follow the Fokker-Planck equation

$$\partial_t p^\dagger(\boldsymbol{x},t;\{v_\alpha^\dagger\}) = -\nabla \boldsymbol{j}^\dagger(\boldsymbol{x},t;\{v_\alpha^\dagger\}) \tag{B.16}$$

with auxiliary density $p^\dagger(\boldsymbol{x}, t; \{v_\alpha^\dagger\})$ and auxiliary current

$$\boldsymbol{j}^\dagger(\boldsymbol{x}, t; \{v_\alpha^\dagger\}) \equiv \left(\boldsymbol{B}^\dagger(\boldsymbol{x}, \boldsymbol{\lambda}_t^\dagger, t) - \mathbf{D}^\dagger(\boldsymbol{x}, \boldsymbol{\lambda}_t^\dagger)\nabla\right) p^\dagger(\boldsymbol{x}, t; \{v_\alpha^\dagger\}). \quad \text{(B.17)}$$

Here, the auxiliary diffusion process is generated by the drift vector $\boldsymbol{B}^\dagger(\boldsymbol{x}, \boldsymbol{\lambda}_t^\dagger, t)$ and diffusion matrix $\mathbf{D}^\dagger(\boldsymbol{x}, \boldsymbol{\lambda}_t^\dagger) \equiv \mathbf{G}^\dagger(\boldsymbol{x}, \boldsymbol{\lambda}_t^\dagger)[\mathbf{G}^\dagger(\boldsymbol{x}, \boldsymbol{\lambda}_t^\dagger)]^T$, where we introduce the auxiliary protocol given by $\boldsymbol{\lambda}_t^\dagger \equiv \boldsymbol{\lambda}_t^\dagger\left(\{v_\alpha^\dagger\}\right) \equiv \{\lambda_1^\dagger(v_1^\dagger t), ..., \lambda_1^\dagger(v_{N_\lambda}^\dagger t)\}$ with auxiliary speed parameter $v_\alpha^\dagger$ and $\alpha \in [1, N_\lambda]$.

We choose the auxiliary dynamics such that it describes an original dynamics that evolves slower or faster in time, i.e., $t \to (1+\epsilon)t$ and $v_\alpha \to v_\alpha/(1+\epsilon)$ and that is driven with the same protocol functions $\{\lambda_\alpha\}$. Here, $\epsilon = \mathcal{O}(z)$ is assumed to be a small parameter, i.e., the auxiliary dynamics is considered in a linear response regime around the original dynamics [75]. Hence, the protocol and the speed parameter of the auxiliary dynamics read

$$\boldsymbol{\lambda}_t^\dagger = \boldsymbol{\lambda}_{(1+\epsilon)t}\left(\{v_\alpha^\dagger\}\right) = \{\lambda_1(v_1 t), ..., \lambda_{N_\lambda}(v_{N_\lambda} t)\} = \boldsymbol{\lambda}_t \quad \text{(B.18)}$$

and

$$v_\alpha^\dagger \equiv v_\alpha/(1+\epsilon), \quad \text{(B.19)}$$

respectively. Thus, the protocol is the same as for the original dynamics. The auxiliary density and current are consequently given by

$$p^\dagger(\boldsymbol{x}, t; \{v_\alpha^\dagger\}) \equiv p(\boldsymbol{x}, [1+\epsilon]t; \{v_\alpha^\dagger\}), \quad \text{(B.20)}$$

and

$$\boldsymbol{j}^\dagger(\boldsymbol{x}, t; \{v_\alpha^\dagger\}) \equiv (1+\epsilon)\boldsymbol{j}(\boldsymbol{x}, [1+\epsilon]t; \{v_\alpha^\dagger\}), \quad \text{(B.21)}$$

respectively, where we assume that both processes start in the same initial condition $p(\boldsymbol{x}(0), 0)$. Furthermore, we assume that the initial condition does not depend on the speed parameter $v_\alpha$. If this was not the case, like, e.g., for a system in a periodic steady-state, an additional boundary term would occur for finite observation times (see Section A.2). The auxiliary dynamics introduced above describing a "time-scaled" diffusion process can be considered as a process generated by an additional drift vector and the original diffusion matrix according to

$$\boldsymbol{B}^\dagger(\boldsymbol{x}, \boldsymbol{\lambda}_t^\dagger, t) = \boldsymbol{B}(\boldsymbol{x}, \boldsymbol{\lambda}_t) + \epsilon \boldsymbol{Y}(\boldsymbol{x}, [1+\epsilon]t; \{v_\alpha^\dagger\}) \quad \text{(B.22)}$$

and

$$\mathbf{D}^\dagger(\boldsymbol{x}, \boldsymbol{\lambda}_t^\dagger) = \mathbf{D}(\boldsymbol{x}, \boldsymbol{\lambda}_t), \ \mathbf{G}^\dagger(\boldsymbol{x}, \boldsymbol{\lambda}_t^\dagger) = \mathbf{G}(\boldsymbol{x}, \boldsymbol{\lambda}_t), \quad \text{(B.23)}$$

respectively. The drift term $\boldsymbol{B}^\dagger(\boldsymbol{x}, \boldsymbol{\lambda}_t^\dagger, t)$ contains the small additional force

$$\epsilon \boldsymbol{Y}(\boldsymbol{x}, [1+\epsilon]t; \{v_\alpha^\dagger\}) \equiv \epsilon \boldsymbol{j}(\boldsymbol{x}, [1+\epsilon]t; \{v_\alpha^\dagger\})/p(\boldsymbol{x}, [1+\epsilon]t; \{v_\alpha^\dagger\}) \quad \text{(B.24)}$$

and is called a *virtual perturbation* [75]. The diffusion matrix $\mathbf{D}(\boldsymbol{x}, \boldsymbol{\lambda}_t)$ is the same as for the original process. Thus, the normalization constant (B.9) is the same for both dynamics.

Next, we insert the auxiliary path weight

$$\mathcal{P}^\dagger[\boldsymbol{x}(t)] \equiv \mathcal{N} \exp\left(-\mathcal{S}^\dagger[\boldsymbol{x}(t), \boldsymbol{\lambda}_t]\right) \tag{B.25}$$

with action

$$\begin{aligned}\mathcal{S}^\dagger[\boldsymbol{x}(t), \boldsymbol{\lambda}_t] \equiv \frac{1}{4}\int_0^T \mathrm{d}t \left(\dot{\boldsymbol{x}}(t) - \boldsymbol{B}^\dagger(\boldsymbol{x}(t), \boldsymbol{\lambda}_t, t)\right)^T \mathbf{D}(\boldsymbol{x}(t), \boldsymbol{\lambda}_t)^{-1} \\ \times \left(\dot{\boldsymbol{x}}(t) - \boldsymbol{B}^\dagger(\boldsymbol{x}(t), \boldsymbol{\lambda}_t, t)\right) \\ + \frac{1}{2}\int_0^T \mathrm{d}t\, \nabla \boldsymbol{B}^\dagger(\boldsymbol{x}(t), \boldsymbol{\lambda}_t, t) + \Gamma[\mathbf{G}(\boldsymbol{x}(t), \boldsymbol{\lambda}_t)],\end{aligned} \tag{B.26}$$

and the auxiliary drift term defined in Eq. (B.22) into Eq. (B.15) and obtain the bound

$$\lambda(z) \geq z \langle X_T \rangle^\dagger - \frac{\epsilon^2}{4}\sigma(T^\dagger, \{v_\alpha^\dagger\}). \tag{B.27}$$

The total entropy production rate

$$\sigma(T^\dagger, \{v_\alpha^\dagger\}) \equiv \frac{1}{T^\dagger}\int_0^{T^\dagger} \mathrm{d}t' \, \frac{\boldsymbol{j}(\boldsymbol{x}, t'; \{v_\alpha^\dagger\})^T \mathbf{D}(\boldsymbol{x}, \boldsymbol{\lambda}_{t'}(\{v_\alpha^\dagger\}))^{-1} \boldsymbol{j}(\boldsymbol{x}, t'; \{v_\alpha^\dagger\})}{p(\boldsymbol{x}, t'; \{v_\alpha^\dagger\})} \tag{B.28}$$

is the one of a system with observation time $T^\dagger \equiv (1+\epsilon)T$ and speed parameter $v^\dagger = v_\alpha/(1+\epsilon)$, where we used the substitution $t' = (1+\epsilon)t$.

We take the limit $\epsilon \to 0$ and calculate the leading orders of the two terms in Eq. (B.27). The first term in Eq. (B.27) depends on the

observable $X_T$ and is given by one of the following four expectation values depending on the choice of $X_T \in \{a_T, A_T, J_T^{\mathrm{I,II}}\}$

$$\begin{aligned}\langle a_T \rangle^\dagger &= a(T^\dagger, \{v_\alpha^\dagger\}) \\ &= \int \mathrm{d}\boldsymbol{x}\, a(\boldsymbol{x}, \boldsymbol{\lambda}_{T^\dagger}(\{v_\alpha^\dagger\}))p(\boldsymbol{x}, T^\dagger; \{v_\alpha^\dagger\}),\end{aligned} \tag{B.29}$$

$$\begin{aligned}\langle A_T \rangle^\dagger &= A(T^\dagger, \{v_\alpha^\dagger\}) \\ &= \frac{1}{T^\dagger}\int_0^{T^\dagger} \mathrm{d}t' \int \mathrm{d}\boldsymbol{x}\, a(\boldsymbol{x}, \boldsymbol{\lambda}_{t'}(\{v_\alpha^\dagger\}))p(\boldsymbol{x}, t'; \{v_\alpha^\dagger\}),\end{aligned} \tag{B.30}$$

$$\begin{aligned}\left\langle J_T^{\mathrm{I}} \right\rangle^\dagger &= J^{\mathrm{I}}(T^\dagger, \{v_\alpha^\dagger\}) \\ &= \frac{1}{T^\dagger}\int_0^{T^\dagger} \mathrm{d}t' \int \mathrm{d}\boldsymbol{x}\, (1+\epsilon)\boldsymbol{d}^{\mathrm{I}}(\boldsymbol{x}, \boldsymbol{\lambda}_{t'}(\{v_\alpha^\dagger\})) \cdot \boldsymbol{j}(\boldsymbol{x}, t'; \{v_\alpha^\dagger\}),\end{aligned} \tag{B.31}$$

$$\begin{aligned}\left\langle J_T^{\mathrm{II}} \right\rangle^\dagger &= J^{\mathrm{II}}(T^\dagger, \{v_\alpha^\dagger\}) \\ &= \frac{1}{T^\dagger}\int_0^{T^\dagger} \mathrm{d}t' \int \mathrm{d}\boldsymbol{x}\, (1+\epsilon) d^{\mathrm{II}}(\boldsymbol{x}, \boldsymbol{\lambda}_{t'}(\{v_\alpha^\dagger\}))p(\boldsymbol{x}, t'; \{v_\alpha^\dagger\}).\end{aligned} \tag{B.32}$$

The increment

$$d^{\mathrm{II}}(\boldsymbol{x}, \boldsymbol{\lambda}_t) \equiv \partial_t \boldsymbol{\lambda}_t \cdot \nabla_{\boldsymbol{\lambda}_t} b(\boldsymbol{x}, \boldsymbol{\lambda}_t), \tag{B.33}$$

involves the time-derivative of a state function $b(\boldsymbol{x}, \boldsymbol{\lambda}_t)$. The vector $\boldsymbol{d}^{\mathrm{I}}(\boldsymbol{x}, \boldsymbol{\lambda}_t)$ is arbitrary. Calculating the leading order in $\epsilon = \mathcal{O}(z)$ in Eq. (B.27) via Eqs. (B.28)–(B.32) and optimizing with respect to $\epsilon$ leads to a local quadratic bound on the generating function that implies with Eqs. (B.13) and (B.14) our main results. These are the bounds on the diffusion coefficients

$$D_J(T, \{v_\alpha\}) \geq \frac{[J(T, \{v_\alpha\}) + \Delta J(T, \{v_\alpha\})]^2}{\sigma(T, \{v_\alpha\})} \tag{B.34}$$

and

$$D_{\mathcal{A}}(T, \{v_\alpha\}) \geq \frac{[\Delta \mathcal{A}(T, \{v_\alpha\})]^2}{\sigma(T, \{v_\alpha\})} \tag{B.35}$$

with currents $J(T, \{v_\alpha\}) \in \{J^{\mathrm{I}}(T, \{v_\alpha\}), J^{\mathrm{II}}(T, \{v_\alpha\})\}$ and state variables $\mathcal{A}(T, \{v_\alpha\}) \in \{a(T, \{v_\alpha\}), A(T, \{v_\alpha\})\}$. The differential operator

$$\Delta \equiv T\partial_T - \sum_\alpha v_\alpha \partial_{v_\alpha} \tag{B.36}$$

is a generalization of the operator defined in Eq. (6.2) to multiple speed parameters. These relations prove the inequalities (6.1) and (6.16) for continuous degrees of freedom.

Finally, we connect the above introduced formalism to the FRI (6.17) in Chapter 6 by deriving it explicitly for a system with one speed

parameter $v$ and one degree of freedom $x$. Instead of using the specific perturbation in Eq. (B.24), we use an arbitrary perturbation of the drift term as

$$B^\dagger(x,\lambda_t,t) \equiv B(x,\lambda_t) + \epsilon Y(x,t;\epsilon), \tag{B.37}$$

where the additional drift term $Y(x,t;\epsilon)$ depends on a parameter $\epsilon$. Inserting Eq. (B.37) into (B.15) yields the lower bound on the cumulant generating function

$$\lambda(z) \geq z \langle X_T \rangle^\dagger - \frac{\epsilon^2}{4} \left\langle Y(x(t),t;\epsilon)^2/D \right\rangle^\dagger, \tag{B.38}$$

where $D$ denotes the diffusion constant. Next, we consider the limit $\epsilon = \mathcal{O}(z) \to 0$, i.e., the perturbed dynamics is in a linear response regime around the original dynamics. Optimizing Eq. (B.38) with respect to $\epsilon$ and calculating the leading order in Eq. (B.38) leads to a bound on the diffusion coefficient

$$D_X(T,v) \geq \frac{(\partial_\epsilon \langle X_T \rangle^\dagger |_{\epsilon=0})^2}{1/T \int_0^T \mathrm{d}t \left\langle Y(x(t),t;\epsilon)^2/D \right\rangle^\dagger |_{\epsilon=0}}. \tag{B.39}$$

This inequality is called a FRI [75] and is identical to Eq. (6.17). Using the special choice of the force in Eq. (B.24) and inserting Eqs. (B.29)–(B.32) into the FRI (B.39) leads to our main results Eqs. (B.69) and (B.70), i.e., Eqs. (6.1) and (6.16) in Chapter 6. We note that the FRI in Eq. (B.39) is a special case of a FRI due to the linear response assumption. For arbitrary strong perturbations a more general FRI can be derived, which involves higher-order cumulants (see Ref. [75] for details).

## B.2 DERIVATION OF THE MAIN RESULTS: DISCRETE STATES

### B.2.1 *Setup*

Here, we consider systems with $N_s$ discrete states. These systems obey a Markovian dynamics described by the master equation

$$\partial_t p_i(t;\{v_\alpha\}) = -\sum_j j_{ij}(t;\{v_\alpha\}) \tag{B.40}$$

with probability current

$$j_{ij}(t;\{v_\alpha\}) \equiv p_i(t;\{v_\alpha\}) k_{ij}(\boldsymbol{\lambda}_t) - p_j(t;\{v_\alpha\}) k_{ji}(\boldsymbol{\lambda}_t). \tag{B.41}$$

Here, $k_{ij}(\boldsymbol{\lambda}_t)$ denotes the transition rate from state $i$ to state $j$ at time $t$, when the system is driven by the protocol $\boldsymbol{\lambda}_t \equiv \boldsymbol{\lambda}_t(\{v_\alpha\}) \equiv \{\lambda_1(v_1 t), ..., \lambda_{N_\lambda}(v_{N_\lambda} t)\}$ with $N_\lambda$ speed parameter $v_\alpha$ and $\alpha \in [1, N_\lambda]$. For thermodynamic consistency, the rates $k_{ij}(\boldsymbol{\lambda}_t)$ must fulfill the so-called *local detailed balance condition* [9]

$$\frac{k_{ij}(\boldsymbol{\lambda}_t)}{k_{ji}(\boldsymbol{\lambda}_t)} = \exp\left[-\beta \Delta E_{ij}(\boldsymbol{\lambda}_t) + \mathcal{A}_{ij}(\boldsymbol{\lambda}_t)\right], \tag{B.42}$$

where $\beta$ is the inverse temperature of the heat bath, $\Delta E_{ij}(\boldsymbol{\lambda}_t) \equiv E_j(\boldsymbol{\lambda}_t) - E_i(\boldsymbol{\lambda}_t)$ is the energy difference between state $i$ and $j$, and $\mathcal{A}_{ij}(\boldsymbol{\lambda}_t)$ is a driving affinity, e.g, a non-conservative force, which drives the system in addition to the time-dependent energies. Both, the energies and the driving affinities depend on the protocol $\boldsymbol{\lambda}_t$.

Similarly to systems with continuous degrees of freedom, we can define a probability density for a discrete trajectory $n_t$ of length $T$ with initial condition $p_{n_0}(0)$

$$\mathcal{P}[n_t] \equiv \exp\left(-\int_0^T \mathrm{d}t \sum_i r_i(\boldsymbol{\lambda}_t)\delta_{n_t,i} + \int_0^T \mathrm{d}t \sum_{ij} \ln\left[k_{ij}(\boldsymbol{\lambda}_t)\right] \dot{m}_{ij}(t)\right) \times p_{n_0}(0), \tag{B.43}$$

where $r_i(\boldsymbol{\lambda}_t) \equiv \sum_j k_{ij}(\boldsymbol{\lambda}_t)$ is the escape, or exit rate, of state $i$, $\delta_{n_t,i}$ is a variable that is 1 if state $i$ is occupied and 0, otherwise, and $m_{ij}(T)$ counts the total number of transitions from state $i$ to state $j$. The time derivative of the latter one

$$\dot{m}_{ij}(t) \equiv \sum_l \delta(t - t_l^{(ij)}) \tag{B.44}$$

depends on the times $t_l^{(ij)}$ at which transitions from $i$ and $j$ occur. The path probability (B.43) is normalized, i.e., $\sum_{n_t} \mathcal{P}[n_t] = 1$, where $\sum_{n_t}$ denotes the summation over all paths. The mean values of the variables $\delta_{n_t,i}$ and $\dot{m}_{ij}(t)$ describing a trajectory are given by

$$\langle \delta_{n_t,i} \rangle \equiv \sum_{n_t} \mathcal{P}[n_t]\delta_{n_t,i} = p_i(t;\{v_\alpha\}), \tag{B.45}$$

$$\langle \dot{m}_{ij}(t) \rangle \equiv \sum_{n_t} \mathcal{P}[n_t]\dot{m}_{ij}(t) = p_i(t;\{v_\alpha\})k_{ij}(\boldsymbol{\lambda}_t). \tag{B.46}$$

For systems with discrete states, the analogues of observables $a_T$, $A_T$ and $J_T^{\mathrm{I,II}}$ defined in Eqs. (6.8)–(6.11) in Section 6.3, are given by

$$a_T \equiv a(n_T, \boldsymbol{\lambda}_T), \tag{B.47}$$

$$A_T \equiv \frac{1}{T}\int_0^T \mathrm{d}t\, a(n_t, \boldsymbol{\lambda}_t), \tag{B.48}$$

$$J_T^{\mathrm{I}} \equiv \frac{1}{T}\int_0^T \mathrm{d}t \sum_{ij} d_{ij}^{\mathrm{I}}(\boldsymbol{\lambda}_t)\dot{m}_{ij}(t), \tag{B.49}$$

$$J_T^{\mathrm{II}} \equiv \frac{1}{T}\int_0^T \mathrm{d}t\, d^{\mathrm{II}}(n_t, \boldsymbol{\lambda}_t), \tag{B.50}$$

where $a(n_t, \boldsymbol{\lambda}_t)$ is an arbitrary state variable, $d_{ij}^{\mathrm{I}}(\boldsymbol{\lambda}_t) = -d_{ji}^{\mathrm{I}}(\boldsymbol{\lambda}_t)$ are anti-symmetric increments and

$$d^{\mathrm{II}}(n_t, \boldsymbol{\lambda}_t) \equiv \partial_t \boldsymbol{\lambda}_t \cdot \nabla_{\boldsymbol{\lambda}_t} b(n_t, \boldsymbol{\lambda}_t) \tag{B.51}$$

can be written as a time-derivative of a state variable $b(n_t, \boldsymbol{\lambda}_t)$. The mean values of Eqs. (B.47)-(B.50) are given by

$$\langle a_T \rangle \equiv a(T, \{v_\alpha\}) = \sum_i a(i, \boldsymbol{\lambda}_T) p_i(T, \{v_\alpha\}), \tag{B.52}$$

$$\langle A_T \rangle \equiv A(T, \{v_\alpha\}) = \frac{1}{T} \int_0^T \mathrm{d}t \sum_i a(i, \boldsymbol{\lambda}_t) p_i(t; \{v_\alpha\}), \tag{B.53}$$

$$\left\langle J_T^{\mathrm{I}} \right\rangle \equiv J^{\mathrm{I}}(T, \{v_\alpha\}) = \frac{1}{T} \int_0^T \mathrm{d}t \sum_{i>j} d_{ij}^{\mathrm{I}}(\boldsymbol{\lambda}_t) j_{ij}(t; \{v_\alpha\}), \tag{B.54}$$

$$\left\langle J_T^{\mathrm{II}} \right\rangle \equiv J^{\mathrm{II}}(T, \{v_\alpha\}) = \frac{1}{T} \int_0^T \mathrm{d}t \sum_i d^{\mathrm{II}}(i, \boldsymbol{\lambda}_t) p_i(t; \{v_\alpha\}). \tag{B.55}$$

### B.2.2 *Bound on the diffusion coefficient*

We use the same formalism as used above for systems with continuous degrees of freedom to bound the generating function (B.12) for systems with discrete states. The generating function for an observable $X_T = X_T[n_t] \in \{a_T, A_T, J_T^{\mathrm{I,II}}\}$ is bounded analogously to Eq. (B.15) by introducing an auxiliary process with path weight $\mathcal{P}^\dagger[n_t]$, where the integral $\int \mathrm{d}[\boldsymbol{x}(t)]$ is replaced by the summation over all paths $\sum_{n_t}$ in Eq. (B.15).

We require the auxiliary path weight $\mathcal{P}^\dagger[n_t]$ to describe a master equation

$$\partial_t p_i^\dagger(t; \{v_\alpha^\dagger\}) = -\sum_j j_{ij}^\dagger(t; \{v_\alpha^\dagger\}) \tag{B.56}$$

with probability current

$$j_{ij}^\dagger(t; \{v_\alpha^\dagger\}) \equiv p_i^\dagger(t; \{v_\alpha^\dagger\}) k_{ij}^\dagger(\boldsymbol{\lambda}_t^\dagger) - p_j^\dagger(t; \{v_\alpha^\dagger\}) k_{ji}^\dagger(\boldsymbol{\lambda}_t^\dagger) \tag{B.57}$$

and auxiliary transition rates $k_{ij}^\dagger(\boldsymbol{\lambda}_t^\dagger)$. Here, we introduce the auxiliary protocol $\boldsymbol{\lambda}_t^\dagger \equiv \boldsymbol{\lambda}_t^\dagger\left(\{v_\alpha^\dagger\}\right) \equiv \{\lambda_1^\dagger(v_1^\dagger t), ..., \lambda_1^\dagger(v_{N_\lambda}^\dagger t)\}$ with auxiliary speed parameters $v_\alpha^\dagger$ and $\alpha \in [1, N_\lambda]$. By inserting the auxiliary path weight $\mathcal{P}^\dagger[n_t]$ via definition (B.43) with transition rates $k_{ij}^\dagger(\boldsymbol{\lambda}_t^\dagger)$ into the discrete version of Eq. (B.15), we get

$$\lambda(z) \geq z \langle X_T \rangle^\dagger - \frac{1}{T} \int_0^T \mathrm{d}t \sum_{ij} \Bigg( p_i^\dagger(t; \{v_\alpha^\dagger\}) k_{ij}^\dagger(\boldsymbol{\lambda}_t^\dagger) \ln \left[ \frac{k_{ij}^\dagger(\boldsymbol{\lambda}_t^\dagger)}{k_{ij}(\boldsymbol{\lambda}_t)} \right] - p_i^\dagger(t; \{v_\alpha^\dagger\}) \left[ k_{ij}^\dagger(\boldsymbol{\lambda}_t^\dagger) - k_{ij}(\boldsymbol{\lambda}_t) \right] \Bigg). \tag{B.58}$$

Here, we assume that both processes, i.e., the original and the auxiliary process, start with the same initial condition $p_{n_0}(0)$, which we require to be independent of the speed parameters $\{v_\alpha\}$ (cf. the discussion for systems with continuous degrees of freedom given in Section B.1).

We choose the rates of the auxiliary process as

$$k_{ij}^{\dagger}(\boldsymbol{\lambda}_t^{\dagger}) \equiv k_{ij}(\boldsymbol{\lambda}_t)\left(1+\epsilon\left[1-\eta_{ij}(\epsilon,t)\delta\right]\right), \tag{B.59}$$

where $\epsilon = \mathcal{O}(z)$ is a small parameter, $\delta$ is a free parameter that can be chosen as 1 or 0 and

$$\eta_{ij}(\epsilon,t) \equiv \frac{2p_j([1+\epsilon]t;\{v_\alpha/[1+\epsilon]\})k_{ji}(\boldsymbol{\lambda}_t)}{t_{ij}([1+\epsilon]t;\{v_\alpha/[1+\epsilon]\})}, \tag{B.60}$$

where

$$t_{ij}(t;\{v_\alpha\}) \equiv p_i(t;\{v_\alpha\})k_{ij}(\boldsymbol{\lambda}_t) + p_j(t;\{v_\alpha\})k_{ji}(\boldsymbol{\lambda}_t) \tag{B.61}$$

is the average dynamical activity at link $ij$ of the original process. Here, we have chosen the auxiliary protocol and speed parameter according to Eqs. (B.18) and (B.19). This choice of rates corresponds to a "time-scaled" process with probability and current given by

$$p_i^{\dagger}(t;\{v_\alpha^{\dagger}\}) \equiv p_i([1+\epsilon]t;\{v_\alpha/[1+\epsilon]\}) \tag{B.62}$$

and

$$j_{ij}^{\dagger}(t;\{v_\alpha^{\dagger}\}) \equiv (1+\epsilon)j_{ij}([1+\epsilon]t;\{v_\alpha/[1+\epsilon]\}), \tag{B.63}$$

respectively.

The first term in Eq. (B.58) is given by

$$\langle a_T\rangle^{\dagger} = a(T^{\dagger},\{v_\alpha^{\dagger}\}) = \sum_i a(i,\boldsymbol{\lambda}_{T^{\dagger}}(\{v_\alpha^{\dagger}\}))p_i(T^{\dagger};\{v_\alpha^{\dagger}\}), \tag{B.64}$$

$$\langle A_T\rangle^{\dagger} = A(T^{\dagger},\{v_\alpha^{\dagger}\}) = \frac{1}{T^{\dagger}}\int_0^{T^{\dagger}} \mathrm{d}t' \sum_i a(i,\boldsymbol{\lambda}_{t'}(\{v_\alpha^{\dagger}\}))p_i(t';\{v_\alpha^{\dagger}\}), \tag{B.65}$$

$$\left\langle J_T^{\mathrm{I}}\right\rangle^{\dagger} = J^{\mathrm{I}}(T^{\dagger},\{v_\alpha^{\dagger}\}) = \frac{1}{T^{\dagger}}\int_0^{T^{\dagger}} \mathrm{d}t' \sum_{i>j}(1+\epsilon)d_{ij}^{\mathrm{I}}(\boldsymbol{\lambda}_{t'}(\{v_\alpha^{\dagger}\}))j_{ij}(t';\{v_\alpha^{\dagger}\}), \tag{B.66}$$

$$\left\langle J_T^{\mathrm{II}}\right\rangle^{\dagger} = J^{\mathrm{II}}(T^{\dagger},\{v_\alpha^{\dagger}\}) = \frac{1}{T^{\dagger}}\int_0^{T^{\dagger}} \mathrm{d}t' \sum_i(1+\epsilon)d^{\mathrm{II}}(i,\boldsymbol{\lambda}_{t'}(\{v_\alpha^{\dagger}\}))p_i(t';\{v_\alpha^{\dagger}\}) \tag{B.67}$$

depending on the choice of the observable $X_T$. Here, we have used the substitution $t' = (1+\epsilon)t$, $T^{\dagger} = (1+\epsilon)T$ and $v_\alpha^{\dagger} = v_\alpha/(1+\epsilon)$. The second term in Eq. (B.58) is given by

$$-\frac{\epsilon^2}{2T}\int_0^T \mathrm{d}t \sum_{ij} \frac{\left[p_i(t;\{v_\alpha\})k_{ij}(\boldsymbol{\lambda}_t) + p_j(t;\{v_\alpha\})k_{ji}(\boldsymbol{\lambda}_t)(1-2\delta)\right]^2}{t_{ij}(t;\{v_\alpha\})} + \mathcal{O}(\epsilon^3). \tag{B.68}$$

An expansion for small $\epsilon$ of the r.h.s of Eq. (B.58) and an optimization with respect to $\epsilon$ leads to the bounds on the diffusion coefficient

$$D_J(T,\{v_\alpha\}) \geq \frac{[J(T,\{v_\alpha\}) + \Delta J(T,\{v_\alpha\})]^2}{C_\delta(T,\{v_\alpha\})} \tag{B.69}$$

and

$$D_{\mathcal{A}}(T,\{v_\alpha\}) \geq \frac{[\Delta\mathcal{A}(T,\{v_\alpha\})]^2}{C_\delta(T,\{v_\alpha\})} \tag{B.70}$$

with currents $J(T,\{v_\alpha\}) \in \{J^{\mathrm{I}}(T,\{v_\alpha\}), J^{\mathrm{II}}(T,\{v_\alpha\})\}$, state variables $\mathcal{A}(T,\{v_\alpha\}) \in \{a(T,\{v_\alpha\}), A(T,\{v_\alpha\})\}$ and the cost term

$$C_\delta(T,\{v_\alpha\}) \equiv \frac{2}{T}\int_0^T \mathrm{d}t \sum_{ij} \frac{\left[p_i(t;\{v_\alpha\})k_{ij}(\boldsymbol{\lambda}_t) + p_j(t;\{v_\alpha\})k_{ji}(\boldsymbol{\lambda}_t)(1-2\delta)\right]^2}{t_{ij}(t;\{v_\alpha\})}. \tag{B.71}$$

For the choice $\delta = 1$, the cost term in Eq. (B.71) is equal or smaller than the total entropy production rate

$$\sigma(T,\{v_\alpha\}) \equiv \frac{1}{T}\int_0^T \mathrm{d}t \sum_{i>j} j_{ij}(t;\{v_\alpha\}) \ln\left[\frac{p_i(t;\{v_\alpha\})k_{ij}(\boldsymbol{\lambda}_t)}{p_j(t;\{v_\alpha\})k_{ji}(\boldsymbol{\lambda}_t)}\right], \tag{B.72}$$

i.e.,

$$C_{\delta=1}(T,\{v_\alpha\}) \leq \sigma(T,\{v_\alpha\}), \tag{B.73}$$

which can be shown by using the log-mean inequality

$$(\gamma_1-\gamma_2)\ln(\gamma_1/\gamma_2) \geq 2(\gamma_1-\gamma_2)^2/(\gamma_1+\gamma_2) \tag{B.74}$$

for arbitrary $\gamma_1, \gamma_2 > 0$. Combined with Eqs. (B.69) and (B.70), the inequality (B.73) proves our main results Eqs. (6.1) and (6.16) in Chapter 6 for systems with discrete states.

### B.2.3 *Bound on the total average dynamic activity*

Additionally, from Eqs. (B.69) and (B.70), we obtain bounds on the total average dynamic activity

$$\begin{aligned}\mathcal{A}ct &\equiv \frac{1}{T}\int_0^T \mathrm{d}t \sum_{i>j} t_{ij}(t;\{v_\alpha\}) \\ &= \frac{1}{T}\int_0^T \mathrm{d}t \sum_{i>j} p_i(t;\{v_\alpha\})k_{ij}(\boldsymbol{\lambda}_t) + p_j(t;\{v_\alpha\})k_{ji}(\boldsymbol{\lambda}_t)\end{aligned} \tag{B.75}$$

by choosing $\delta = 0$ in Eq. (B.71), i.e., $C_{\delta=0}(T,\{v_\alpha\}) = \mathcal{A}ct(T,\{v_\alpha\})$.

Finally, we show that the above derived bounds on the average dynamic activity $\mathcal{A}ct(T,\{v_\alpha\})$ can also be applied to jump observables of the type

$$\chi_T \equiv \frac{1}{T}\int_0^T \mathrm{d}t \sum_{ij} d_{ij}^{\mathrm{III}}(\boldsymbol{\lambda}_t)\dot{m}_{ij}(t), \tag{B.76}$$

where $d_{ij}^{\mathrm{III}}$ are arbitrary increments that do not necessarily have to be symmetric or anti-symmetric. With $\delta = 0$ in the ansatz (B.59), the first term in Eq. (B.58) becomes

$$\langle\chi_T\rangle^{\dagger} = \frac{1}{T}\int_0^T \mathrm{d}t\,(1+\epsilon)d_{ij}^{\mathrm{III}}(\boldsymbol{\lambda}_t)p_i([1+\epsilon]t;\{v_\alpha/[1+\epsilon]\})k_{ij}(\boldsymbol{\lambda}_t). \tag{B.77}$$

An expansion for small $\epsilon$ of the r.h.s of Eq. (B.58) and an optimization with respect to $\epsilon$ leads to

$$D_\chi(T,\{v_\alpha\}) \geq \frac{[\chi(T,v)+\Delta\chi(T,v)]^2}{2\mathcal{A}ct(T,\{v_\alpha\})}, \tag{B.78}$$

where

$$D_\chi(T,\{v_\alpha\}) \equiv T\left(\langle\chi_T^2\rangle - \langle\chi_T\rangle^2\right)/2 \tag{B.79}$$

is the diffusion coefficient of the jump observable $\chi_T$ and $\mathcal{A}ct(T,\{v_\alpha\})$ is the total average dynamical activity defined in Eq. (B.75). The bound in Eq. (B.78) is a generalization of bounds that were obtained in [108] for steady-state systems, in [106] for relaxation processes and in Ref. [1], i.e., Section A.3 for periodically driven systems to arbitrary time-dependently driven systems.

## B.3 MOVING TRAP: ONE PARTICLE

In this section, we derive expressions for the mean particle current $\nu(T,v)$, the mean power $P(T,v)$, the diffusion coefficients $D_{\nu,P}$ and the total entropy production rate $\sigma(T,v)$ for the moving trap model with one particle discussed in Section 6.2.

### B.3.1 *Fokker-Planck equation and solution*

The Fokker-Planck equation for the moving trap reads

$$\partial_t p(x,t;v) = -\partial_x\left(-\mu k[x-\lambda(vt)] - D\partial_x\right)p(x,t;v), \tag{B.80}$$

with protocol $\lambda(vt) = vt$ and diffusion constant $D \equiv \mu/\beta$. The solution of Eq. (B.80) is a Gaussian distribution

$$p(x,t;v) \equiv \frac{1}{2\pi y_t^2}\exp\left(-[x-c_t]^2/[2y_t^2]\right) \tag{B.81}$$

with mean

$$c_t \equiv c(t;v) \equiv \langle x(t) \rangle \tag{B.82}$$

and variance

$$y_t^2 \equiv y^2(t;v) \equiv \left\langle x^2(t) \right\rangle - \langle x(t) \rangle^2 . \tag{B.83}$$

In general, both, mean and variance depend on the speed $v$. The system is initially prepared in equilibrium, i.e., $c_0 = 0$ and $y_{t=0}^2 = 1/(\beta k)$. Consequently, mean and variance are given by

$$c_t = vt - \frac{v}{\mu k} \left[ 1 - \exp\left( -\mu k t \right) \right], \tag{B.84}$$

$$y_t^2 = 1/(\beta k). \tag{B.85}$$

With these expressions the probability current can be written as

$$j(x,t;v) = v(1 - \exp\left[ -\mu k t \right]) p(x,t;v). \tag{B.86}$$

### B.3.2 *Mean values and response terms*

Using Eq. (B.84), the mean value of the velocity of the particle is given by

$$v(T,v) = \langle x(T) \rangle / T = c_T / T = v \left( 1 - \frac{1}{\mu k T} \left[ 1 - \exp\left( -\mu k T \right) \right] \right). \tag{B.87}$$

The response term becomes

$$\begin{aligned} \Delta v(T,v) &\equiv (T\partial_T - v\partial_v) v(T,v) \\ &= v \left( \frac{2}{\mu k T} \left[ 1 - \exp\left( -\mu k T \right) \right] - \exp\left[ -\mu k T \right] - 1 \right). \end{aligned} \tag{B.88}$$

The mean value of the power reads

$$\begin{aligned} P(T,v) &= \frac{1}{T} \int_0^T \mathrm{d}t \left\langle -kv(x(t) - vt) \right\rangle \\ &= \frac{v^2}{\mu} \left( 1 - \frac{1}{\mu k T} \left[ 1 - \exp\left( -\mu k T \right) \right] \right) \end{aligned} \tag{B.89}$$

with the response term

$$\begin{aligned} \Delta P(T,v) &\equiv (T\partial_T - v\partial_v) P(T,v) \\ &= -2P(T,v) - \frac{v^2}{\mu} \exp(-\mu k T) + \frac{v^2}{\mu^2 k T} (1 - \exp[-\mu k T]). \end{aligned} \tag{B.90}$$

The mean total entropy production rate can be calculated by using Eq. (B.86) and is given by

$$\begin{aligned}\sigma(T,v) &\equiv \frac{1}{T}\int_0^T \mathrm{d}t \int_{-\infty}^{\infty} \mathrm{d}x\, \frac{j(x,t;v)^2}{Dp(x,t;v)} \\ &= \frac{v^2}{TD}\left(T - \frac{2}{\mu k}[1-\exp(-\mu k T)] + \frac{1}{2\mu k}[1-\exp(-2\mu k T)]\right).\end{aligned} \tag{B.91}$$

### B.3.3 *Diffusion coefficients*

For the diffusion coefficients

$$D_J(T,v) \equiv T\left(\left\langle J_T^2\right\rangle - \left\langle J_T\right\rangle^2\right)/2 \tag{B.92}$$

the term $\left\langle J_T^2\right\rangle$ must be calculated. The correlation function $\langle \dot{x}(t)\dot{x}(t')\rangle$ that enters in the correlation $\left\langle v_T^2\right\rangle$ for the velocity can be written in terms of correlations between state functions as

$$\begin{aligned}\left\langle \dot{x}(t)\dot{x}(t')\right\rangle &= 2D\delta(t-t') \\ &\quad + \left\langle [2\nu(x(t'),t') - \mu F(x(t'),\lambda(vt'))]\mu F(x(t),\lambda(vt))\right\rangle \Theta(t-t') \\ &\quad + \left\langle [2\nu(x(t),t) - \mu F(x(t),\lambda(vt))]\mu F(x(t'),\lambda(vt'))\right\rangle \Theta(t'-t).\end{aligned} \tag{B.93}$$

Hence, in both correlation functions, i.e., in $\left\langle v_T^2\right\rangle$ for the velocity and in $\left\langle P_T^2\right\rangle$ for the power, correlation functions $\langle x(t)x(t')\rangle$ occur that can be directly evaluated by solving the Langevin equation and taking the average over all noise realizations. Inserting these expressions into Eq. (B.92) yields the diffusion coefficient

$$D_v(T,v) = \frac{D}{\mu k T}\left(1-\exp\left[-\mu k T\right]\right) \tag{B.94}$$

for the velocity and

$$D_P(T,v) = \frac{v^2}{\beta\mu}\left(1 - \frac{1}{\mu k T}\left[1-\exp\left(-\mu k T\right)\right]\right) = P(T,v)/\beta \tag{B.95}$$

for the power. The latter relation between the diffusion coefficient of the power and its mean value arises due to the Gaussian nature of the work statistics [160]. With Eqs. (B.87)–(B.91), (B.94) and (B.95) the quality factors $\mathcal{Q}_{P,\nu}$ defined in Eq. (6.4) in Section 6.2 can be calculated.

### B.3.4 *Violation of the TUR for steady-state systems*

In this section, we will show that the TUR for steady-state systems

$$\frac{D_J\sigma}{J^2} \geq 1 \tag{B.96}$$

is strictly violated for the power, i.e., $J = P(T,v)$. With Eq. (B.95) the l.h.s of (B.96) can be written as $\sigma(T,v)/[\beta P(T,v)]$ for the moving trap. Thus, if the TUR for steady-state systems was valid, it would state $\sigma(T,v) \geq \beta P(T,v)$. However, as we now show in the case for the moving trap, the power rather fulfills the opposite inequality

$$\sigma(T,v) \leq \beta P(T,v). \tag{B.97}$$

First, the mean entropy of the system $\langle S_{\text{sys}} \rangle$ is constant in time due to the fact that the variance $y_t^2$ is constant. Hence, the mean entropy change of the system $\langle \Delta S_{\text{sys}} \rangle$ is zero. Second, using

$$\langle \Delta V(x(t),t) \rangle = \langle V(x(t),t) - V(x(0),0) \rangle = \frac{k}{2} \langle x^2(t) \rangle \geq 0 \tag{B.98}$$

the first law of thermodynamics leads to

$$\begin{aligned} \sigma(T,v) &= \frac{1}{T} \langle \Delta S_{\text{tot}} \rangle = \frac{1}{T} \left( \beta \langle Q \rangle + \langle \Delta S_{\text{sys}} \rangle \right) \\ &= \beta P(T,v) - \langle \Delta V(x(t),t) \rangle / T \leq \beta P(T,v), \end{aligned} \tag{B.99}$$

where $\langle Q \rangle$ is the mean heat dissipated in the medium.

## B.4 MOVING TRAP: TWO INTERACTING PARTICLES

In this section, we give further details about the moving trap with two interacting particles in a harmonic potential. The two particles with mobility $\mu$ are embedded in a solution with temperature $\beta$ and dragged by a harmonic trap with velocity $v$ up to time $T$ as shown in the inset of Fig. 6.1. The positions $x_1(t)$ and $x_2(t)$ of the two interacting particles obey a set of coupled Langevin equations

$$\begin{aligned} \dot{x}_1(t) = \mu \Big[ &- \partial_{x_1} V_{\text{ext}}(x_1, \lambda(vt))|_{x_1 = x_1(t)} \\ &- \partial_{x_1} V_{\text{int}}(x_1, x_2(t))|_{x_1 = x_1(t)} \Big] + \zeta_1(t), \end{aligned} \tag{B.100}$$

$$\begin{aligned} \dot{x}_2(t) = \mu \Big[ &- \partial_{x_2} V_{\text{ext}}(x_2, \lambda(vt))|_{x_2 = x_2(t)} \\ &- \partial_{x_2} V_{\text{int}}(x_1(t), x_2)|_{x_2 = x_2(t)} \Big] + \zeta_2(t), \end{aligned} \tag{B.101}$$

where the noises fulfill

$$\langle \zeta_i(t) \rangle = 0, \tag{B.102}$$

$$\langle \zeta_i(t) \zeta_j(t') \rangle = 2D\delta_{i,j}\delta(t-t') \tag{B.103}$$

with $i,j \in \{1,2\}$ and $D = \mu/\beta$. The external potential generated by the harmonic trap reads

$$V_{\text{ext}}(x, \lambda(vt)) \equiv k(x - \lambda(vt))^2/2, \tag{B.104}$$

where $k$ denotes the stiffness of the trap and $\lambda(vt) \equiv vt$ is the protocol. The interaction between the particles is chosen as a Lennard-Jones potential

$$V_{\text{int}}(x_1, x_2) = V_0 \left[ \left( \frac{r_{\min}}{|x_1 - x_2|} \right)^{12} - 2 \left( \frac{r_{\min}}{|x_1 - x_2|} \right)^{6} \right] \tag{B.105}$$

with $V_0 > 0$ the depth of the potential well and $r_{\min}$ the distance at which the potential reaches its minimum $-V_0$.

For calculating the quality factors $\mathcal{Q}_P$ and $\mathcal{Q}_\nu$ shown in Fig. 6.1 in Section 6.2, we perform a Langevin simulation. As initial condition, we choose two independent Gaussian distributions

$$p_1(x_1, t = 0) = \frac{1}{\sqrt{2\pi y_1^2}} \exp\left( -\frac{[x_1 - c_1]^2}{2y_1^2} \right) \tag{B.106}$$

and

$$p_2(x_2, t = 0) = \frac{1}{\sqrt{2\pi y_2^2}} \exp\left( -\frac{[x_2 - c_2]^2}{2y_2^2} \right). \tag{B.107}$$

In the Langevin simulation, we fix the values of the means and standard deviations to $c_1 = 2.0$, $c_2 = -2.0$ and $y_1 = y_2 = 0.1$, respectively. We further keep the parameters $\mu = 1.0, k = 1.0, r_{\min} = 1.0, V_0 = 1.0, vT = 10.0$ and $\beta = 10.0$ fixed and vary the speed of driving $v$ and the observation time $T$ as shown in Fig. 6.1.

## B.5 TRANSITION RATES FOR THE UNFOLDING OF CALMODULIN

In this section, we give further information about the transition rates between two conformational mesostates of Calmodulin that we extract from the experimental data from Ref. [26] as follows. In this experiment, an external force is applied to Calmodulin through optical tweezers. At constant force $f$ the folding and unfolding processes are observed and the force-dependent transition rates are measured. The rates at zero force are extrapolated using appropriate models for the folding and unfolding processes (see supplemental material of [26]).

We parameterize the transition rates according to

$$k_{ij}(f) \equiv k_{ij}^{(0)} \exp\left( \kappa_{ij} f \right), \tag{B.108}$$

where $i, j \in \{U, F_{12}, F_{23}, F_{34}, F_{1234}\}$ with $i \neq j$ and $k_{ij}^{(0)}$ and $\kappa_{ij}$ are parameters listed for each individual link in Table B.1. We determine the parameters by using the zero force rates listed in Table 2 in Ref. [26] and Fig. S8 in the supplemental material of Ref. [26]. The exponential force dependence in (B.108) is used for the unfolding rates in Ref. [26].

Table B.1: Parameters for the transition rates (B.108) as extracted from the experimental data given in Ref. [26].

| transition | $k_{ij}^{(0)}\,[\mathrm{s}^{-1}]$ | $\kappa_{ij}\,[\mathrm{pN}^{-1}]$ | transition | $k_{ij}^{(0)}\,[\mathrm{s}^{-1}]$ | $\kappa_{ij}\,[\mathrm{pN}^{-1}]$ |
|---|---|---|---|---|---|
| $F_{1234} \to F_{12}$ | 0.2 | 0.33 | $F_{12} \to U$ | $1 \times 10^{-5}$ | 1.2 |
| $F_{12} \to F_{1234}$ | $3.8 \times 10^{8}$ | $-1.9$ | $U \to F_{12}$ | $2.9 \times 10^{10}$ | $-2.5$ |
| $F_{1234} \to F_{34}$ | 0.16 | 0.43 | $F_{34} \to U$ | $7.9 \times 10^{-5}$ | 1 |
| $F_{34} \to F_{1234}$ | $2.4 \times 10^{9}$ | $-2.2$ | $U \to F_{34}$ | $1.3 \times 10^{11}$ | $-2.6$ |
| $F_{123} \to F_{12}$ | 0.74 | 0.47 | $F_{23} \to U$ | 0.04 | 0.89 |
| $F_{12} \to F_{123}$ | $1.1 \times 10^{7}$ | $-1$ | $U \to F_{23}$ | $4.9 \times 10^{7}$ | $-1.7$ |

For the folding rates, a more complex model was used in Ref. [26] to fit the experimental data. However, in the region around $6 - 13\,\mathrm{pN}$ using (B.108) is a sufficient approximation to reproduce the experimental measured folding rates. The force-dependent transition rates $k_{ij}(f)$ thus obtained are shown in Fig. B.1.

For the time dependent driving, we vary the force $f(t) \equiv \lambda(vt) = f_0 + vt(f_1 - f_0)$, where $v$ is the speed parameter, $f_1$ is the final force and $f_0$ is the initial force applied to the protein.

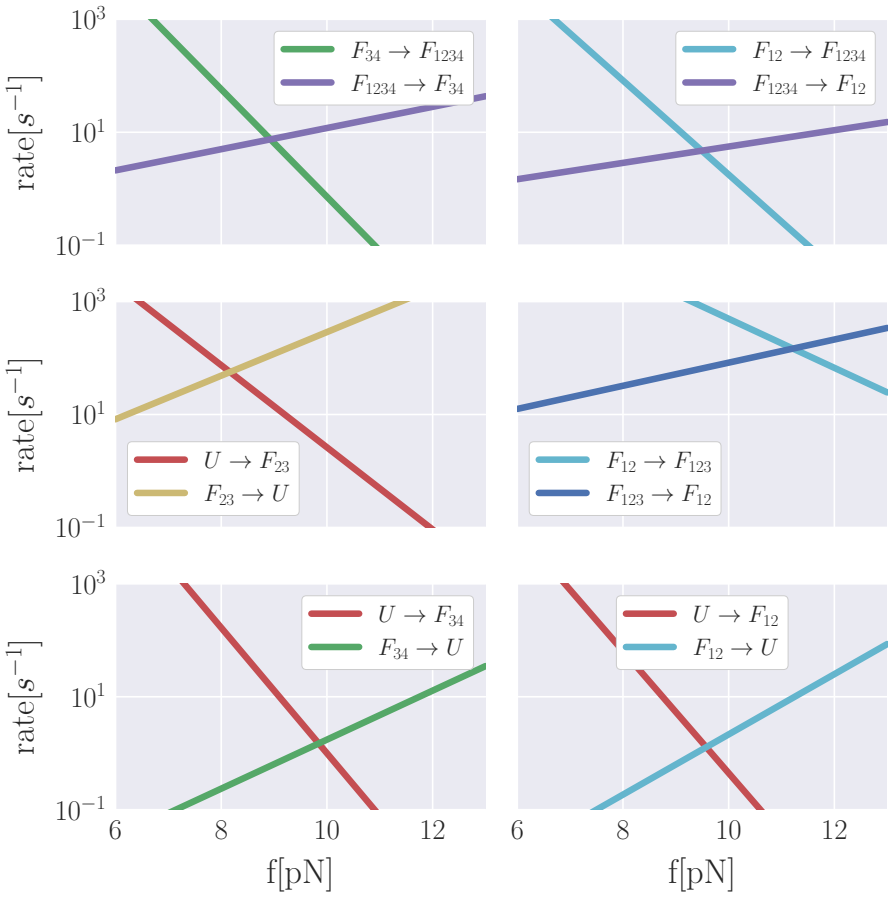


Figure B.1: Force-dependent transition rates for Calmodulin as used for the simulation in Chapter 6. Similar curves can be found in Fig. S8 of the supplemental material of Ref. [26].

# C

# FAST AND SLOW DRIVING

## C.1 DIFFUSION COEFFICIENTS AND CORRELATION FUNCTIONS

### C.1.1 *Diffusion coefficients*

In this section, we give the explicit expressions for the diffusion coefficients of the observables defined in Eqs. (7.7)–(7.10). The diffusion coefficients of the state variables (7.7) and (7.8) in terms of the scaled time $\tau$ are given by

$$D_a(T,v) = T\left(\int \mathrm{d}x\, a^2(x,\lambda_{\tau_f})p(x,\tau_f;v) - a(T,v)^2\right)/2 \tag{C.1}$$

and

$$\begin{aligned} D_A(T,v) =& \frac{T}{\tau_f^2}\int_0^{\tau_f}\mathrm{d}\tau\int_0^{\tau}\mathrm{d}\tau'\int\mathrm{d}x\int\mathrm{d}x'\, a(x,\lambda_\tau)p(x,\tau|x',\tau')a(x',\lambda_\tau)p(x',\tau;v) \\ & - T/2A(T,v)^2, \end{aligned} \tag{C.2}$$

respectively. Analogously, the diffusion coefficient of the the current (7.9) is given by

$$\begin{aligned} D_{J^b}(T,v) =& \frac{v}{\tau_f}\int_0^{\tau_f}\mathrm{d}\tau\int_0^{\tau}\mathrm{d}\tau'\int\mathrm{d}x\int\mathrm{d}x'\, \dot{b}(x,\lambda_\tau)p(x,\tau|x',\tau')\dot{b}(x',\lambda_\tau)p(x',\tau;v) \\ & - T/2J_b(T,v)^2. \end{aligned} \tag{C.3}$$

In order to write the diffusion coefficient of the current in Eq. (7.10) in terms of correlation functions between state functions, we use the relation (C.6) in Section C.1.2. Plugging Eq. (C.6) into the diffusion coefficient (7.12) of the current depending on the velocity and changing to the timescale $\tau$ yields

$$\begin{aligned} D_{J^d}(T,v) =& \frac{1}{t_{\mathrm{sys}}\tau_f}\int_0^{\tau_f}\mathrm{d}\tau\int\mathrm{d}x\,\tilde{D}d^2(x,\lambda_\tau)p(x,\tau;v) \\ & + \frac{(vt_{\mathrm{sys}})^{-1}}{t_{\mathrm{sys}}\tau_f}\int_0^{\tau_f}\mathrm{d}\tau\int_0^{\tau}\mathrm{d}\tau'\int\mathrm{d}x\int\mathrm{d}x'\,\tilde{J}(x,\tau)p(x,\tau|x',\tau') \\ & \qquad \times\{\tilde{J}(x',\tau')p(x',\tau';v) - 2\tilde{D}\left[d(x',\lambda_{\tau'})p(x',\tau';v)\right]'\} \\ & - \frac{T}{2}J_d(T,v)^2 \end{aligned} \tag{C.4}$$

with

$$\tilde{J}(x,\tau) \equiv d(x,\lambda_\tau)j(x,\tau;v)/p(x,\tau;v) + \tilde{D}\{d(x,\lambda_\tau)p(x,\tau;v)\}'/p(x,\tau;v). \tag{C.5}$$

### C.1.2 *Correlation functions*

Throughout this section, we use the original notation for the Fokker-Planck equation introduced in Eq. (7.5) and not the time-scaled notation introduced in Section 7.1.4. In the following, we derive the relation

$$\begin{aligned}
&\langle d(x_t,\lambda_t)\circ\dot{x}_t d(x_{t'},\lambda_{t'})\circ\dot{x}_{t'}\rangle \\
=&2D\left\langle d^2(x_t,\lambda_t)\right\rangle\delta(t-t') \\
&+\theta(t-t')\left\langle J(x_{t'},t')\left[J(x_t,t)-2D\{d(x_t,\lambda_t)p(x_t,t;v)\}'/p(x_t,t)\right]\right\rangle \\
&+\theta(t'-t)\left\langle J(x_t,t)\left[J(x_{t'},t')-2D\{d(x_t,\lambda_t)p(x_t,t;v)\}'/p(x_{t'},t')\right]\right\rangle
\end{aligned} \tag{C.6}$$

with

$$J(x_t,t)\equiv d(x_t,\lambda_t)j(x_t,t)/p(x_t,t)+D\{d(x_t,\lambda_t)p(x_t,t)\}'/p(x_t,t), \tag{C.7}$$

where

$$\{d(x_t,\lambda_t)p(x_t,t)\}'\equiv\partial_x d(x,\lambda_t)p(x,t)|_{x=x_t}. \tag{C.8}$$

We introduce the shorthand notation $C_t\equiv C(x_t,\lambda_t)$ for an arbitrary state function $C(x_t,\lambda_t)$. First, we use the Langevin Eq. (7.1) to rewrite the expression

$$\begin{aligned}
\langle d_t\circ\dot{x}_t d_{t'}\circ\dot{x}_{t'}\rangle =&\langle d_t\circ\zeta_t d_{t'}\circ\zeta_{t'}\rangle-\langle d_t\mu F_t d_{t'}\mu F_{t'}\rangle+\langle d_t\mu F_t d_{t'}\circ\dot{x}_{t'}\rangle \\
&+\langle d_{t'}\mu F_{t'} d_t\circ\dot{x}_t\rangle
\end{aligned} \tag{C.9}$$

in terms of the noise. Then, we use Itô's Lemma [47] to write the first term in Eq. (C.9) in terms of non-anticipating functions and the noise, i.e.,

$$\begin{aligned}
\langle d_t\circ\zeta_t d_{t'}\circ\zeta_{t'}\rangle =&\langle d_t\cdot\zeta_t d_{t'}\cdot\zeta_{t'}\rangle-D^2\left\langle d'_t d'_{t'}\right\rangle+\left\langle Dd'_t d_{t'}\circ[\dot{x}_{t'}-\mu F_{t'}]\right\rangle \\
&+\left\langle Dd'_{t'} d_t\circ[\dot{x}_t-\mu F_t]\right\rangle,
\end{aligned} \tag{C.10}$$

where $\cdot$ denotes the Itô product and

$$d'_t\equiv\partial_x d(x,\lambda_t)|_{x=x_t}. \tag{C.11}$$

Next, we use Itô's Isometry [47] to evaluate the first term in Eq. (C.10), which reads

$$\langle d_t\cdot\zeta_t d_{t'}\cdot\zeta_{t'}\rangle=2D\delta(t-t')\left\langle d_t^2\right\rangle. \tag{C.12}$$

Using Eqs. (C.10) and (C.12) we can rewrite Eq. (C.9) as

$$\begin{aligned}
\langle d_t\circ\dot{x}_t d_{t'}\circ\dot{x}_{t'}\rangle =&2D\delta(t-t')\left\langle d_t^2\right\rangle-\left\langle\left[d_t\mu F_t+Dd'_t\right]\left[d_{t'}\mu F_{t'}+Dd'_{t'}\right]\right\rangle \\
&+\left\langle\left[d_{t'}\mu F_{t'}+Dd'_{t'}\right]d_t\circ\dot{x}_t\right\rangle+\left\langle\left[d_t\mu F_t+Dd'_t\right]d_{t'}\circ\dot{x}_{t'}\right\rangle.
\end{aligned} \tag{C.13}$$

Now, we rewrite the last two terms of Eq. (C.13) in terms of correlation functions between state functions. To do so, we define a variable $B(x,\lambda_t)$ such that $\partial_x B(x,\lambda_t) = d(x,\lambda_t)$ and, hence, $d(x_t,\lambda_t)\circ\dot{x}_t = \dot{B}(x_t,\lambda_t) - \dot{\lambda}\partial_\lambda B(x,\lambda)|_{\lambda=\lambda_t}$, where $\dot{B}(x_t,\lambda_t) \equiv (\mathrm{d}/\mathrm{d}t)B(x_t,\lambda_t)$ is the total time-derivative of the state function $B(x,\lambda_t)$. The last term in Eq. (C.13) can be written as

$$\left\langle \left[d_t\mu F_t + Dd'_t\right] d_{t'}\circ\dot{x}_{t'}\right\rangle = \left\langle A_t \circ \left[\dot{B}_{t'} - \dot{\lambda}\partial_\lambda B(x_{t'},\lambda)|_{\lambda=\lambda_{t'}}\right]\right\rangle, \tag{C.14}$$

with $A_t \equiv d_t\mu F_t + Dd'_t$. Next, we can rewrite the first term on the r.h.s of Eq. (C.14) by applying the derivative after averaging because average values and time derivatives commute in the Stratonovich convention [161], i.e.,

$$\left\langle A_t\dot{B}_{t'}\right\rangle = (\mathrm{d}/\mathrm{d}t')\left\langle A_tB_{t'}\right\rangle = (\mathrm{d}/\mathrm{d}t')\int \mathrm{d}x\, A(x,\lambda_t)U\left(x,t,t'\right)B(x,\lambda_{t'}) \tag{C.15}$$

for $t > t'$ and

$$\left\langle A_t\dot{B}_{t'}\right\rangle = (\mathrm{d}/\mathrm{d}t')\int \mathrm{d}x\, B(x,\lambda_{t'})U\left(x,t',t\right)A(x,\lambda_t) \tag{C.16}$$

for $t' > t$ with time evolution operator

$$U\left(x,t',t\right) \equiv \overrightarrow{\exp}\left(\int_t^{t'} \mathrm{d}t''\,\mathcal{L}_{\mathrm{FP}}\left(x,\lambda_{t''}\right)\right) \tag{C.17}$$

and Fokker-Planck operator

$$\mathcal{L}_{\mathrm{FP}}\left(x,\lambda_\tau\right) \equiv -\partial_x\left(\mu F(x,\lambda_\tau) - D\partial_x\right). \tag{C.18}$$

Using $(\mathrm{d}/\mathrm{d}t')U\left(x,t',t\right) = \mathcal{L}_{\mathrm{FP}}\left(x,t'\right)U\left(x,t',t\right)$ and $(\mathrm{d}/\mathrm{d}t')U\left(x,t,t'\right) = U\left(x,t,t'\right)\mathcal{L}_{\mathrm{FP}}\left(x,t'\right)$ for Eqs. (C.15) and (C.16) yields the following expression

$$\begin{aligned}\left\langle A_t\dot{B}_{t'}\right\rangle = {}& \theta(t-t')\left\langle A_t\left[2\nu_{t'}d_{t'} - \mu F_{t'} - Dd'_{t'} + \dot{\lambda}\partial_\lambda B(x_{t'},\lambda)|_{\lambda=\lambda_{t'}}\right]\right\rangle \\ & + \theta(t'-t)\left\langle A_t\left[\mu F_{t'}d_{t'} + Dd'_{t'} + \dot{\lambda}\partial_\lambda B(x_{t'},\lambda)|_{\lambda=\lambda_{t'}}\right]\right\rangle,\end{aligned} \tag{C.19}$$

where $\theta(\cdot)$ is the Heaviside function and $\nu_t \equiv j(x_t,\lambda_t)/p(x_t,\lambda_t)$ is the mean local velocity. Finally, inserting Eq. (C.19) into Eq. (C.13) leads to

$$\begin{aligned}\left\langle d_t\circ\dot{x}_t d_{t'}\circ\dot{x}_{t'}\right\rangle = {}& 2D\delta(t-t')\left\langle d_t^2\right\rangle \\ & + \theta(t-t')\left\langle\left[\mu F_t d_t + Dd'_t\right]\left[2\nu_{t'}d_{t'} - \mu F_{t'}d_{t'} - Dd'_{t'}\right]\right\rangle \\ & + \theta(t'-t)\left\langle\left[\mu F_{t'}d_{t'} + Dd'_{t'}\right]\left[2\nu_t d_t - \mu F_t d_t - Dd'_t\right]\right\rangle,\end{aligned} \tag{C.20}$$

which is identical to Eq. (C.6) when identifying the terms $J(x_t,\lambda_t) = \mu F_{t'}d_{t'} + Dd'_{t'}$ and $J(x_t,\lambda_t) - 2Dd(x_t,\lambda_t)p(x_t,\lambda_t)'/p(x_t,t) = 2\nu_t d_t - \mu F_t d_t - Dd'_t$.

## C.2 LIMIT OF FAST DRIVING

In this section, we derive the scaling properties of the quality factors in the limit of fast driving shown in Table 7.1.

First, we determine the leading order of the total entropy production rate by inserting Eqs. (7.36) and (7.40) into Eq. (7.33), which yields

$$\begin{aligned}\sigma(T,v) &= \frac{1}{t_{\text{sys}}}\sigma^{(0)}(T,v) + \mathcal{O}\left(\epsilon_f/t_{\text{sys}}\right) \\ &\equiv \frac{1}{t_{\text{sys}}\tau_f}\int_0^{\tau_f} \mathrm{d}\tau \int \mathrm{d}x\, \frac{j^{(0)}(x,\tau)^2}{\tilde{D}p(x,0)} + \mathcal{O}\left(\epsilon_f/t_{\text{sys}}\right). \end{aligned} \tag{C.21}$$

Obviously, the entropy production rate is of $\mathcal{O}(1)$ in the limit of fast driving.

Next, we determine the leading orders of the mean values and their response terms. Inserting Eqs. (7.36), (7.37), (7.38) into (7.28) leads to an expression for the instantaneous state variable

$$a(T,v) = a^{(0)}(T,v) + \epsilon_f a^{(1)}(T,v) + \mathcal{O}\left(\epsilon_f^2\right) \tag{C.22}$$

with

$$a^{(0)}(T,v) \equiv \int \mathrm{d}x\, a(x,\lambda_{\tau_f})p(x,0) \tag{C.23}$$

and

$$a^{(1)}(T,v) \equiv \int \mathrm{d}x\, a(x,\lambda_{\tau_f})\hat{\mathcal{L}}_{\text{eff}}\left(x,\tau_f,0\right)\, p(x,0). \tag{C.24}$$

The response term of $a(T,v)$ is consequently given by

$$\mathcal{R}_a(T,v) \equiv [\Delta a(T,v)]^2 = \left[a^{(1)}(T,v)\right]^2 \epsilon_f^2 + \mathcal{O}\left(\epsilon_f^3\right) \tag{C.25}$$

due to the fact that $\Delta f(\tau_f = vT) = 0$ for an arbitrary function $f$ depending only on $\tau_f$ and not depending separately on $v$ and $T$. For time-averaged state variables (7.29) one gets a similar behavior by following the analogous steps above, which leads to the response term

$$\mathcal{R}_A(T,v) \equiv [\Delta A(T,v)]^2 = \left[A^{(1)}(T,v)\right]^2 \epsilon_f^2 + \mathcal{O}\left(\epsilon_f^3\right) \tag{C.26}$$

with

$$A^{(1)}(T,v) \equiv \frac{1}{\tau_f}\int_0^{\tau_f} \int \mathrm{d}x\, a(x,\lambda_\tau)\hat{\mathcal{L}}_{\text{eff}}\left(x,\tau,0\right)\, p(x,0). \tag{C.27}$$

Furthermore, for the current defined in Eq. (7.30) one finds the following expression for the current

$$J_b(T,v) = \frac{1}{\epsilon_f t_{\text{sys}}}\left(J_b^{(0)}(T,v) + \epsilon_f J_b^{(1)}(T,v) + \mathcal{O}\left(\epsilon_f^2\right)\right) \tag{C.28}$$

with zeroth order

$$J_b^{(0)}(T,v) \equiv \frac{1}{\tau_f}\int_0^{\tau_f}\int \mathrm{d}x\, \dot{b}(x,\lambda_\tau)p(x,0) \tag{C.29}$$

and first order

$$J_b^{(1)}(T,v) \equiv \frac{1}{\tau_f}\int_0^{\tau_f}\int \mathrm{d}x\, \dot{b}(x,\lambda_\tau)\hat{\mathcal{L}}_{\text{eff}}\,(x,\tau,0)\; p(x,0). \tag{C.30}$$

Using these expressions leads to the response term

$$\mathcal{R}_{J_b}(T,v) \equiv [J_b(T,v)+\Delta J_b(T,v)]^2 = \left[J_b^{(1)}(T,v)\right]^2 (1/t_{\text{sys}}^2) + \mathcal{O}(\epsilon_f). \tag{C.31}$$

Moreover, for the current depending on the velocity we insert Eqs. (7.40), (7.41) into Eq. (7.32), which leads to

$$J_d(T,v) = \frac{1}{t_{\text{sys}}} J_d^{(0)}(T,v) + \mathcal{O}(\epsilon_f/t_{\text{sys}}) \tag{C.32}$$

with zeroth leading order

$$J_d^{(0)}(T,v) \equiv \frac{1}{\tau_f}\int_0^{\tau_f}\mathrm{d}\tau\int \mathrm{d}x\, d(x,\lambda_\tau)j^{(0)}(x,\tau). \tag{C.33}$$

The response term consequently reads

$$\mathcal{R}_{J_d}(T,v) \equiv [J_d(T,v)+\Delta J_d(T,v)]^2 = \left[J_d^{(0)}(T,v)\right]^2 \frac{1}{t_{\text{sys}}^2} + \mathcal{O}\left(\epsilon_f/t_{\text{sys}}^2\right). \tag{C.34}$$

Now we derive the leading order of the diffusion coefficients. First, using the leading order of the density in (7.37) and plugging it into Eq. (C.1) yields

$$D_a(T,v) = t_{\text{sys}}\tau_f\epsilon_f D_a^{(1)}(T,v) + \mathcal{O}\left(\epsilon_f^2\right) \tag{C.35}$$

with

$$D_a^{(1)}(T,v) \equiv \frac{1}{2}\left(\int \mathrm{d}x\, a(x,\lambda_{\tau_f})^2 p(x,0) - \left[\int \mathrm{d}x\, a(x,\lambda_{\tau_f})p(x,0)\right]^2\right) \tag{C.36}$$

for the instantaneous state variable. For all other diffusion coefficients it is sufficient to use the zeroth order of the propagator defined in Eq. (7.44). Plugging this leading order into the diffusion coefficient (C.2) for time-averaged state variable leads to

$$D_A(T,v) = t_{\text{sys}}\tau_f\epsilon_f D_A^{(1)}(T,v) + \mathcal{O}\left(\epsilon_f^2\right) \tag{C.37}$$

with

$$D_A^{(1)}(T,v) \equiv \frac{1}{\tau_f^2}\int_0^{\tau_f} \mathrm{d}\tau \int_0^{\tau} \mathrm{d}\tau' \int \mathrm{d}x\, a(x,\lambda_\tau)a(x,\lambda_{\tau'})p(x,0) - \frac{1}{2}A^{(0)}(T,v)^2, \tag{C.38}$$

where

$$A^{(0)}(T,v) \equiv \frac{1}{\tau_f}\int_0^{\tau_f} \mathrm{d}\tau \int \mathrm{d}x\, a(x,\lambda_\tau)p(x,0) \tag{C.39}$$

is the leading zeroth order of the time-averaged state variable. Furthermore, plugging Eq. (7.44) into (7.30) yields the diffusion coefficient

$$D_{J_b} = \frac{\tau_f}{t_{\mathrm{sys}}\epsilon_f}\left(D_{J_b}^{(0)}(T,v) + \mathcal{O}(\epsilon_f)\right) \tag{C.40}$$

of the current $J_b(T,v)$ with

$$D_{J_b}^{(0)}(T,v) \equiv \frac{1}{\tau_f^2}\int_0^{\tau_f} \mathrm{d}\tau \int_0^{\tau} \mathrm{d}\tau' \int \mathrm{d}x\, \dot{b}(x,\lambda_\tau)\dot{b}(x,\lambda_{\tau'})p(x,0) - \frac{1}{2}J_b^{(0)}(T,v)^2, \tag{C.41}$$

where $J_b^{(0)}(T,v)$ is defined in Eq. (C.29). For diffusion coefficient of the current depending on the velocity, we insert Eq. (7.44) into (C.4), which leads to

$$D_{J_d}(T,v) = \frac{1}{t_{\mathrm{sys}}}D_{J_d}^{(0)}(T,v) + \mathcal{O}(\epsilon_f/t_{\mathrm{sys}}) \tag{C.42}$$

with leading order

$$D_{J_d}^{(0)}(T,v) \equiv \frac{1}{\tau_f}\int_0^{\tau_f} \mathrm{d}\tau \int \mathrm{d}x\, d^2(x,\lambda_\tau)p(x,0). \tag{C.43}$$

Finally, we use the above derived results to determine the leading orders of all quality factors. First, by using Eqs. (C.21), (C.25) and (C.35) we can determine the quality factor

$$Q_a \equiv \frac{\mathcal{R}_a(T,v)}{\sigma(T,v)D_a(T,v)} \approx \frac{\left[a^{(1)}(T,v)\right]^2}{\sigma^{(0)}(T,v)\tau_f D_a^{(1)}(T,v)}\epsilon_f \tag{C.44}$$

for the instantaneous state variable $a(T,v)$. Furthermore, via Eqs. (C.21), (C.26) and (C.37) we get the asymptotic behavior of the quality factor

$$Q_A \equiv \frac{\mathcal{R}_A(T,v)}{\sigma(T,v)D_A(T,v)} \approx \frac{\left[A^{(1)}(T,v)\right]^2}{\sigma^{(0)}(T,v)\tau_f D_A^{(1)}(T,v)}\epsilon_f \tag{C.45}$$

for the time-averaged observable. Moreover using Eqs. (C.21), (C.31) and (C.40) yields the quality factor

$$Q_{J_b} \equiv \frac{\mathcal{R}_{J_b}(T,v)}{\sigma(T,v)D_{J_b}(T,v)} \approx \frac{\left[J_b^{(1)}(T,v)\right]^2}{\sigma^{(0)}(T,v)\tau_f D_{J_b}^{(0)}(T,v)}\epsilon_f \tag{C.46}$$

for the current depending on the time spent in a certain state. Last but not least, using Eqs. (C.21), (C.34) and (C.42) leads to the expression for the quality factor

$$Q_{J_d} \equiv \frac{\mathcal{R}_{J_d}(T,v)}{\sigma(T,v)D_{J_d}(T,v)} \approx \frac{\left[J_d^{(0)}(T,v)\right]^2}{\sigma^{(0)}(T,v)D^{(0)}(T,v)} \tag{C.47}$$

for the current depending on the velocity. We remark that the explicit expression for the quality factor (C.47) is given by Eq. (7.48) in the main text, which can be verified by using Eqs. (C.21), (C.32) and (C.42).

## C.3 LIMIT OF SLOW DRIVING

In this section, we derive the generic scaling properties of the quality factors in the limit of slow driving shown in Table 7.2. A system prepared in an arbitrary initial condition relaxes into the stationary state at $\lambda_0$ on a timescale that is much shorter than the timescale of the external driving on which the protocol changes. We are interested in the dynamics on a timescale that is comparable with the timescale of the driving and, hence, assume that the system has already reached the stationary state at $\lambda_0$.

We first derive an expression for the total entropy production rate. For this, we insert Eqs. (7.51) and (7.54) into Eq. (7.33), which leads to

$$\sigma(T,v) = \frac{1}{t_{\rm sys}\tau_f}\int_0^{\tau_f} \mathrm{d}\tau \int \mathrm{d}x \, \frac{\left(j^{(0)}(x,\tau) + \epsilon_s j^{(1)}(x,\tau)\right)^2}{\tilde{D}p^{(0)}(x,\tau)}. \tag{C.48}$$

If the system is driven around an equilibrium state, the entropy production rate vanishes, i.e., $\sigma(T,v) = \mathcal{O}(\epsilon_s)$. If the system is driven around a NESS, the entropy production rate is finite and, hence, $\sigma(T,v) = \mathcal{O}(1)$.

Next, we derive the leading orders of the mean values and their response terms. Due to the fact that the density (7.52) is a function of the protocol in the leading order, the response term of the zeroth order of the instantaneous state variable vanishes. As a consequence, the response term of this quantity is given by

$$\mathcal{R}_a(T,v) = \left[a^{(1)}(T,v)\right]^2 \epsilon_s^2 + \mathcal{O}(\epsilon_s^3), \tag{C.49}$$

where we used that $\Delta\epsilon_s = -\epsilon_s$. This implies that the response terms for the time-averaged state variable

$$\mathcal{R}_A(T,v) = \left[A^{(1)}(T,v)\right]^2 \epsilon_s^2 + \mathcal{O}(\epsilon_s^3) \tag{C.50}$$

as well as for the current depending on the residence time

$$\mathcal{R}_{J_b}(T,v) = \left[J_b^{(2)}(T,v)\right]^2 \epsilon_s^4/t_{\text{sys}}^2 + \mathcal{O}(\epsilon_s^5) \tag{C.51}$$

vanish asymptotically. The response term for the current depending on the velocity is given by

$$\mathcal{R}_{J_d}(T,v) = \left[J_d^{(0)}(T,v) - \epsilon_s^2 J_d^{(2)}(T,v) + \mathcal{O}(\epsilon_s^3)\right]^2 (1/t_{\text{sys}})^2, \tag{C.52}$$

where the linear term in $\epsilon_s$ of the current vanishes due to $\Delta\epsilon_s = -\epsilon_s$. Depending on whether a non-conservative force is applied or not, the response term (C.52) is either of $\mathcal{O}(1)$ or $\mathcal{O}(\epsilon_s^4)$, respectively.

Now, we derive the leading orders of the diffusion coefficients. First, for the instantaneous state variable we plug Eq. (7.51) into (C.1) and obtain

$$D_a(T,v) = \frac{\tau_f t_{\text{sys}}}{\epsilon_s}\left[D_a^{(0)}(T,v) + \mathcal{O}(\epsilon_s)\right] \tag{C.53}$$

with

$$D_a^{(0)}(T,v) \equiv \frac{1}{2}\int \mathrm{d}x\, a^2(x,\lambda_{\tau_f}) p^{(0)}(x,\tau_f) - \left[\int \mathrm{d}x\, a(x,\tau_f) p^{(0)}(x,\tau_f)\right]^2. \tag{C.54}$$

For the time-averaged observables, we insert the propagator (7.59) in the limit of slow driving into the diffusion coefficients (C.2), (C.3) and (C.4). The leading order of the variance of the time-averaged state variable vanishes such that its diffusion coefficient is given by

$$D_A(T,v) = \tau_f t_{\text{sys}} D_A^{(0)}(T,v) + \mathcal{O}(\epsilon_s) \tag{C.55}$$

with leading order $D_A^{(0)}(T,v)$. Analogously, for the current $J_b(T,v)$ we find

$$D_{J_b}(T,v) = \frac{\epsilon_s^2}{\tau_f t_{\text{sys}}} D_{J_b}^{(2)}(T,v) + \mathcal{O}(\epsilon_s^3) \tag{C.56}$$

with leading order $D_{J_b}^{(2)}(T,v)$. Furthermore, the diffusion coefficient for the current $J_d(T,v)$ converges to

$$D_{J_d}(T,v) = \frac{1}{t_{\text{sys}}} D_{J_d}^{(0)}(T,v) + \mathcal{O}(\epsilon_s) \tag{C.57}$$

with leading order $D_{J_d}^{(0)}(T,v)$ as the last two terms in Eq. (C.4) compensate each other, when using (7.59).

Lastly, we determine the leading orders of all quality factors by using the above derived results. Using Eqs. (C.48), (C.49), and (C.53) leads to the quality factor

$$\mathcal{Q}_a \equiv \frac{\mathcal{R}_a(T,v)}{\sigma(T,v) D_a(T,v)} \approx \frac{\left[a^{(1)}(T,v)\right]^2 \epsilon_s^3}{D_a^{(0)}(T,v) \int_0^{\tau_f} \mathrm{d}\tau \int \mathrm{d}x\, \frac{\left(j^{(0)}(x,\tau) + \epsilon_s j^{(1)}(x,\tau)\right)^2}{\tilde{D} p^{(0)}(x,\tau)}}$$

(C.58)

of the instantaneous state variable. Depending on whether a non-conservative force is applied or not the quality factor (C.58) vanishes like $\epsilon_s^3$ or $\epsilon_s$, respectively. The quality factor of the time-averaged state variable can be calculated by using Eqs. (C.48), (C.50) and (C.55) and reads

$$\mathcal{Q}_A \equiv \frac{\mathcal{R}_A(T,v)}{\sigma(T,v)D_A(T,v)} \approx \frac{\left[A^{(1)}(T,v)\right]^2 \epsilon_s^2}{D_A^{(0)}(T,v)\int_0^{\tau_f} \mathrm{d}\tau \int \mathrm{d}x \, \frac{\left(j^{(0)}(x,\tau)+\epsilon_s j^{(1)}(x,\tau)\right)^2}{\tilde{D}p^{(0)}(x,\tau)}}. \tag{C.59}$$

This quality factor is either of $\mathcal{O}(\epsilon_s^2)$ or $\mathcal{O}(1)$ depending on whether the system is in a NESS or in an equilibrium state at fixed $\lambda_\tau$. Furthermore, we use Eqs. (C.48), (C.51) and (C.56) to determine the leading order of the quality factor for current $J_b(T,v)$

$$\mathcal{Q}_{J_b} \equiv \frac{\mathcal{R}_{J_b}(T,v)}{\sigma(T,v)D_{J_b}(T,v)} \approx \frac{\left[J_b^{(2)}(T,v)\right]^2 \epsilon_s^2 \tau_f^2}{D_{J_b}(T,v)\int_0^{\tau_f} \mathrm{d}\tau \int \mathrm{d}x \, \frac{\left(j^{(0)}(x,\tau)+\epsilon_s j^{(1)}(x,\tau)\right)^2}{\tilde{D}p^{(0)}(x,\tau)}}, \tag{C.60}$$

which vanishes like $\epsilon_s^2$, if a non-conservative force is applied and is of $\mathcal{O}(1)$, when only conservative forces are applied. Using eqs. (C.48), (C.52) and (C.57) yields the quality factor for the current $J_d(T,v)$

$$\mathcal{Q}_{J_d} \equiv \frac{\mathcal{R}_{J_d}(T,v)}{\sigma(T,v)D_{J_d}(T,v)} \approx \frac{\left[J_d^{(0)}(T,v) - \epsilon_s^2 J_d^{(2)}(T,v)\right]^2 \tau_f}{D_{J_d}^{(0)}(T,v)\int_0^{\tau_f} \mathrm{d}\tau \int \mathrm{d}x \, \frac{\left(j^{(0)}(x,\tau)+\epsilon_s j^{(1)}(x,\tau)\right)^2}{\tilde{D}p^{(0)}(x,\tau)}}. \tag{C.61}$$

The quality factor (C.61) is of $\mathcal{O}(1)$, if a non-conservative force is applied and vanishes like $\epsilon_s^2$, if only conservative forces are present.

# BIBLIOGRAPHY


[1] T. Koyuk and U. Seifert, *Operationally accessible bounds on fluctuations and entropy production in periodically driven systems*, Phys. Rev. Lett. **122**, 230601 (2019).

[2] T. Koyuk and U. Seifert, *Thermodynamic uncertainty relation for time-dependent driving*, Phys. Rev. Lett. **125**, 260604 (2020).

[3] T. Koyuk and U. Seifert, *Quality of the thermodynamic uncertainty relation for fast and slow driving*, J. Phys. A: Math. Theor. **54**, 414005 (2021).

[4] T. Koyuk, U. Seifert, and P. Pietzonka, *A generalization of the thermodynamic uncertainty relation to periodically driven systems*, J. Phys. A Math. Theor. **52**, 02LT02 (2019).

[5] J. Degünther, T. Koyuk, and U. Seifert, *Phase shift in periodically driven non-equilibriumsystems: its identification and a bound*, J. Stat. Mech.: Theor. Exp., 033207 (2022).

[6] T. Koyuk and U. Seifert, *Thermodynamic uncertainty relation in interacting many-body systems*, arXiv:2202.12220 (2022).

[7] U. Seifert, *Entropy production along a stochastic trajectory and an integral fluctuation theorem*, Phys. Rev. Lett. **95**, 040602 (2005).

[8] U. Seifert, *Stochastic thermodynamics, fluctuation theorems, and molecular machines*, Rep. Prog. Phys. **75**, 126001 (2012).

[9] U. Seifert, *Stochastic thermodynamics: from principles to the cost of precision*, Physica A **504**, 176–191 (2018).

[10] U. Seifert, *From stochastic thermodynamics to thermodynamic inference*, Ann. Rev. Cond. Mat. Phys. **10**, 171–192 (2019).

[11] U. Seifert, *Lecture notes on advanced statistical physics.* Universität Stuttgart (unpublished) (2022).

[12] R. Clausius, *Ueber verschiedene für die Anwendung bequeme Formen der Hauptgleichungen der mechanischen Wärmetheorie*, Ann. Phys. **201**, 353–400 (1865).

[13] L. Boltzmann, *Über die mechanische Bedeutung des zweiten Hauptsatzes der Wärmetheorie*, Wiener Berichte. **53**, 195–220 (1866).

[14] J. W. Gibbs, *Elementary principles in statistical mechanics* (Charles Scribner's Sons, 1902).

[15] R. Clausius, *Ueber die bewegende Kraft der Wärme und die Gesetze, welche sich daraus für die Wärmelehre selbst ableiten lassen*, Ann. Phys. **155**, 500–524 (1850).

[16] R. Clausius, *Ueber eine veränderte Form des zweiten Hauptsatzes der mechanischen Wärmetheorie*, Ann. Phys. **169**, 481–506 (1854).

[17] F. Schwabl, *Statistische Mechanik* (Springer-Verlag, Berlin Heidelberg New York, 2000).

[18] S. Carnot, *Réflexions sur la puissance motrice du feu*, (1824).

[19] R. Brown, *XXVII. A brief account of microscopical observations made in the months of June, July and August 1827, on the particles contained in the pollen of plants; and on the general existence of active molecules in organic and inorganic bodies*, Philosophical Magazine Series 2 **4**, 161–173 (1828).

[20] A. Einstein, *Über die von der molekularkinetischen Theorie der Wärme geforderte Bewegung von in ruhenden Flüssigkeiten suspendierten Teilchen*, Ann. Phys. **17**, 549 (1905).

[21] M. von Smoluchowski, *Zur kinetischen Theorie der Brownschen Molekularbewegung und der Suspensionen*, Ann. Phys. **326**, 756–780 (1906).

[22] M. P. Langevin, *Sur la théorie du mouvement brownien*, Comptes Rend. Acad. Sci. (Paris) **146**, 530 (1908).

[23] D. S. Lemons and A. Gythiel, *Paul Langevin's 1908 paper "On the theory of Brownian motion" ["sur la théorie du mouvement brownien," c. r. acad. sci. (paris) 146, 530–533 (1908)]*, American Journal of Physics **65**, 1079–1081 (1997).

[24] J. Perrin, *Mouvement brownien et réalité moléculaire*, Annales de Chimie et de Physique **18**, 5–104 (1909).

[25] S. Ciliberto, *Experiments in stochastic thermodynamics: short history and perspectives*, Phys. Rev. X **7**, 021051 (2017).

[26] J. Stigler, F. Ziegler, A. Gieseke, J. C. M. Gebhardt, and M. Rief, *The complex folding network of single calmodulin molecules*, Science **334**, 512–516 (2011).

[27] A. C. Barato and U. Seifert, *Thermodynamic uncertainty relation for biomolecular processes*, Phys. Rev. Lett. **114**, 158101 (2015).

[28] T. R. Gingrich, J. M. Horowitz, N. Perunov, and J. L. England, *Dissipation bounds all steady-state current fluctuations*, Phys. Rev. Lett. **116**, 120601 (2016).

[29] P. Pietzonka and U. Seifert, *Universal trade-off between power, efficiency and constancy in steady-state heat engines*, Phys. Rev. Lett. **120**, 190602 (2018).

[30] K. Proesmans and C. van den Broeck, *Discrete-time thermodynamic uncertainty relation*, EPL **119**, 20001 (2017).

[31] A. C. Barato and U. Seifert, *Cost and precision of Brownian clocks*, Phys. Rev. X **6**, 041053 (2016).

[32] H.-M. Chun, L. P. Fischer, and U. Seifert, *Effect of a magnetic field on the thermodynamic uncertainty relation*, Phys. Rev. E **99**, 042128 (2019).

[33] L. P. Fischer, H.-M. Chun, and U. Seifert, *Free diffusion bounds the precision of currents in underdamped dynamics*, Phys. Rev. E **102**, 012120 (2020).

[34] P. Pietzonka, *Classical pendulum clocks break the thermodynamic uncertainty relation*, Phys. Rev. Lett. **128**, 130606 (2022).

[35] K. Sekimoto, *Kinetic characterisation of heat bath and the energetics of thermal ratchet models*, J. Phys. Soc. Jpn. **66**, 1234–1237 (1997).

[36] K. Sekimoto, *Stochastic energetics* (Springer, Berlin, Heidelberg, 2010).

[37] A. W. C. Lau and T. C. Lubensky, *State-dependent diffusion: thermodynamic consistency and its path integral formulation*, Phys. Rev. E **76**, 011123 (2007).

[38] H. Risken, *The Fokker-Planck equation*, 2nd (Springer-Verlag, Berlin, 1989).

[39] P. Hänggi and F. Marchesoni, *Artificial brownian motors: controlling transport on the nanoscale*, Rev. Mod. Phys. **81**, 387–442 (2009).

[40] U. Seifert, *Stochastic thermodynamics of single enzymes and molecular motors*, Eur. Phys. J. E **34**, 26 (2011).

[41] V. Blickle and C. Bechinger, *Realization of a micrometre-sized stochastic heat engine*, Nature Phys. **8**, 143 (2012).

[42] I. A. Martínez, E. Roldan, L. Dinis, D. Petrov, J. M. R. Parrondo, and R. A. Rica, *Brownian Carnot engine*, Nature Phys. **12**, 67–70 (2016).

[43] S. Erbas-Cakmak, D. A. Leigh, C. T. McTernan, and A. L. Nussbaumer, *Artificial molecular machines*, Chem. Rev. **115**, 10081–10206 (2015).

[44] A. Rosas, C. van den Broeck, and K. Lindenberg, *Stochastic thermodynamics for a periodically driven single-particle pump*, Phys. Rev. E **96**, 052135 (2017).

[45] A. C. Barato, É. Roldán, I. A. Martínez, and S. Pigolotti, *Arcsine laws in stochastic thermodynamics*, Phys. Rev. Lett. **121**, 090601 (2018).

[46] S. Machlup and L. Onsager, *Fluctuations and irreversible process. II. Systems with kinetic energy*, Phys. Rev. **91**, 1512–1515 (1953).

[47] C. W. Gardiner, *Handbook of stochastic methods*, 3rd (Springer-Verlag, Berlin, 2004).

[48] C. Jarzynski, *Nonequilibrium equality for free energy differences*, Phys. Rev. Lett. **78**, 2690 (1997).

[49] C. Maes and K. Netocný, *Time-reversal and entropy*, J. Stat. Phys. **110**, 269 (2003).

[50] A. Berman and R. J. Plemmons, *Nonnegative matrices in the mathematical sciences* (SIAM, Philadelphia, 1994).

[51] J. M. Horowitz and T. R. Gingrich, *Thermodynamic uncertainty relations constrain non-equilibrium fluctuations*, Nat. Phys. **16**, 15–20 (2020).

[52] H. Touchette, *The large deviation approach to statistical mechanics*, Phys. Rep. **478**, 1–69 (2009).

[53] C. Jarzynski, *Equalities and inequalities: irreversibility and the second law of thermodynamics at the nanoscale*, Ann. Rev. Cond. Mat. Phys. **2**, 329–351 (2011).

[54] C. van den Broeck and M. Esposito, *Ensemble and trajectory thermodynamics: a brief introduction*, Physica A **418**, 6–16 (2015).

[55] R. Kubo, *Fluctuation-dissipation theorem*, Rep. Progr. Phys. **29**, 255 (1966).

[56] D. J. Evans, E. G. D. Cohen, and G. P. Morriss, *Probability of second law violations in shearing steady states*, Phys. Rev. Lett. **71**, 2401 (1993).

[57] G. Gallavotti and E. G. D. Cohen, *Dynamical ensembles in nonequilibrium statistical mechanics*, Phys. Rev. Lett. **74**, 2694 (1995).

[58] J. Kurchan, *Fluctuation theorem for stochastic dynamics*, J. Phys. A: Math. Gen. **31**, 3719 (1998).

[59] J. L. Lebowitz and H. Spohn, *A Gallavotti-Cohen-type symmetry in the large deviation functional for stochastic dynamics*, J. Stat. Phys. **95**, 333 (1999).

[60] D. J. Evans and D. J. Searles, *Equilibrium microstates which generate second law violating steady states*, Phys. Rev. E **50**, 1645 (1994).

[61] C. Jarzynski, *Equilibrium free-energy differences from nonequilibrium measurements: a master-equation approach*, Phys. Rev. E **56**, 5018 (1997).

[62] G. E. Crooks, *Entropy production fluctuation theorem and the nonequilibrium work relation for free energy differences*, Phys. Rev. E **60**, 2721 (1999).

[63] G. E. Crooks, *Path-ensemble averages in systems driven far from equilibrium*, Phys. Rev. E **61**, 2361 (2000).

[64] U. Seifert, *Fluctuation theorem for a single enzym or molecular motor*, Europhys. Lett. **70**, 36 (2005).

[65] U. Marconi, A. Puglisi, L. Rondoni, and A. Vulpiani, *Fluctuation-dissipation: response theory in statistical physics*, Phys. Rep. **461**, 111–195 (2008).

[66] M. Baiesi, C. Maes, and B. Wynants, *Fluctuations and response of nonequilibrium states*, Phys. Rev. Lett. **103**, 010602 (2009).

[67] J. Prost, J.-F. Joanny, and J. M. R. Parrondo, *Generalized fluctuation-dissipation theorem for steady-state systems*, Phys. Rev. Lett. **103**, 090601 (2009).

[68] U. Seifert and T. Speck, *Fluctuation-dissipation theorem in nonequilibrium steady states*, EPL **89**, 10007 (2010).

[69] M. Baiesi and C. Maes, *An update on nonequilibrium linear response*, New J. Phys. **15**, 013004 (2013).

[70] T. Harada and S. I. Sasa, *Equality connecting energy dissipation with a violation of the fluctuation-response relation*, Phys. Rev. Lett. **95**, 130602 (2005).

[71] T. Harada and S. Sasa, *Energy dissipation and violation of the fluctuation-response relation in nonequilibrium Langevin systems*, Phys. Rev. E **73**, 026131 (2006).

[72] P. Pietzonka, F. Ritort, and U. Seifert, *Finite-time generalization of the thermodynamic uncertainty relation*, Phys. Rev. E **96**, 012101 (2017).

[73] J. M. Horowitz and T. R. Gingrich, *Proof of the finite-time thermodynamic uncertainty relation for steady-state currents*, Phys. Rev. E **96**, 020103(R) (2017).

[74] A. Dechant and S. I. Sasa, *Current fluctuations and transport efficiency for general Langevin systems*, J. Stat. Mech. Theor. Exp., 063209 (2018).

[75] A. Dechant and S. I. Sasa, *Fluctuation–response inequality out of equilibrium*, Proc. Natl. Acad. Sci. U.S.A. **117**, 6430 (2020).

[76] A. Dechant and S. I. Sasa, *Entropic bounds on currents in Langevin systems*, Phys. Rev. E **97**, 062101 (2018).

[77] Y. Hasegawa and T. Van Vu, *Uncertainty relations in stochastic processes: an information inequality approach*, Phys. Rev. E **99**, 062126 (2019).

[78] P. Pietzonka, A. C. Barato, and U. Seifert, *Universal bound on the efficiency of molecular motors*, J. Stat. Mech.: Theor. Exp., 124004 (2016).

[79] W. Hwang and C. Hyeon, *Energetic costs, precision, and transport efficiency of molecular motors*, J. Phys. Chem. Lett. **9**, 513–520 (2018).

[80] M. Nguyen and S. Vaikuntanathan, *Design principles for nonequilibrium self-assembly*, Proc. Natl. Acad. Sci. U.S.A. **113**, 14231–14236 (2016).

[81] D. Hartich and A. Godec, *Thermodynamic uncertainty relation bounds the extent of anomalous diffusion*, Phys. Rev. Lett. **127**, 080601 (2021).

[82] D. B. Brückner, P. Ronceray, and C. P. Broedersz, *Inferring the dynamics of underdamped stochastic systems*, Phys. Rev. Lett. **125**, 058103 (2020).

[83] A. Frishman and P. Ronceray, *Learning force fields from stochastic trajectories*, Phys. Rev. X **10**, 021009 (2020).

[84] D. J. Skinner and J. Dunkel, *Improved bounds on entropy production in living systems*, Proc. Natl. Acad. Sci. U.S.A. **118** (2021).

[85] D. J. Skinner and J. Dunkel, *Estimating entropy production from waiting time distributions*, Phys. Rev. Lett. **127**, 198101 (2021).

[86] T. R. Gingrich, G. M. Rotskoff, and J. M. Horowitz, *Inferring dissipation from current fluctuations*, J. Phys. A: Math. Theor. **50**, 184004 (2017).

[87] J. Li, J. M. Horowitz, T. R. Gingrich, and N. Fakhri, *Quantifying dissipation using fluctuating currents*, Nat. Commun. **10**, 1666 (2019).

[88] S. Otsubo, S. Ito, A. Dechant, and T. Sagawa, *Estimating entropy production by machine learning of short-time fluctuating currents*, Phys. Rev. E **101**, 062106 (2020).

[89] S. K. Manikandan, D. Gupta, and S. Krishnamurthy, *Inferring entropy production from short experiments*, Phys. Rev. Lett. **124**, 120603 (2020).

[90] L. P. Fischer, P. Pietzonka, and U. Seifert, *Large deviation function for a driven underdamped particle in a periodic potential*, Phys. Rev. E **97**, 022143 (2018).

[91] J. S. Lee, J.-M. Park, and H. Park, *Thermodynamic uncertainty relation for underdamped Langevin systems driven by a velocity-dependent force*, Phys. Rev. E **100**, 062132 (2019).

[92] T. Van Vu and Y. Hasegawa, *Uncertainty relations for underdamped Langevin dynamics*, Phys. Rev. E **100**, 032130 (2019).

[93] T. Van Vu and Y. Hasegawa, *Thermodynamic uncertainty relations under arbitrary control protocols*, Phys. Rev. Research **2**, 013060 (2020).

[94] J. S. Lee, J.-M. Park, and H. Park, *Universal form of thermodynamic uncertainty relation for Langevin dynamics*, Phys. Rev. E **104**, L052102 (2021).

[95] H. K. L. Chulan Kwon Youngchae Kwon, *Thermodynamic uncertainty relation for underdamped dynamics driven by time-dependent protocols*, New J. Phys. **24**, 013029 (2022).

[96] K. Brandner, T. Hanazato, and K. Saito, *Thermodynamic bounds on precision in ballistic multiterminal transport*, Phys. Rev. Lett. **120**, 090601 (2018).

[97] N. Shiraishi, K. Saito, and H. Tasaki, *Universal trade-off relation between power and efficiency for heat engines*, Phys. Rev. Lett. **117**, 190601 (2016).

[98] V. Holubec and A. Ryabov, *Cycling tames power fluctuations near optimum efficiency*, Phys. Rev. Lett. **121**, 120601 (2018).

[99] T. Ekeh, M. E. Cates, and É. Fodor, *Thermodynamic cycles with active matter*, Phys. Rev. E **102**, 010101(R) (2020).

[100] A. C. Barato, R. Chetrite, A. Faggionato, and D. Gabrielli, *Bounds on current fluctuations in periodically driven systems*, New J. Phys. **20**, 103023 (2018).

[101] K. Proesmans and J. M. Horowitz, *Hysteretic thermodynamic uncertainty relation for systems with broken time-reversal symmetry*, J. Stat. Mech.: Theor. Exp. **2019**, 054005 (2019).

[102] O. Niggemann and U. Seifert, *Field-theoretic thermodynamic uncertainty relation*, J. Stat. Phys. **178**, 1142 (2020).

[103] O. Niggemann and U. Seifert, *Numerical study of the thermodynamic uncertainty relation for the kpz-equation*, J. Stat. Phys. **182**, 25 (2021).

[104] C. Maes, *Frenetic bounds on the entropy production*, Phys. Rev. Lett. **119**, 160601 (2017).

[105] C. Nardini and H. Touchette, *Process interpretation of current entropic bounds*, Eur. Phys. J. B **91**, 16 (2018).

[106] I. Terlizzi and M. Baiesi, *Kinetic uncertainty relation*, J. Phys. A **52**, 02LT03 (2019).

[107] T. R. Gingrich and J. M. Horowitz, *Fundamental bounds on first passage time fluctuations for currents*, Phys. Rev. Lett. **119**, 170601 (2017).

[108] J. P. Garrahan, *Simple bounds on fluctuations and uncertainty relations for first-passage times of counting observables*, Phys. Rev. E **95**, 032134 (2017).

[109] K. Hiura and S.-i. Sasa, *Kinetic uncertainty relation on first-passage time for accumulated current*, Phys. Rev. E **103**, L050103 (2021).

[110] K. Macieszczak, K. Brandner, and J. P. Garrahan, *Unified thermodynamic uncertainty relations in linear response*, Phys. Rev. Lett. **121**, 130601 (2018).

[111] B. K. Agarwalla and D. Segal, *Assessing the validity of the thermodynamic uncertainty relation in quantum systems*, Phys. Rev. B **98**, 155438 (2018).

[112] K. Ptaszyński, *Coherence-enhanced constancy of a quantum thermoelectric generator*, Phys. Rev. B **98**, 085425 (2018).

[113] M. Carrega, M. Sassetti, and U. Weiss, *Optimal work-to-work conversion of a nonlinear quantum brownian duet*, Phys. Rev. A **99**, 062111 (2019).

[114] G. Guarnieri, G. T. Landi, S. R. Clark, and J. Goold, *Thermodynamics of precision in quantum non equilibrium steady states*, Phys. Rev. Research **1**, 033021 (2019).

[115] F. Carollo, R. L. Jack, and J. P. Garrahan, *Unraveling the large deviation statistics of markovian open quantum systems*, Phys. Rev. Lett. **122**, 130605 (2019).

[116] S. Pal, S. Saryal, D. Segal, T. S. Mahesh, and B. K. Agarwalla, *Experimental study of the thermodynamic uncertainty relation*, Phys. Rev. Research **2**, 022044(R) (2020).

[117] H. M. Friedman, B. K. Agarwalla, O. Shein-Lumbroso, O. Tal, and D. Segal, *Thermodynamic uncertainty relation in atomic-scale quantum conductors*, Phys. Rev. B **101**, 195423 (2020).

[118] L. M. Cangemi, V. Cataudella, G. Benenti, M. Sassetti, and G. De Filippis, *Violation of thermodynamics uncertainty relations in a periodically driven work-to-work converter from weak to strong dissipation*, Phys. Rev. B **102**, 165418 (2020).

[119] E. Potanina, C. Flindt, M. Moskalets, and K. Brandner, *Thermodynamic bounds on coherent transport in periodically driven conductors*, Phys. Rev. X **11**, 021013 (2021).

[120] P. E. Harunari, C. E. Fiore, and K. Proesmans, *Exact statistics and thermodynamic uncertainty relations for a periodically driven electron pump*, J. Phys. A: Math. Theor. **53**, 374001 (2020).

[121] D. M. Busiello and S. Pigolotti, *Hyperaccurate currents in stochastic thermodynamics*, Phys. Rev. E **100**, 060102(R) (2019).

[122] T. Van Vu, V. T. Vo, and Y. Hasegawa, *Entropy production estimation with optimal current*, Phys. Rev. E **101**, 042138 (2020).

[123] N. Shiraishi, *Optimal thermodynamic uncertainty relation in Markov jump processes*, J. Stat. Phys. **185**, 19 (2021).

[124] G. Falasco, M. Esposito, and J.-C. Delvenne, *Unifying thermodynamic uncertainty relations*, New J. Phys. **22**, 053046 (2020).

[125] L. Ziyin and M. Ueda, *Universal thermodynamic uncertainty relation in non-equilibrium dynamics*, arXiv:2202.13311 (2022).

[126] A. Dechant, *Multidimensional thermodynamic uncertainty relations*, English, J. Phys. A: Math. Theor. **52**, 035001 (2018).

[127] I. V. Girsanov, *On transforming a certain class of stochastic processes by absolutely continuous substitution of measures*, Theory of Probability & Its Applications **5**, 285–301 (1960).

[128] K. Liu, Z. Gong, and M. Ueda, *Thermodynamic uncertainty relation for arbitrary initial states*, Phys. Rev. Lett. **125**, 140602 (2020).

[129] P. Pietzonka, A. C. Barato, and U. Seifert, *Universal bounds on current fluctuations*, Phys. Rev. E **93**, 052145 (2016).

[130] B. Rutten, M. Esposito, and B. Cleuren, *Reaching optimal efficiencies using nanosized photoelectric devices*, Phys. Rev. B **80**, 235122 (2009).

[131] R. Filliger and P. Reimann, *Brownian gyrator: a minimal heat engine on the nanoscale*, Phys. Rev. Lett. **99**, 230602 (2007).

[132] K.-H. Chiang, C.-L. Lee, P.-Y. Lai, and Y.-F. Chen, *Electrical autonomous Brownian gyrator*, Phys. Rev. E **96**, 032123 (2017).

[133] A. Argun, J. Soni, L. Dabelow, S. Bo, G. Pesce, R. Eichhorn, and G. Volpe, *Experimental realization of a minimal microscopic heat engine*, Phys. Rev. E **96**, 052106 (2017).

[134] K. Hayashi, S. de Lorenzo, M. Manosas, J. M. Huguet, and F. Ritort, *Single-molecule stochastic resonance*, Phys. Rev. X **2**, 031012 (2012).

[135] S. Rahav, J. Horowitz, and C. Jarzynski, *Directed flow in nonadiabatic stochastic pumps*, Phys. Rev. Lett. **101**, 140602 (2008).

[136] V. Y. Chernyak and N. A. Sinitsyn, *Pumping restriction theorem for stochastic networks*, Phys. Rev. Lett. **101**, 160601 (2008).

[137] T. Schmiedl and U. Seifert, *Efficiency at maximum power: an analytically solvable model for stochastic heat engines*, EPL **81**, 20003 (2008).

[138] M. Esposito, R. Kawai, K. Lindenberg, and C. van den Broeck, *Quantum-dot Carnot engine at maximum power*, Phys. Rev. E **81**, 041106 (2010).

[139] O. Abah, J. Roßnagel, G. Jacob, S. Deffner, F. Schmidt-Kaler, K. Singer, and E. Lutz, *Single-ion heat engine at maximum power*, Phys. Rev. Lett. **109**, 203006 (2012).

[140] G. Verley, M. Esposito, T. Willaert, and C. van den Broeck, *The unlikely Carnot efficiency*, Nat. Commun. **5**, 4721 (2014).

[141] K. Brandner, K. Saito, and U. Seifert, *Thermodynamics of micro- and nano-systems driven by periodic temperature variations*, Phys. Rev. X **5**, 031019 (2015).

[142] J. Roßnagel, S. T. Dawkins, K. N. Tolazzi, O. Abah, E. Lutz, F. Schmidt-Kaler, and K. Singer, *A single-atom heat engine*, Science **352**, 325–329 (2016).

[143] I. A. Martínez, E. Roldan, L. Dinis, and R. A. Rica, *Colloidal heat engines: a review*, Soft Matter **13**, 22–36 (2017).

[144] M. Campisi and R. Fazio, *The power of a critical heat engine*, Nat. Commun. **7**, 11895 (2016).

[145] M. Polettini and M. Esposito, *Carnot efficiency at divergent power output*, EPL **118**, 40003 (2017).

[146] A. C. Barato, R. Chetrite, A. Faggionato, and D. Gabrielli, *A unifying picture of generalized thermodynamic uncertainty relations*, J. Stat. Mech., 084017 (2019).

[147] G. M. Rotskoff, *Mapping current fluctuations of stochastic pumps to nonequilibrium steady states*, Phys. Rev. E **95**, 030101(R) (2017).

[148] A. Bérut, A. Arakelyan, A. Petrosyan, S. Ciliberto, R. Dillenschneider, and E. Lutz, *Experimental verification of Landauer's principle linking information and thermodynamics*, Nature **483**, 187–189 (2012).

[149] K. Proesmans, J. Ehrich, and J. Bechhoefer, *Finite-time Landauer principle*, Phys. Rev. Lett. **125**, 100602 (2020).

[150] K. Proesmans, J. Ehrich, and J. Bechhoefer, *Optimal finite-time bit erasure under full control*, Phys. Rev. E **102**, 032105 (2020).

[151] Y.-Z. Zhen, D. Egloff, K. Modi, and O. Dahlsten, *Universal bound on energy cost of bit reset in finite time*, Phys. Rev. Lett. **127**, 190602 (2021).

[152] S. Asban and S. Rahav, *Stochastic pumping of particles with zero-range interactions*, New Journal of Physics **17**, 055015 (2015).

[153] O. Raz, Y. Subasi, and C. Jarzynski, *Mimicking nonequilibrium steady states with time-periodic driving*, Phys. Rev. X **6**, 021022 (2016).

[154] I. A. Martínez, É. Roldán, L. Dinis, D. Petrov, and R. A. Rica, *Adiabatic processes realized with a trapped brownian particle*, Phys. Rev. Lett. **114**, 120601 (2015).

[155] A. Dechant and S.-i. Sasa, *Continuous time reversal and equality in the thermodynamic uncertainty relation*, Phys. Rev. Research **3**, L042012 (2021).

[156] M. T. Woodside and S. M. Block, *Reconstructing folding energy landscapes by single-molecule force spectroscopy*, Annual Review of Biophysics **43**, 19–39 (2014).

[157] A. Dechant and S. I. Sasa, *Improving thermodynamic bounds using correlations*, Phys. Rev. X **11**, 041061 (2021).

[158] A. P. Solon and J. M. Horowitz, *Phase transition in protocols minimizing work fluctuations*, Phys. Rev. Lett. **120**, 180605 (2018).

[159] R. Landauer, *Irreversibility and heat generation in the computing process*, IBM J. Res. Dev. **5**, 183–191 (1961).

[160] T. Speck and U. Seifert, *Dissipated work in driven harmonic diffusive systems: general solution and application to stretching rouse polymers*, Eur. Phys. J. B **43**, 521 (2005).

[161] J. Zinn-Justin, *Quantum field theory and critical phenomena*, Fourth (Oxford University Press, New York, 2002).

# LIST OF FIGURES

## LIST OF TABLES

# ERKLÄRUNG

Die eingereichte Dissertation zum Thema „Thermodynamic Uncertainty Relations for Time-Dependent Driving“ stellt meine eigenständig erbrachte Leistung dar.
Ich habe ausschließlich die angegebenen Quellen und Hilfsmittel benutzt. Wörtlich oder inhaltlich aus anderen Werken übernommene Angaben habe ich als solche kenntlich gemacht.
Die Richtigkeit der hier getätigten Angaben bestätige ich und versichere, nach bestem Wissen die Wahrheit erklärt zu haben.

*Stuttgart, den 14. Juni 2022*

Timur Koyuk

# ERKLÄRUNG ZUR ÜBEREINSTIMMUNG DER DIGITALEN VERSION MIT DER VORGELEGTEN PRINTVERSION DER DISSERTATION

Hiermit erkläre ich, Timur Koyuk, geboren am 11. Mai 1995, dass das von mir eingereichte pdf-Dokument zur Dissertation mit dem Thema „Thermodynamic Uncertainty Relations for Time-Dependent Driving“ in Inhalt und Wortlaut der ebenfalls eingereichten Printversion meiner Dissertationsschrift entspricht.

*Stuttgart, den 14. Juni 2022*

Timur Koyuk

# DANKSAGUNG

An dieser Stelle möchte ich mich ganz herzlich bei allen Menschen bedanken, die mich sowohl während meines Studiums als auch während der Promotion stets begleitet und unterstützt haben.

Als Erstes möchte ich mich bei Herrn Prof. Dr. Udo Seifert bedanken, der sich stets Zeit für interessante Diskussionen genommen und mich mit großem Einsatz gefördert hat. Sowohl während meiner Masterarbeit als auch während der Promotion konnte ich dabei viel lernen und mich stets weiterentwickeln.

Bei Herrn Prof. Dr. Christian Holm bedanke ich mich für die Anfertigung des Zweitgutachtens und bei Herrn Prof. Dr. Peter Michler für die Übernahme des Prüfungsvorsitzes.

Darüber hinaus danke ich allen aktuellen und ehemaligen Mitgliedern des Instituts, die ich während meiner Laufbahn kennenlernen durfte. Frau Steinhauser gebührt hierbei ein großer Dank, da sie bei vielen organisatorischen Angelegenheiten stets auf freundliche und professionelle Art und Weise weiterhelfen konnte. Ebenso bedanke ich mich bei allen Kollegen am Institut für die freundschaftliche Atmosphäre. Zudem bedanke ich mich für die erfolgreiche Zusammenarbeit im Rahmen von Bachelor- und Masterarbeiten bei Felix Schwab, Jonas Schmid, Tim Gomez, Julius Degünther, Robin Bebon und Michel Mom.

Des Weiteren möchte ich mich bei den beiden ehemaligen Adminkollegen Dr. Matthias Uhl und Dr. Lukas Fischer bedanken, die mich gewissenhaft in die Netzwerkinfrastuktur des Instituts eingearbeitet haben und mit ihrer Arbeit dazu beigetragen haben, beständige und wartbare Serverstrukturen zu schaffen. Weiterhin möchte ich mich bei den Adminkollegen Bendedikt Remlein, Julius Degünther und Benjamin Ertel für die tolle, freundliche sowie produktive Zusammenarbeit bedanken.

Weiterhin gebührt Dr. Patrick Pietzonka ein besonderer Dank für die großartige Betreuung meiner Masterarbeit, die Möglichkeit einer Dienstreise zum DAMPT (Cambridge) und natürlich für die vielen interessanten fachlichen Diskussionen.

Ebenso gebührt Christoph Lohrmann ein besonderer Dank, der mich schon seit den ersten Tagen des Studiums in Vorlesungen, Praktika, Prüfungsvorbereitungen sowie während der Masterarbeit als Büropartner begleitet hat.

Schließlich möchte ich mich ganz besonders herzlich bei meiner Familie bedanken, die mich immer gefördert, unterstützt und mir somit das Studieren und Promovieren überhaupt erst ermöglicht hat.